UNIVERSIDADE FEDERAL DO CEARÁ
CENTRO DE CIÊNCIAS
DEPARTAMENTO DE BIOQUÍMICA E BIOLOGIA MOLECULAR
PROGRAMA DE PÓS-GRADUAÇÃO EM BIOQUÍMICA

FRANCISCO BRUNO SILVA FREIRE

APOPLASTIC SUCROSE CONCENTRATION IS A KEY REGULATOR OF THE DIEL COURSE STOMATAL MOVEMENTS

FORTALEZA
2024

FRANCISCO BRUNO SILVA FREIRE

APOPLASTIC SUCROSE CONCENTRATION IS A KEY REGULATOR OF THE DIEL COURSE STOMATAL MOVEMENTS

Tese apresentada ao Curso de Doutorado em Bioquímica do Departamento de Bioquímica e Biologia Molecular da Universidade Federal do Ceará, como requisito parcial à obtenção do título de Doutor em Bioquímica. Área de Concentração: Bioquímica Vegetal.

Orientador: Prof. Dr. Danilo de Menezes Daloso.

FORTALEZA

2024

Dados Internacionais de Catalogação na Publicação
Universidade Federal do Ceará
Sistema de Bibliotecas
Gerada automaticamente pelo módulo Catalog, mediante os dados fornecidos pelo(a) autor(a)

F933a Freire, Francisco Bruno Silva.
Apoplastic sucrose concentration is a key regulator of the diel course stomatal movements / Francisco Bruno Silva Freire. – 2024.
116 f. : il. color.

Tese (doutorado) – Universidade Federal do Ceará, Centro de Ciências, Programa de Pós-Graduação em Bioquímica , Fortaleza, 2024.
Orientação: Prof. Dr. Danilo de Menezes Daloso.

1. Células-guarda. 2. Espaço apoplástico. 3. Técnica de infiltração-centrifugação. 4. Metabolômica. 5. Regulação estomática. I. Título.

CDD 572

FRANCISCO BRUNO SILVA FREIRE

APOPLASTIC SUCROSE CONCENTRATION IS A KEY REGULATOR OF THE DIEL COURSE STOMATAL MOVEMENTS

Tese apresentada ao Curso de Doutorado em Bioquímica do Departamento de Bioquímica e Biologia Molecular da Universidade Federal do Ceará, como requisito parcial à obtenção do título de Doutor em Bioquímica. Área de Concentração: Bioquímica Vegetal.

Aprovado em: 17/05/2024

BANCA EXAMINADORA

_____

Prof. Dr. Danilo de Menezes Daloso (Orientador)
Universidade Federal do Ceará (UFC)

_____

Prof. Dr Cleiton Breder Eller
Universidade Federal do Ceará (UFC)

_____

Prof. Dr. Werner Camargos Antunes
Universidade Estadual de Maringá (UEM)

_____

Prof. Dr. Wagner Luiz Araújo
Universidade Federal de Viçosa (UFV)

_____

Dra. Valéria Freitas Lima
Universidade Federal de Viçosa (UFV)

Aos meus pais, Francisco e Marluce.

À minha família e amigos.

AGRADECIMENTOS

À minha família, que sempre me ajudou e me apoiou em alcançar meus objetivos.

Ao meu orientador, Professor Dr. Danilo de Menezes Daloso, por me acolher, instruir e acompanhar por toda minha formação, além de ser mentor para o meu aprendizado.

Ao Professor Dr. Joaquim Albenísio Silveira, pela disponibilidade de seu laboratório e por todos os ensinamentos durante o doutorado.

Ao CNPq pelo apoio financeiro durante o doutorado.

À Universidade Federal do Ceará e ao programa de Pós-graduação em Bioquímica, por me conceder recursos e a oportunidade de desenvolvimento pessoal.

A todos os professores do Departamento de Bioquímica e Biologia Molecular por serem as pessoas mais prestativas e solícitas que já conheci.

À minha amada esposa, Eva Gomes Morais, por estar comigo desde o início de nosso caminho na formação acadêmica, me ajudando nos momentos mais difíceis.

A todos meus amigos, pelos momentos de auxílio e diversão.

A todos os meus colegas do laboratório de metabolismo de plantas, pela amizade, carinho e imenso auxílio.

RESUMO

Evidências recentes sugerem que a sacarose é uma molécula capaz de induzir o fechamento estomático em altas concentrações, em que o acúmulo de sacarose no apoplasto seria uma forma de induzir o fechamento estomático em períodos de alta taxa fotossintética e, assim, otimizar a eficiência do uso da água em plantas (WUE). Entretanto, não está claro como esse processo contribui para a regulação diária da WUE e sua relação com o papel da sacarose dentro das células-guarda (GC) durante o fechamento estomático. Dentro desta perspectiva, este projeto irá testar a hipótese de que a sacarose é uma molécula chave que integra fotossíntese e movimentos estomáticos e que seus níveis presentes no apoplasto foliar se correlacionam positivamente durante a abertura e negativamente durante o fechamento estomático com a condutância estomática (g_s). Para isso, inicialmente foi estabelecido método eficiente de coleta do apoplasto foliar utilizando metanol (MeOH) e água (ddH_2O) como fluidos de infiltração visando análises metabólicas via cromatografia gasosa acoplada a um espectrometro de massas usando folhas de tabaco e Arabidopsis. Posteriormente, foram realizados experimentos determinando a dinâmica dos movimentos estomáticos com o perfil metabólico de folhas e do apoplasto ao longo do dia utilizando plantas de tabaco selvagem (NtWT) e transgênicas com expressão reduzida do transportador de sacarose *SUT1* nas GC (Nt*SUT1*), que possui menor capacidade de importar sacarose do apoplasto para o simplasto das GC. Foram realizadas análises multivariadas englobando dados de trocas gasosas e metabolômica bem como cinéticas de g_s sob diferentes concentrações de sacarose, glicose e frutose. Finalmente, foi determinada a dinâmica da abertura estomática e o nível interno de açúcares em fragmentos epidérmicos submetidos a 25 mM de sacarose na luz, juntamente com seu perfil metabólico. Os resultados do método de coleta do apoplasto demonstraram que MeOH aumentou o volume de recuperação do apoplasto, mas também elevou a contaminação com simplasto, principalmente em Arabidopsis. Ao utilizar MeOH como fluido de infiltração, recomendamos o cálculo de um fator de correção ao utilizar atividades enzimáticas como forma de atestar a pureza do apoplasto. Pela ausência de diferenças nas análises metabólicas entre ambos fluidos de infiltração, o uso de ddH_2O é o mais recomendado por ser de fácil acesso e não tóxico. Através do curso diário das análises em plantas NtWT e Nt*SUT1*, a abertura e fechamento estomáticos foram associados a baixas e altas concentrações de sacarose apoplástica, respectivamente. Além disso, pelo efeito da aplicação exógena de açúcares, a velocidade de abertura e fechamento se mostraram serem positivamente e negativamente correlacionadas com a concentração de sacarose em de folhas iluminadas, respectivamente. Adicionalmente, a resposta estomática

mediada por sacarose se mostrou bastante reduzida em fragmentos epidérmicos de plantas Nt*SUT1*. Tomados em conjunto, nossos resultados indicam que a sacarose é, de fato, um regulador mestre da g_s, sendo capaz de induzir a abertura e o fechamento estomáticos de maneira dependente de sua concentração e localização.

Palavras-chave: células-guarda; espaço apoplástico; técnica de infiltração-centrifugação; metabolômica; regulação estomática; regulação metabólica.

ABSTRACT

Recent evidence suggests that sucrose is a molecule capable of inducing stomatal closure at high concentrations, in which the accumulation of sucrose in the apoplast would induce stomatal closure in periods of high photosynthetic rate and, thus, optimizing the efficiency of use of water in plants (WUE). However, it is unclear how this process contributes to the daily regulation of WUE and its relationship with the role of sucrose within guard cells (GC) during stomatal closure. Within this perspective, this project will test the hypothesis that sucrose is a key molecule that integrates photosynthesis and stomatal movements and that its levels present in the leaf apoplast correlate positively during opening and negatively during stomatal closure with the stomatal conductance (g_s). First of all, an efficient method of leaf apoplast collection was established using methanol (MeOH) and water (ddH_2O) as infiltration fluids for metabolic analysis via gas chromatography coupled to mass spectrometry using tobacco and Arabidopsis leaves. Subsequently, experiments were carried out to determine the dynamics of stomatal movements along with the metabolic profile of leaves and apoplast throughout the day using wild-type (NtWT) and transgenic tobacco plants with reduced expression of the sucrose transporter SUT1 in GC (Nt*SUT1*), which has a lower capacity to import sucrose from the apoplast to the GC symplast. Multivariate analyzes were performed with gas exchange and metabolomics data as well as g_s kinetics under different concentrations of sucrose, glucose and fructose. Finally, was determined the dynamics of the stomatal opening and the internal level of sugars in epidermal fragments subjected to 25 mM sucrose under light, along with their metabolic profile. The results of the apoplast collection method demonstrated that the MeOH increased the apoplast volume recovery yield, but also increased symplast contamination, mainly in Arabidopsis. When using MeOH as infiltration fluid, we recommend the calculation of a correction factor by using enzymatic activities to attest the apoplast purity. Due to the absence of differences in metabolic analyzes between both infiltration fluids, the use of ddH_2O is the most recommended as it is easily accessible and non-toxic. Across the diel course of analyzes in NtWT and Nt*SUT1* plants, the stomatal opening and closure were associated with low and high apoplastic sucrose concentrations, respectively. Furthermore, due to the effect of exogenous application of sugars, the opening and closure rapidity were positively and negatively correlated with the sucrose concentration in illuminated leaves, respectively. Additionally, the sucrose-mediated stomatal response was significantly reduced in epidermal fragments of Nt*SUT1* plants. Taken together, our results indicate that sucrose is, in fact, a master

regulator of g_s, being capable of inducing stomatal opening and closure in a concentration and location dependent manner.

Keywords: guard cells; apoplastic space; infiltration-centrifugation technique; metabolomics; stomatal regulation; metabolic regulation.

CONTENTS

1. GENERAL INTRODUCTION

Stomata are structures composed by two guard cells (GC) located mainly in the leaf epidermis of almost all groups of terrestrial plants. In some cases, GCs may be associated with other cells in the epidermis, called subsidiary cells, such as those found in many monocots (Lima *et al.*, 2018). The structure of GCs is highly conserved, presenting kidney or bean shape in most plant groups, mainly in dicotyledons, and dumbbell shape in grasses and other monocotyledons (Chater *et al.*, 2017). These two cells together form the stomatal pore, which opening and closure are actively regulated through changes that lead to the movement of different osmolytes into or out of GC. The difference in the osmotic potential allows water to enter or leave the cell, determining the opening or closure of the pore, respectively (Medeiros *et al.*, 2015). Due to an uneven deposition of cellulose microfibrils on the cell wall, this kind of change in shape through water movement is possible in GC. In kidney-shaped cells, the cell wall is thicker on the side facing the pore and thinner on the opposite side, whereas in dumbbell-shaped cells, its cell wall is thicker along the pore and thinner at the ends (McCormick, 2017; Woolfenden *et al.*, 2017).

The GCs greatly differ from any other kind of plant cell. They are highly specialized, integrating endogenous and environmental signals related to the water conditions of the plant, hormonal stimuli, quantity and quality of light, carbon dioxide (CO_2) concentration, air humidity, among other conditions. This provide the perception of any necessary stimulus for the opening or closure of the stomatal pore (Lawson *et al.*, 2014; Matthews; Vialet-Chabrand; Lawson, 2017).

Stomata are responsible for the gas exchange between plants and atmosphere. Through them, plants import CO_2 for the photosynthesis and release transpired water (Hetherington; Woodward, 2003). Thus, they are considered the key regulators of water use efficacy (WUE), defined as the ratio between net photosynthesis (A) and stomatal conductance (g_s) or transpiration (E) at leaf level (Leakey *et al.*, 2019). Therefore, the stomatal movement regulation is primordial to the plant acclimation and survival. In addition, it exercise a direct impact on productivity and water consumption, which can be evaluated by WUE (Brodribb; Sussmilch; McAdam, 2019).

The control of the pore opening involves reversible changes in the concentration of several different osmolytes in GC, such as ions potassium (K^+) and counter ions malate ($malate^{-2}$), chloride (Cl^-) and nitrate (NO^{-3}) (Eisenach; De Angeli, 2017; Hedrich; Marten, 1993). The presence of light is one of the primary ways of inducing stomatal opening. The stomata must

open to allow CO_2 to enter the cell for photosynthesis to occur. The mechanism of induction of stomatal opening by light demands large amounts of ATP that initially involves the activation of phototropins by blue light in GC. The blue light induces phototropin autophosphorylation, which initiates a signal transduction pathway involving the 14-3-3 protein that activates the H^+-ATPase proton pump, justifying the high consumption of ATP. The flux of H^+ leaving the cell to the apoplast leads to the hyperpolarization of the membrane and activation of K^+ influx channels. This proton accumulates in the vacuole, which drives water to enter the GCs and leads the stomata to open (Inoue; Kinoshita, 2017).

For most species, the phytohormone abscisic acid (ABA) is the main inductor of stomatal closure (Roelfsema; Hedrich, 2005), except for some fern species, which are insensitive or show a very slow responses to ABA (Hõrak; Kollist; Merilo, 2017; Voss *et al.*, 2018). In angiosperms, ABA is recognized by the cell through receptors that trigger signals, such as the internal increase of pH and concentration of calcium (Ca^{2+}), inositol 1,4,5-triphosphate (IP_3) and pH. The interaction between ABA and its receptors induces the synthesis of IP_3, nitric oxide (NO) and reactive oxygen species that activate Ca^{2+} influx channels into the cytosol. The increase of internal Ca^{2+} and IP_3 promotes the release of more Ca^{2+} from the vacuole. Excess Ca^{2+} blocks K^+ influx channels and opens Cl^- efflux channels that depolarize the membrane, inducing the opening of K^+ efflux channels. The increase in Ca^{2+} inhibits the proton pump H^+-ATPase and thus the concentration of solutes in the cell's apoplast increases, leading to water loss and the stomata to close (Neill *et al.*, 2002; Pei *et al.*, 2000).

The apoplast is defined as the extracellular space between cells and the internal portion of cell walls (Parkhurst, 1982). The leaf apoplastic space is well known to contain several metabolites and other substances that modulate different physiological processes (Chikov; Bakirova, 2004; Steudle; Frensch, 1996). These compounds are derived from the vascular system and mesophyll cells, being used as a transportation route to distribute sugars and other metabolites, as well as nutrients and ions absorbed by the root system throughout the plant (Parkhurst, 1982; Rodríguez-Celma *et al.*, 2016). Furthermore, there are a variety of evidences suggesting that the apoplast plays an important role in the modulation of the gas exchange between leaves and the atmosphere, in which metabolites derived from mesophyll would operate as the regulators of the stomatal movements (Kang, YUN *et al.*, 2007; Lima *et al.*, 2018). Consequently, it is reasonable to assume that the identification and comprehension of the apoplast composition dynamics, such as sucrose, may expose key players for the photosynthesis-stomatal movements trade-off regulation.

Sucrose is the most abundant disaccharide found in plants and it is the main photoassimilate transported. It can be metabolized, converted into starch in plastids or stored in vacuoles. Its synthesis occurs in the cytosol of cells by two possible routes. The main pathway is carried out by two enzymes, sucrose phosphate synthase, which uses UDP-glucose and fructose-6-phosphate, releasing sucrose-6-phosphate, and sucrose-phosphate phosphatase, which dephosphorylates sucrose-6-phosphate, releasing sucrose. Another route of synthesis occurs by the sucrose synthase enzyme combining UDP-glucose and fructose to release sucrose (Yahia; Carrillo-López; Bello-Perez, 2019). The reaction catalyzed by sucrose synthase is reversible and also occurs in the direction of degradation. A second enzyme is also responsible for its degradation, the invertase. (Fettke; Fernie, 2015; Sturm; Tang, 1999). In leaves, during periods of light, sucrose synthesis is supported by the products of photosynthesis and its excess is transported via the phloem to sink tissues.

In the apoplast, a fraction of sucrose can reach the GC through the transpiration stream (Kang, Yun *et al.*, 2007; Kang, YUN *et al.*, 2007). Due the lack of plasmodesmata in these cells (Wille; Lucas; Zea, 1984), except of those found in some ferns (Voss *et al.*, 2018), the input of sucrose and hexoses from its degradation in the GC is mainly realized by the symplastic pathway via transporters in the plasma membrane (Daloso; dos Anjos; Fernie, 2016). In fact, genes from several transporters are highly expressed in GC of Arabidopsis thaliana, such as *SUCROSE TRANSPORTER 1 (SUT1), SUPPRESSOR OF G PROTEIN BETA 1 (SGB1), SUGAR TRANSPORTER 1 (STP1), SUGAR TRANSPORTER 4 (STP4), SUGAR TRANSPORT PROTEIN 13 (MSS1)* and many members of the exporter family *SUGARS WILL EVENTUALLY BE EXPORTED (SWEET)* (Bates *et al.*, 2012; Bauer *et al.*, 2013; Leonhardt *et al.*, 2004; Wang *et al.*, 2011). The *Arabidopsis thaliana SWEET11;12* double mutant was previously characterized as presenting approximately 3-fold higher sucrose content in leaves than in wild type plants, due to the lower capability to load this sugar in the phloem, as it is the main function of these transporters (Chen *et al.*, 2012). In addition, changes in *SUT1* genes, specifically in tobacco GC, lead to less accumulation of sucrose in GC's symplast (Antunes *et al.*, 2017). Photosynthetic activity is known to be an important source of sucrose for mesophyll cells. However, although most GC present functional chloroplasts, its number is lower compared to mesophyll cells, 3 to 5 times less, followed by low RubisCO activity in most species (Lawson, 2009; Outlaw; De Vlieghere-He, 2001; Vavasseur; Raghavendra, 2005). Together, this evidence suggests that most of the sucrose found and accumulated in GC comes from the

apoplast, which in turn is produced by mesophyll cells, characterizing stomata as structures more similar to sink than source tissues.

Several works indicate the importance of carbohydrate metabolism to the regulation of the stomatal movements (Kopka; Provart; Muller-Rober, 1997; Outlaw; De Vlieghere-He, 2001; Wang *et al.*, 2019). Initially, the role of sucrose in controlling stomatal movements was attributed to being purely osmotic, and that its accumulation in the GC symplast would be a way of maintaining stomatal opening during periods of light in which the K^+ concentration is low (Amodeo; Talbott; Zeiger, 1996; Talbott; Zeiger, 1996, 1998). However, there is another evidence demonstrating that the addition of high concentrations of sucrose in the light leads to stomatal closure (Kang, YUN *et al.*, 2007; Lu *et al.*, 1995; Medeiros *et al.*, 2018). Currently, several results support some non-osmotic hypotheses of the role of sucrose. For example, increased saccharolytic activity by the overexpression of invertase or sucrose synthase enzymes in GCs from potato or tobacco, respectively, led to greater stomatal conductance under light (Antunes *et al.*, 2012; Daloso *et al.*, 2016). In contrast, antisense silencing of the sucrose synthase gene in tobacco GC resulted in plants with lower g_s and stomatal opening speed (Freire *et al.*, 2021). Additionally, the monosaccharide transporters, *STP1* and *STP4*, were identified as the main importers of glucose into GC and important contributors to light-induced stomatal opening (Glucose uptake to guard cells via STP transporters provides carbon sources for stomatal opening and plant growthFlütsch *et al.*, 2020). These works demonstrate the energetic role of sucrose in GC, in which the products generated by sucrose degradation assist the process of stomatal opening induced by light (Lima *et al.*, 2019; Medeiros *et al.*, 2018; Ni, 2012; Robaina-Estévez *et al.*, 2017).

The signaling role that sucrose breakdown hexoses play in ABA-mediated stomatal closure has also been demonstrated. Overexpression of the hexokinase enzyme in GC from Arabidopsis, tomato, orange and tobacco led to lower g_s, higher closure speed and WUE (Kelly *et al.*, 2013, 2019; Lugassi *et al.*, 2015, 2019, 2020). The association with ABA was demonstrated by the use of tomato or Arabidopsis mutants deficient in ABA or its receptors (PYR/RCAR), respectively, whose stomata do not respond to changes in sugar levels (Kelly *et al.*, 2013; Li *et al.*, 2018). These authors hypothesized that hexokinase acts as a sensor of sugar levels in GC, inducing stomatal closure in response to elevated concentrations of sugars mediated by abscisic acid (ABA), which leads to an increase in the internal production of nitric oxide and hydrogen peroxide (Granot; Kelly, 2019).

According to the hypotheses described above, i.e., energetic function of sucrose during opening and signaling function of its hydrolysis products (glucose and fructose) during stomatal closure, sucrose can enter and be hydrolyzed inside the GC or be hydrolyzed in the apoplast by invertase and enter the GC in the form of glucose and fructose. Most likely, both situations occur and complement each other in the control of stomatal movements. Despite the apparent conflict between these hypotheses, both suggest that sucrose originated from mesophyll cells coordinates the processes of photosynthesis and stomatal movements. For example, in a condition of high photosynthetic rate, the sucrose level is negatively correlated with g_s (Gago *et al.*, 2016; Lima *et al.*, 2019), probably as a way to reduce water loss through transpiration under favorable conditions for photosynthesis. Furthermore, there are evidence demonstrating the dual role of hexokinase in stomatal movements. Overexpression of hexokinase in orange GC resulted in greater and lesser g_s at low and high light intensity, respectively (Lugassi *et al.*, 2015), suggesting that hexokinase may mediate the control of g_s depending on the concentration of sucrose and hexoses available in GC.

However, the exact concentration of sucrose in the apoplast that would act on stomatal opening and closure for different species is not known. To date, few studies have tested the effects that the external addition of sucrose has on stomatal movements. Furthermore, some studies used extremely high concentrations of sucrose, which makes it difficult to understand how sucrose regulates stomatal movements. Also, since the major sugar source for GC comes from the apoplastic space through the transpiration stream (Kang et al., 2007a; Kang et al., 2007b), it is reasonable to assume that the sucrose levels found in the apoplast would determine the stomatal behavior. Therefore, the sugar levels in the apoplast alone must be evaluated together with the stomatal movements. However, each apoplast collection method needs to be specific adapted depending on the species, sample size and main objective of interest.

There are several methods to collect the apoplast from leaves, yet not all are suitable for different species and the availability of limited amounts of leaf material (Chincinska, 2021; Lohaus *et al.*, 2001). The main limitations of these methods are the contamination with symplastic fluids, the need for substantial amount of leaf material and the low yield of collected apoplast and compounds found. It is thus important to use an appropriate washing solution to improve the extraction and the solubility of metabolites present in the apoplast without compromising the cellular structure, which leads to a decreased symplastic contamination. However, collecting the apoplast totally free of any contamination is extremely difficult (Figueiredo *et al.*, 2021; O'Leary *et al.*, 2014; Rodríguez-Celma *et al.*, 2016). The best possible

solution is to choose an acceptable threshold of symplastic contamination, which is quantified by different markers such as the level of phosphorylated hexoses, malate dehydrogenase (MDH) activity and ion leakage.

Given the need of an appropriate protocol to collect the apoplast from small scale samples suitable for metabolomic analysis and due the scarcity of results found in the literature and the complexity of GC metabolism, the role of apoplastic sucrose in controlling stomatal movements needs to be better studied. Therefore, here we aimed to established an improved and efficient method for collecting the leaf apoplast for metabolic analysis and to reveal which correlation exists between sucrose concentrations in the apoplast and stomatal movements in *Nicotiana tabacum*.

2. HYPOTHESIS

Chapter I - Methanol as infiltration fluid enhances the apoplast recovery yield and increases the solubility of metabolites for identification from tobacco and Arabidopsis leaves.

Chapter II - Sucrose levels present in the leaf apoplast correlate positively during opening and negatively during closure with the stomatal conductance rate of tobacco leaves.

3. OBJECTIVES

3.1 General objective

Chapter I - To adapt and evaluate an apoplast collection method for tobacco and Arabidopsis leaves metabolomics analysis.

Chapter II - To elucidate the role of sucrose in controlling stomatal movements in tobacco plants.

3.2 Specific objective

Chapter I

1. To adapt the apoplast collection method for small samples.
2. To evaluate the efficiency of the apoplast collection method for tobacco and Arabidopsis leaves.
3. To evaluate the purity of the collected apoplast.

Chapter II

1. To analyze the gas exchange, stomatal opening and the metabolic profile of leaves and leaf apoplast throughout the diel course.
2. To determine the relationship between sugar concentrations from leaves and leaf apoplast and stomatal movements throughout the diel course.
3. To evaluate the effects that the exogenous application of different concentrations of sugars have on the kinetics of stomatal movements.
4. To determine the relationship between internal sugar content and stomatal aperture in tobacco guard cells under exogenous application of sucrose.

4. CHAPTER I - Toward the apoplast metabolome: establishing a leaf apoplast collection approach suitable for metabolomics analysis

(Submitted manuscript)

Toward the apoplast metabolome: establishing a leaf apoplast collection approach suitable for metabolomics analysis

Francisco Bruno S. Freire[1], Eva G. Morais[1], Danilo M. Daloso[1*]

[1]LabPlant, Department of Biochemistry and Molecular Biology, Federal University of Ceará. Fortaleza-CE, 60451-970, Brazil.

*Author for correspondence
Tel: +55 85 33669821
Email address: daloso@ufc.br

Abstract

The leaf apoplast contains several compounds that play important roles in the regulation of different physiological processes in plants. However, this compartment has been neglected in several experimental and modelling studies, which is mostly associated to the difficulty to collect apoplast washing fluid (AWF) in sufficient amount for metabolomics analysis and as free as possible from symplastic contamination. Here, we established an approach based in an infiltration-centrifugation technique that use little leaf material but allows sufficient AWF collection for gas chromatography mass spectrometry (GC-MS)-based metabolomics analysis. Up to 54 metabolites were annotated in leaf and apoplast samples from both tobacco and Arabidopsis using either 20% (v/v) methanol (MeOH) or distilled deionized water (ddH_2O) as infiltration fluids. The use of MeOH increased the yield of the AWF collected but also the level of symplastic contamination, especially in Arabidopsis. We propose a correction factor and recommend the use of multiple markers to verify the level of symplastic contamination in MeOH-based protocols. Neither the concentration of sugars nor the level of primary metabolites diverges between apoplast samples extracted with ddH_2O or MeOH. Therefore, the approach described here can be carried out using little leaf material and ddH_2O, a non-toxic and highly accessible infiltration fluid.

Keywords: Apoplastic space, GC-MS, infiltration-centrifugation technique, metabolomics, metabolite profiling, *Nicotiana tabacum*, *Arabidopsis thaliana*.

Introduction

The apoplast is characterized as the extracellular space found among the cells and within the cell walls (Parkhurst, 1982). The leaf apoplastic space is known to contain a variety of metabolites and other substances derived from the vascular system and mesophyll cells that can modulate different physiological processes (Chikov; Bakirova, 2004; Steudle; Frensch, 1996). For instance, the apoplastic transpiration stream is a route to distribute sugars and other metabolites from mesophyll cells as well as nutrients and ions absorbed in the roots throughout the plant (Outlaw; De Vlieghere-He, 2001; Rodríguez-Celma *et al.*, 2016; Sattelmacher, 2001). This route is also associated to the transport of regulatory RNAs, as a mechanism to regulate gene expression *in planta* (Kehr; Morris; Kragler, 2022). Furthermore, several lines of evidence suggest that the apoplast is key to influence the gas exchange between leaves and the surrounding environment, in which mesophyll-derived metabolites would act as stomatal movements regulators (Kang, YUN *et al.*, 2007; Lima *et al.*, 2018). Therefore, understanding the composition and the dynamic of the compounds present in the apoplast may aid to unveil key players in the photosynthesis-stomatal movements trade-off regulation and several other physiological processes. As consequence, this not only can open several biotechnological possibilities to obtain plants with improved water use efficiency, but also offers the possibility to connect different source and sink tissue models as well as to improve our understanding on how different plant organs/tissues are connected.

There are several methods to obtain the apoplast washing fluid (AWF) from leaves, yet not all are suitable for different species and some of them require large amounts of leaf material, are too laborious, lead to substantial contamination with symplastic fluid and/or result in low yield of compounds (Chincinska, 2021; Lohaus *et al.*, 2001). This hampers the use of the AWF for omics analysis and aids to explain why our understanding concerning the metabolic aspects of the apoplast space is very limited and why several integrative metabolic models do not include biochemical information from this space (Figueiredo *et al.*, 2021; Floerl *et al.*, 2012; Rohwer, 2012; Zakhartsev *et al.*, 2016). It is thus important to establish new methods or to improve the current ones used to collect the AWF. For this, it is crucial to consider an infiltration fluid that improve the extraction and the solubility of metabolites present at the apoplast without compromising the cellular structure, leading to a lower symplastic contamination. However, collecting the AWF totally free of any contamination is nearly impossible (Figueiredo *et al.*, 2021; O'Leary *et al.*, 2014; Rodríguez-Celma *et al.*, 2016). Alternatively, plant scientists have been delimiting an acceptable threshold of symplastic contamination in AWF samples, which

is quantified by different markers such as the level of phosphorylated hexoses, malate dehydrogenase (MDH) activity and ion leakage, among others (Gentzel *et al.*, 2019; Lohaus *et al.*, 2001; O'Leary *et al.*, 2014).

The common methods to collect the apoplast are: the vacuum perfusion method (Bernstein, 1971), the forced pressure method (Hartung; Radin; Hendrix, 1988), the elution method (Long; Widders, 1990), the filter strip method (Dragišic Maksimovic *et al.*, 2014) and the infiltration and/or centrifugation method (Klement 1965). The principle of the vacuum perfusion method uses vacuum to aspirate the apoplast from the plant tissue, but this method requires a specific apparatus connected to a pump to work (Bernstein, 1971). The forced pressure method uses a Scholander bomb to force the apoplast out by placing the leaf in a high-pressure chamber. This method collects very small apoplast amounts (~10 µL) and it is difficult to assure the complete recovery of the apoplast without damaging the tissue (Hartung; Radin; Hendrix, 1988). The elution method is based on the elution of the apoplast by removing the epidermis and adding a solution to wash the apoplast from the tissue, which has a great risk of damaging the tissue and dilutes the AWF (Long; Widders, 1990). The filter strip method uses a filter paper placed in the surface of the tissue to collect the apoplast by capillary forces. It takes up to 30 min to collect sufficient material and requires a further step to extract the apoplast from the filter paper (Dragišic Maksimovic *et al.*, 2014). The infiltration and/or centrifugation method is one of the most used and it has several variations depending on the species, the tissue and the analysis that will be carried out. This method can be performed using either infiltration or centrifugation or both, named the infiltration-centrifugation technique (Chincinska, 2021; Joosten, 2012; Kingsbury; McDonald, 2014; Madsen; Nour-Eldin; Halkier, 2016).

Recent studies have adapted the infiltration-centrifugation technique to collect AWF using small amounts of *Zea mays* and *Arabidopsis thaliana* leaves (Ekanayake; Gohmann; Mackey, 2022; Gentzel *et al.*, 2019). The method established using excised maize and Arabidopsis leaves and methanol as infiltration fluid has great potential to be extended to other plant species as well as to perform metabolomics analysis, which could improve our understanding on the biochemistry of the apoplastic space. However, due to the great morpho-anatomical variability in angiosperm leaves, which can hamper the use of this method in other plant species, it remains unclear whether the AWF collected from this method is suitable for other plant species and to perform metabolomics analysis. Here, we have fulfilled these gaps and provided an infiltration-centrifugation-based approach that allows sufficient AWF

collection from small leaf material and using either methanol or distilled deionized water as infiltration fluids.

Materials and Methods

Plant material and growth conditions

The model plants *Nicotiana tabacum* cv Havana 425 and *Arabidopsis thaliana* ecotype Columbia, both wild type (WT), were used in this study. Tobacco plants were cultivated in 5 L pots with substrate composed by a mixture of vermiculite, sand and soil (1:1:1) and kept well-watered under greenhouse conditions with natural 12 h photoperiod (maximum of 800 µmol photons m^{-2} s^{-1}, 30 ± 4 ºC and relative humidity 70 ± 10%). Arabidopsis plants were cultivated in 0.1 L pots with substrate composed by a mixture of vermiculite, sand and vegetal compound (1:1:1) under well-watered and growth chamber conditions with 8 h photoperiod (maximum of 100 µmol photons m^{-2} s^{-1}, 25 ± 1 ºC and relative humidity 60 ± 10%). Tobacco and Arabidopsis plants were irrigated with Hoagland and Arnon nutritive solution (Hoagland; Arnon, 1950) two times per week and cultivated during 45 and 60 days, respectively, until apoplast and leaf collection.

Leaf and apoplast collection

The apoplast collection was performed using an adapted protocol for small quantities (Gentzel *et al.*, 2019; O'Leary *et al.*, 2014). Leaves from tobacco and Arabidopsis plants were excised, washed in distilled deionized water (ddH_2O) and vacuum-infiltrated with cold (4 ºC) 20% (v/v) methanol (20% MeOH) or ddH_2O using a 20 mL syringe. For tobacco plants, only the very tip of the leaves was used and for Arabidopsis plants three to five leaves were used without petiole (Fig. S1). The infiltrated leaves were gently dried, wrapped by parafilm around a 200 µL cut pipette tip and inserted in a 1.5 mL microcentrifuge tube with the leaf tips down. The assembled tubes were kept in ice until centrifugation at 1,000 *g* per 10 min at 4 ºC. The leaves were removed from the tubes and only the AWF was centrifugated again at 11,000 *g* per 10 min at 4 ºC for removal of any solids. The AWF was transferred to a new 1.5 mL tube, which was immediately frozen in liquid nitrogen, as well as intact fresh leaves, and stored at -80 ºC until further use for metabolite profiling analysis, protein quantification and malate dehydrogenase (MDH) activity. The weight of the leaves used for AWF extraction was measured before the start of the extraction (which represents the fresh leaf weight) and after the infiltration and the spin in the centrifuge steps.

Determination of sample conductivity

Leaves from each step of apoplast collection and AWF were subjected to conductivity measurements in order to access cell damaged through ion leakage (Gentzel *et al.*, 2019; O'Leary *et al.*, 2016). Leaves and the AWF were incubated in 35 mL of ddH_2O for 1 h with 100 rpm of agitation in 50 mL falcon tubes. The conductivity of the liquid obtained after the incubation period was measured using a conductivity meter TEC-4MP (Tecnal®). The control (blank) for AWFs collected using ddH_2O and 20% MeOH was pure ddH_2O and a solution of 20% MeOH diluted in 35 mL of ddH_2O, respectively. The conductivity was also measured in a solution of 35 mL of 20% MeOH. The values of AWF samples were normalized by the leaf fresh weight (Eq. 1).

$$Conductivity\ (\mu S/cm/mg) = \frac{Leaf\ conductivity\ - blank}{Leaf\ fresh\ weight} \qquad \text{(Eq. 1)}$$

For the normalization of AWF conductivity, it was used the conductivity of the respective leaf in which the AWF was collected. The relative conductivity (%) was calculated using the maximum conductivity of each leaf after boiled in water bath at 95 °C for 1 h (Eq. 2).

$$\%\ conductivity = \frac{Leaf\ conductivity\ - blank}{Bolied\ leaf\ conductivity\ - blank} \times 100 \qquad \text{(Eq. 2)}$$

Metabolomics analysis

Intact leaves and AWF collected previously were used for metabolite profiling analysis. Metabolite extractions were performed using ~60 mg of leaves and ~150 µL of AWF, both frozen in liquid nitrogen. The grinded powder of leaves and AWF were shaken for 15 min at 350 rpm and incubated at 70 °C with pure methanol containing 0.2 mg mL^{-1} of ribitol as internal quantitative standard followed by 10 min of centrifugation at 11,000 *g*. After, chloroform plus water was added to the supernatant collected. After 15 min of centrifugation at 11,000 *g*, 200-400 µL of the polar phase was collected and dried in a vacuum concentrator. The derivatization and the subsequently analysis in gas chromatography coupled to mass spectrometry (GC-MS, QP-PLUS 2010, Shimadzu, Japan) was carried out using a well-established platform (Lisec *et al.*, 2006). The mass spectral analysis and identification were performed using the software Xcalibur® 2.1 (Thermo Fisher Scientific, Waltham, MA, USA) and by the Golm Metabolome Database (http://gmd.mpimp-golm.mpg.de/), as described earlier (Kopka *et al.*, 2005; Medeiros *et al.*, 2018). The absolute quantification of sugars was performed using linear calibration

curves of authentic standards of fructose, glucose and sucrose (i.e., >99% purity; e.g., Sigma-Aldrich) ran in the GC-MS, as previously described in literature (Jayasinghe et al., 2018; Rosado-Souza et al., 2019).

Determination of protein content and MDH activity

Intact fresh leaves and AWF collected previously were used for protein quantification and MDH activity to determine the level of symplastic contamination (O'Leary *et al.*, 2016). Around ~60 mg of fresh leaves were powdered using liquid nitrogen and extracted by adding 600 µL of 20% MeOH or ddH_2O or protein extraction buffer (200 mM HEPES/NaOH pH 8.0, 10 mM $MgCl_2$, 2 mM aminocaproic, 2 mM benzamidine, 1 mM EDTA, 1mM DTT, 0.5 mM PMSF, 10% (v/v) glycerol and 2% (w/v) polyvinylpyrrolidone) in 1.5 mL microcentrifuge tubes (Gregory *et al.*, 2009; Shi *et al.*, 2015). The tubes were centrifuged at 14,000 *g* per 15 min at 4 ºC and the supernatant transferred to a new 1.5 ml tube for analysis.

It is known that methanol inhibits enzyme activity and precipitate proteins (Chen *et al.*, 2000; Gupta, 1992; Smith; Canady, 1992; Yu *et al.*, 2016). We then established a methanol correction factor (MCF) to determine how much the concentration of proteins and the activity of MDH are reduced by the use of this solvent. For this, the leaves were macerated using mortar and pestle with liquid nitrogen until a fine powder was obtained. Approximately 60 mg of leaf fresh weight was used to extract leaf proteins using 600 µl of ddH_2O. After centrifugation 14,000 *g* per 15 min at 4 ºC, 300 µl was transferred to two different tubes, in which 75 µl of ddH_2O or 100% MeOH (final concentration 20% MeOH) was added to them. The MDH activity and the concentration of proteins were then measured in these two extracts (Fig. S2). The MCF was calculated for both parameters in each replicate (n = 5) (Eq. 3).

$$MCF = \frac{Leaf\ ddH_2O\ MDH\ activity\ or\ protein}{Leaf\ ddH_2O\ plus\ MeOH\ MDH\ activity\ or\ protein} \qquad \text{(Eq. 3)}$$

Protein was quantified in both AWF and leaf extracts as described earlier (Ernst; Zor, 2010). Each sample was read in triplicate at A_{590} and A_{450} using an Epoch microplate reader (BioTek®) in 300 µL well microplate. Bovine serum albumin (BSA) was used as protein standard. The protein concentration, after applying the MCF for 20% MeOH samples, was transformed as total protein content expressed as protein by fresh weight (FW) (Eq. 4) and used for the calculation of total protein content percentage in AWF (Eq. 5).

$$Total\ protein\ content = \frac{Protein\ concentration\ (g/mL) \times Extracted\ volume}{Leaf\ fresh\ weight} \qquad \text{(Eq. 4)}$$

$$\%\ total\ protein\ content = \frac{Apoplast\ protein\ content}{Average\ leaf\ protein\ content} \times 100 \quad \text{(Eq. 5)}$$

MDH activity was carried out as described previously (O'Leary *et al.*, 2014, 2016). The activity was calculated following the NADH oxidation at A_{340} using its molar absorption coefficient (ε = 6.22 mM^{-1} cm^{-1}) (Eq. 6). Each sample was read in triplicate using an Epoch microplate reader (BioTek®) in 0.2 mL well microplate with reaction buffer (100 mM HEPES/NaOH pH 7.0, 10% (v/v) glycerol, 0.15 mM NADH and 2 mM oxaloacetate (start)) and 1-40 µL of leaf extract or AWF. The MDH activity, after applying the MCF for 20% MeOH samples, was transformed to Final MDH activity expressed as U by FW (Eq. 7) and used for the calculation of final MDH activity percentage in the AWF (Eq. 8).

$$MDH\ activity\ (U/mL) = \frac{(\Delta abs_{340}\ per\ min) \times 0.2}{6.22 \times Leaf\ extract\ or\ AWF\ volume\ added} \quad \text{(Eq. 6)}$$

$$Final\ MDH\ activity = \frac{MDH\ activity\ (U/mL) \times Extracted\ volume}{Leaf\ fresh\ weight} \quad \text{(Eq. 7)}$$

$$\%\ final\ MDH\ activity = \frac{Apoplast\ final\ MDH\ activity}{Average\ final\ leaf\ MDH\ activity} \times 100 \quad \text{(Eq. 8)}$$

Statistical analysis

All data are expressed as the mean of five replicates and standard error (SE). For apoplast samples, each replicate represents the AWF collected from one and twelve leaves for tobacco and Arabidopsis, respectively. The statistical differences between all treatments and conditions were assessed by using one-way ANOVA and the Tukey test at 5% of probability ($P < 0.05$), while apoplast extractions and correction factor using 20% MeOH were compared to those extracted using only ddH_2O by using Student's *t*-test ($P < 0.05$). All statistical and regression analyses were carried out using SigmaPlot 14 (Systat Software Inc., San Jose, CA, USA), Microsoft Excel (Microsoft, Redmond, WA, USA) or Minitab 17 statistical software (Minitab Inc., State College, PA, USA). The metabolomics data were mean-centered normalized and analyzed using the MetaboAnalyst platform (Chong *et al.*, 2018).

Results

Establishing a method to collect the leaf apoplast fluid

The leaf apoplast fluid was obtained by using an infiltration-centrifugation technique and cold distilled deionized water (ddH_2O) or 20% (v/v) methanol (20% MeOH) as infiltration fluids (Fig. 1). The method consists of the input of infiltration fluids onto the leaf via a simple procedure, in which a syringe is used to slowly apply pressure in a small amount of leaf tissues (Fig. 1), as previously described (Chincinska, 2021; DURAN-CARRIL; BUJAN, 1998; Matsuo; Fukuzawa; Matsumura, 2016). The tip of a fully expanded tobacco leaf and twelve Arabidopsis leaves were sufficient to collect a substantial amount of the AWF using either ddH_2O or 20% MeOH (Fig. S1A-D). Before the centrifugation, the infiltrated samples were wrapped by parafilm around a 200 µL cut pipette tip and inserted into a 1.5 mL microcentrifuge tube (Fig. S1E-G). These tubes were maintained on ice until the centrifugation step, as previously recommended (Gentzel *et al.*, 2019). The AWF is collected by centrifuging the prepared tubes, removing the leaves, centrifuging again to remove any solids and carefully transferred to a fresh tube (Fig. S1H). The use of microtubes to place the infiltrated samples and to collect the AWF allows the use of a refrigerated microcentrifuge at low temperature (4 ºC) and centrifugation force (1,000 *g*), an equipment available in most plant laboratories, as well as increases the number of replicates that can be carried out simultaneously and speed up the AWF collection (Fig. 1). To access the collection efficiency of the method, we calculated the AWF recovery of each sample. The yield of the apoplast volume collected linearly increases with the leaf fresh weight of either Arabidopsis or tobacco leaves (Figs. S3A-D). However, the yield of apoplast collected (µL of apoplast collected g^{-1} FW) increased ~20% in the extractions using 20% MeOH, when compared to ddH_2O in both species (Fig. S4).

Determining the level of symplastic contamination in the apoplast washing fluid

The level of symplastic contamination in the AWF collected was investigated through the level of phosphorylated hexoses, MDH enzymes activity, total protein content and ion leakage. The phosphorylated hexoses were neither detected in leaves nor in apoplast samples by GC-MS (described in the next section). The conductivity of leaves was measured in the solutions used for AWF collection (i.e. ddH_2O and 20% MeOH), in solutions derived from each extraction step and in the final AWF collected (Fig. 1). As expected, the conductivity was higher in 20% MeOH than ddH_2O solutions. However, the conductivity did not differ between the ddH_2O solution and the leaf infiltrate volume made with 20% MeOH (Fig. S5). Tobacco leaves and their AWF have 3.8 to 4.9-fold higher conductivity in 20% MeOH than ddH_2O, respectively (Fig. 2A; Table S1). The conductivity percentage was ~4% and 19% for ddH_2O and 20%

MeOH, respectively (Fig. 2B). Although Arabidopsis exhibits the same trend, i.e. 1.7 to 2.1-fold higher conductivity in 20% MeOH than ddH_2O, it was not statistically significant for most steps, including the AWF conductivity (Fig. 2C; Table S1). In average, the conductivity percentage was ~2.5% and 5% for ddH_2O and 20% MeOH, respectively (Figs. 2D).

The use of 20% MeOH negatively affected all measurements in both species, but the MCF obtained varied between MDH activity and protein content and was species-dependent (Figs. 2E-H). The values of both MDH activity (U g^{-1} FW) and the total protein content (mg protein g^{-1} FW) were lower in leaf extracts using 20% MeOH than those obtained using a proper protein extraction buffer, even after applying the MCF (Figs. 3A-D). There was no difference in either total protein content or MDH activity between 20% MeOH and ddH_2O leaf extracts in both species. These parameters were higher in leaf than AWFs, except the total protein content from leaf extracts using 20% MeOH in tobacco that was not statistically different from AWF extracted with either 20% MeOH or ddH_2O (Figs. 3A-D). The percentage of MDH activity and protein content in the apoplast (related to the values observed in leaves) were higher in 20% MeOH than ddH_2O (Figs. 3E-H; Table S2). Although the MDH activity in tobacco AWF was only 0.08% in 20% MeOH, this value was 13% in Arabidopsis. Comparing 20% MeOH with ddH_2O alone, the percentage of conductivity and MDH activity are approximately 2 and 4-fold higher in 20% MeOH for Arabidopsis and tobacco, respectively (Tables S1,3). These results demonstrate that the use of 20% MeOH increase the symplastic contamination of the AWF in both species, but such effect has a greater extent in Arabidopsis.

The feasibility of the AWF collected for metabolomics analysis

The small amount of AWF collected was sufficient to carried out a good GC-MS-based metabolite profiling analysis. This is evidenced by the quantity of peaks presented in the chromatograms (Fig. 4) and the number of metabolites that could be detected and identified in apoplast samples (Table 1), as compared to leaves. Up to 54 metabolites were identified in AWF samples, pertaining to the groups of amino acids, sugars, sugar alcohols and organic acids, as typically observed in GC-MS-based studies (Medeiros *et al.*, 2019). Certain metabolites were found exclusively in tobacco, such as quinic acid and *trans*-caffeoyl quinic acid, while raffinose, trehalose, allo-inositol and asparagine were only detected in Arabidopsis samples (Table 1). Lyxose was detected only in apoplast samples using both infiltration fluids and trehalose was identified only in leaf samples. Fructose-6-phosphate and glucose-6-phosphate are good markers used to detect the level of symplastic contamination in AWF (Garchery *et al.*,

2013; Malinova *et al.*, 2020; O'Leary *et al.*, 2014). However, although we detected these metabolites in GC-MS using purified compounds, they were not detected in leaves and AWF samples from both species (Table 1). These analyses highlight that our protocol is suitable for metabolomics analysis, opening new avenues to investigate the metabolic dynamic of the apoplast space.

Leaf and apoplastic primary metabolism diverge substantially

Principal component analysis (PCA) indicates that the primary metabolism of leaves and the AWF diverge substantially, as evidenced by the separation between these samples by the PC1 in both species (Fig. 5A-B). Interestingly, the apoplast samples collected using 20% MeOH or ddH_2O were clustered together in both species. This idea is strengthened by hierarchical cluster analysis, in which both infiltration fluids belong to a separate cluster from leaf samples, and by the fact that the level of the metabolites identified is very similar between 20% MeOH and ddH_2O in both species (Figs. 6-7). Similarly, the content (ng mg^{-1} FW) of glucose, fructose and sucrose did not differ between 20% MeOH and ddH_2O and was higher in leaves than both AWF in both species (Fig. 8A-B). These analyses indicate that the metabolism of leaves and the apoplast is substantially different, in which the level of several primary metabolites is higher in leaves than in the AWF. Our results further highlight that the use of 20% MeOH did not alter the apoplast metabolite profile and, most importantly, that ddH_2O can be used as infiltration fluid for GC-MS-based metabolomics analysis.

Discussion

Establishing an approach suitable for apoplast metabolomics analysis

Plants are biological systems separated in different modules (e.g. organs) that present autonomous responses to changes in the surrounding environment but are interconnected via the transport of metabolites and other compounds through the vascular system and the transpiration stream at the apoplast space (Chikov; Bakirova, 2004; Cramer *et al.*, 2011; Farvardin *et al.*, 2020). However, the apoplastic route is frequently neglected as a source of compounds that integrate the different plant modules. The restricted information from the metabolic dynamic of the apoplast space is mostly associated to the difficulty to obtain sufficient AWF for metabolomics analysis in different species and with good purity (Lohaus *et al.*, 2001). Here, we provide an infiltration-centrifugation-based approach suitable for

collecting the apoplast fluid using small quantity of tobacco and Arabidopsis leaves and to perform GC-MS-based metabolomic analysis.

We could detect several metabolites in the AWF from both infiltration fluids and species (Table 1). Metabolites pertaining to the groups of amino acids, sugars, sugar alcohols and organic acids were annotated in all AWF samples. The relative content of primary metabolites was similar among the biological replicates of the AWF samples in both species (Figs. 6-7), highlighting that the method has a high reproducibility. These results further highlight that the use of 20% MeOH did not improve the metabolite profiling analysis. This is evidenced by the similarity in the mass spectra (Fig. 4), in the number of metabolites identified (Table 1) and in the level of them (Figs. 6-7), when compared to apoplast samples extracted with ddH_2O. Furthermore, the feasibility of the use of ddH_2O is undoubtedly confirmed by the no separation in the PCA (Fig. 5) and by the lack of differences in glucose, fructose and sucrose concentrations between ddH_2O and 20% MeOH AWF samples from both species (Figs. 8A-B). Therefore, the approach described here is highly efficient using ddH_2O, a safe and highly accessible infiltration fluid present in most plant biology laboratories. Further studies may unveil whether this approach is also suitable for other metabolomic platforms, such as those based in liquid chromatography coupled to MS (LC-MS) and nuclear magnetic resonance (NMR).

On the level of purity of the leaf apoplast collected

The level of symplastic contamination of the AWF was investigated here by measuring MDH activity, total protein content, the level of hexose phosphates and the ion leakage via conductivity measurements. This last analysis has been used as apoplast purity parameter in several previous works (Azevedo *et al.*, 2008; Ekanayake; Gohmann; Mackey, 2022; Gentzel *et al.*, 2019; Marentes *et al.*, 1993; O'Leary *et al.*, 2016). However, increased electrolyte leakage may be associated to changes in other variables such as ion efflux and relative water content of the tissue rather than an increase in membrane permeability (Almeida; Huber, 2010). In this context, our results highlight that, multiple markers of symplastic contamination should be used to better determine the level of AWF purity, which also ranges according to the species investigated. For instance, the use of 20% MeOH increased 19% in the conductivity, while the MDH activity and protein content increased approximately ~1% in tobacco (Figs. 2B, 3E-F). In Arabidopsis, the 20% MeOH-mediated increase in conductivity was below 5%, in agreement with a previous study (Ekanayake; Gohmann; Mackey, 2022). However, the use of 20% MeOH

increased substantially (up to 13%) both protein content and MDH activity in this species (Figs. 2D, 3G-H). These results indicate that the use of single markers can under or overestimate the level of symplastic contamination, depending on the marker used and the species under investigation.

Beyond ion leakage, the activities of hexose-phosphate isomerases and glucose-6-phosphate dehydrogenase as well as the level of hexose phosphates have been used as symplastic markers in several apoplast collection methods (Gupta *et al.*, 2021; Jaswanthi *et al.*, 2019; Martínez-González *et al.*, 2018; Montano *et al.*, 2020). Here, although both fructose-6-phosphate and glucose-6-phosphate could be detected using reference compounds, demonstrating that the GC-MS protocol used here is suitable for the analysis of these compounds (Roessner-Tunali *et al.*, 2004), they were not detected in apoplast or leaf samples. This can be associated to their low concentration in plant tissues and/or to their high instability when in a complex mixture (Koley *et al.*, 2022; Liu *et al.*, 2021). The use of hexose phosphates as symplastic contamination markers may need another metabolomics platform rather than GC-MS, in which several LC-MS-based protocols may be used (Jorge; António, 2018). Our results further highlight that the use of 20% MeOH as infiltration fluid can increase cell damage, as revealed by the higher conductivity in tobacco (Fig. 2A-B) and the higher MDH activity and protein content in Arabidopsis (Fig. 3G-H). This is likely associated to the fact that methanol can interact with membrane lipids increasing its fluidity (Dyrda *et al.*, 2019; Joo *et al.*, 2012).

Recommendations to use methanol as infiltration fluid to collect leaf apoplast

The method can be further used with methanol as infiltration fluid, but it requires some adjustments and caution to interpret the level of purity of the AWF collected. Methanol is largely used in metabolite extraction protocols for GC-MS and liquid chromatography coupled to MS analysis (Lisec *et al.*, 2006; Perez de Souza *et al.*, 2021). Thus, the effectiveness of metabolite extraction by this solvent is not questionable. However, it is well known that methanol inhibits enzyme activity by changing the proteins conformation, which decrease solubility and, consequently, increase their precipitation (Chen *et al.*, 2000; Yu *et al.*, 2016). It is thus reasonable to assume that the presence of methanol in the AWF may overestimate apoplast purity when this is determined by MDH activity and/or total protein concentration, given that centrifugation is one of the steps of this method and may therefore precipitate proteins. Indeed, both MDH activity and protein concentration were lower in leaf samples extracted with ddH_2O plus 20% MeOH, as compared to pure ddH_2O (Figs. 2E-H). This

highlights that the use of methanol as infiltration fluid requires a correction factor to certify the real level of purity of the AWF collected. We propose a straightforward procedure to obtain a MCF that can be used via analysis of protein concentration and MDH activity using leaf proteins extracted with ddH_2O followed by the addition of ddH_2O (control) or MeOH (Fig. S2). The difference between protein concentration and MDH activity measured in the extracts with and without MeOH is used to calculate the MCF of each replicate and parameter. This is important given that the values of these parameters are presumably underestimated by the presence of the MeOH. Thus, the MCF allows a fair comparison with other solvents used for AWF collection and better represent the level of contamination of the AWF with symplast fluids.

Concluding remarks

Our results collectively highlight that the use of 20% MeOH as infiltration fluid increase the yield but also the level of symplastic contamination of the AWF collected, which can be partially corrected by the use of the methanol correction factor proposed here. We further showed that the level of symplastic contamination depends on the species, highlighting that the level of the symplastic contamination of the AWF collected may be carefully evaluated before the use to other plant species. In this context, we recommend verifying the purity of the AWF collected by multiple markers, such as MDH activity, protein content and conductivity measurements. Both infiltration fluids used here are suitable for GC-MS-based metabolomics analysis. However, given that 20% MeOH did not improve the apoplast metabolomics analysis, the use of ddH_2O is preferable, as it is a non-toxic and highly accessible infiltration fluid.

Acknowledgments

This work was partially supported by the National Institute of Science and Technology in Plant Physiology under Stress Conditions (INCT Plant Stress Physiology – Grant: 406455/2022–8) and the National Council for Scientific and Technological Development (CNPq, Grant No. 404817/2021–1). The authors gratefully acknowledge the CNPq for the PhD fellowship to F.B.S.F. (CNPq, Grant 141043/2020-2) and the research fellowship to D.M.D. We also thank the scholarship granted by the Brazilian Federal Agency for Support and Evaluation of Graduate Education (CAPES-Brazil) to E.G.M.

Author contributions

F.B.S.F. and D.M.D. designed the research and experiments; F.B.S.F., E.G.M. and D.M.D. performed the experiments; all authors contributed to write the final manuscript; D.M.D. obtained funding.

Conflict of interest

The authors declare no conflict of interest.

References

ALMEIDA, D.; HUBER, D. Chilling-induced changes in the apoplastic solution of tomato pericarp. **The Journal of Horticultural Science and Biotechnology**, [*s. l.*], v. 85, n. 4, p. 312–316, 2010. Disponível em: http://www.tandfonline.com/doi/full/10.1080/14620316.2010.11512673.

AZEVEDO, I. G. *et al.* P-type H+-ATPases activity, membrane integrity, and apoplastic pH during papaya fruit ripening. **Postharvest Biology and Technology**, [*s. l.*], v. 48, n. 2, p. 242–247, 2008. Disponível em: https://linkinghub.elsevier.com/retrieve/pii/S0925521407003730.

BERNSTEIN, L. Method for Determining Solutes in the Cell Walls of Leaves. **Plant Physiology**, [*s. l.*], v. 47, n. 3, p. 361–365, 1971.

CHEN, Q. X. *et al.* Effect of methanol on the activity and conformation of acid phosphatase from the prawn Penaeus penicillatus. **Biochemistry. Biokhimiia**, [*s. l.*], v. 65, n. 4, p. 452–456, 2000. Disponível em: http://www.ncbi.nlm.nih.gov/pubmed/10810183.

CHIKOV, V. I.; BAKIROVA, G. G. Role of the Apoplast in the Control of Assimilate Transport, Photosynthesis, and Plant Productivity. **Russian Journal of Plant Physiology**, [*s. l.*], v. 51, n. 3, p. 420–431, 2004. Disponível em: http://link.springer.com/10.1023/B:RUPP.0000028691.49600.c2.

CHINCINSKA, I. A. Leaf infiltration in plant science: old method, new possibilities. **Plant Methods**, [*s. l.*], v. 17, n. 1, p. 1–21, 2021. Disponível em: https://doi.org/10.1186/s13007-021-00782-x.

CHONG, J. *et al.* MetaboAnalyst 4.0: towards more transparent and integrative metabolomics analysis. **Nucleic Acids Research**, [*s. l.*], v. 46, n. W1, p. W486–W494, 2018. Disponível em: https://academic.oup.com/nar/article/46/W1/W486/4995686.

CRAMER, G. R. *et al.* Effects of abiotic stress on plants: a systems biology perspective. **BMC Plant Biology**, [*s. l.*], v. 11, n. 1, p. 163, 2011. Disponível em: http://www.biomedcentral.com/content/pdf/1471-2229-11-163.pdf.

DRAGIŠIC MAKSIMOVIC, J. J. *et al.* Filter strip as a method of choice for apoplastic fluid extraction from maize roots. **Plant Science**, [*s. l.*], v. 223, p. 49–58, 2014.

DURAN-CARRIL, M. V; BUJAN, C. R. Antioxidant systems in the leaf apoplast compartment of Pinus pinaster Ait. and Pinus radiata D. Don. Plants exposed to SO 2. **Annals**

of Applied Biology, [*s. l.*], v. 133, n. 3, p. 455–466, 1998. Disponível em: https://onlinelibrary.wiley.com/doi/10.1111/j.1744-7348.1998.tb05843.x.

DYRDA, G. *et al.* The effect of organic solvents on selected microorganisms and model liposome membrane. **Molecular Biology Reports**, [*s. l.*], v. 46, n. 3, p. 3225–3232, 2019. Disponível em: http://link.springer.com/10.1007/s11033-019-04782-y.

EKANAYAKE, G.; GOHMANN, R.; MACKEY, D. A method for quantitation of apoplast hydration in Arabidopsis leaves reveals water-soaking activity of effectors of Pseudomonas syringae during biotrophy. **Scientific Reports**, [*s. l.*], v. 12, n. 1, p. 1–11, 2022. Disponível em: https://doi.org/10.1038/s41598-022-22472-x.

ERNST, O.; ZOR, T. Linearization of the Bradford Protein Assay. **Journal of Visualized Experiments**, [*s. l.*], v. 38, n. e1918, 2010. Disponível em: http://www.jove.com/index/Details.stp?ID=1918.

FARVARDIN, A. *et al.* The apoplast: A key player in plant survival. **Antioxidants**, [*s. l.*], v. 9, n. 7, p. 1–26, 2020.

FIGUEIREDO, J. *et al.* An apoplastic fluid extraction method for the characterization of grapevine leaves proteome and metabolome from a single sample. **Physiologia Plantarum**, [*s. l.*], v. 171, n. 3, p. 343–357, 2021.

FLOERL, S. *et al.* Verticillium longisporum Infection Affects the Leaf Apoplastic Proteome, Metabolome, and Cell Wall Properties in Arabidopsis thaliana. **PLoS ONE**, [*s. l.*], v. 7, n. 2, p. e31435, 2012. Disponível em: https://dx.plos.org/10.1371/journal.pone.0031435.

GARCHERY, C. *et al.* A diminution in ascorbate oxidase activity affects carbon allocation and improves yield in tomato under water deficit. **Plant, Cell & Environment**, [*s. l.*], v. 36, n. 1, p. 159–175, 2013. Disponível em: https://onlinelibrary.wiley.com/doi/10.1111/j.1365-3040.2012.02564.x.

GENTZEL, I. *et al.* A simple method for measuring apoplast hydration and collecting apoplast contents. **Plant Physiology**, [*s. l.*], v. 179, n. 4, p. 1265–1272, 2019.

GREGORY, A. L. *et al.* In vivo regulatory phosphorylation of the phosphoenolpyruvate carboxylase AtPPC1 in phosphate-starved Arabidopsis thaliana. **Biochemical Journal**, [*s. l.*], v. 420, n. 1, p. 57–65, 2009. Disponível em: https://portlandpress.com/biochemj/article/420/1/57/44523/In-vivo-regulatory-phosphorylation-of-the.

GUPTA, S. K. *et al.* Effects of ethylenediurea (EDU) on apoplast and chloroplast proteome in two wheat varieties under high ambient ozone: an approach to investigate EDU's mode of action. **Protoplasma**, [*s. l.*], v. 258, n. 5, p. 1009–1028, 2021. Disponível em: https://link.springer.com/10.1007/s00709-021-01617-1.

GUPTA, M. N. Enzyme function in organic solvents. **European Journal of Biochemistry**, [*s. l.*], v. 203, n. 1–2, p. 25–32, 1992. Disponível em: https://onlinelibrary.wiley.com/doi/10.1111/j.1432-1033.1992.tb19823.x.

HARTUNG, W.; RADIN, J. W.; HENDRIX, D. L. Abscisic Acid Movement into the

Apoplastic solution of Water-Stressed Cotton Leaves. **Plant Physiology**, [*s. l.*], v. 86, n. 3, p. 908–913, 1988.

HOAGLAND, D. R.; ARNON, D. I. The water-culture method for growing plants without soil. **California Agricultural Experiment Station Circular**, [*s. l.*], v. 347, p. 1–32, 1950.

JASWANTHI, N. *et al.* Apoplast proteomic analysis reveals drought stress-responsive protein datasets in chilli (Capsicum annuum L.). **Data in Brief**, [*s. l.*], v. 25, p. 104041, 2019. Disponível em: https://linkinghub.elsevier.com/retrieve/pii/S2352340919303944.

JOO, H.-J. *et al.* The Effect of Methanol on the Structural Parameters of Neuronal Membrane Lipid Bilayers. **The Korean Journal of Physiology & Pharmacology**, [*s. l.*], v. 16, n. 4, p. 255, 2012. Disponível em: https://synapse.koreamed.org/DOIx.php?id=10.4196/kjpp.2012.16.4.255.

JOOSTEN, M. H. A. J. A. J. Isolation of Apoplastic Fluid from Leaf Tissue by the Vacuum Infiltration-Centrifugation Technique. *In*: METHODS IN MOLECULAR BIOLOGY. [*S. l.: s. n.*], 2012. v. 835, p. 603–610. Disponível em: https://link.springer.com/10.1007/978-1-61779-501-5_38.

JORGE, T. F.; ANTÓNIO, C. Quantification of Low-Abundant Phosphorylated Carbohydrates Using HILIC-QqQ-MS/MS. *In*: PLANT METABOLOMICS: METHODS AND PROTOCOLS. [*S. l.: s. n.*], 2018. p. 71–86. Disponível em: http://link.springer.com/10.1007/978-1-4939-7819-9_6.

KANG, Y. *et al.* Guard-cell apoplastic sucrose concentration – a link between leaf photosynthesis and stomatal aperture size in the apoplastic phloem loader Vicia faba L. **Plant, Cell & Environment**, [*s. l.*], v. 30, n. 5, p. 551–558, 2007. Disponível em: http://doi.wiley.com/10.1111/j.1365-3040.2007.01635.x.

KEHR, J.; MORRIS, R. J.; KRAGLER, F. Long-Distance Transported RNAs: From Identity to Function. **Annual Review of Plant Biology**, [*s. l.*], v. 73, p. 457–474, 2022.

KINGSBURY, N. J.; MCDONALD, K. A. Quantitative Evaluation of E1 Endoglucanase Recovery from Tobacco Leaves Using the Vacuum Infiltration-Centrifugation Method. **BioMed Research International**, [*s. l.*], v. 2014, p. 1–10, 2014. Disponível em: http://www.hindawi.com/journals/bmri/2014/483596/.

KOLEY, S. *et al.* An efficient LC-MS method for isomer separation and detection of sugars, phosphorylated sugars, and organic acids. **Journal of Experimental Botany**, [*s. l.*], v. 73, n. 9, p. 2938–2952, 2022.

KOPKA, J. *et al.* GMD@CSB.DB: the Golm Metabolome Database. **Bioinformatics**, [*s. l.*], v. 21, n. 8, p. 1635–1638, 2005. Disponível em: https://academic.oup.com/bioinformatics/article-lookup/doi/10.1093/bioinformatics/bti236.

LIMA, V. F. *et al.* Toward multifaceted roles of sucrose in the regulation of stomatal movement. **Plant Signaling and Behavior**, [*s. l.*], v. 13, n. 8, p. 1–8, 2018. Disponível em: https://doi.org/10.1080/15592324.2018.1494468.

LISEC, J. *et al.* Gas chromatography mass spectrometry–based metabolite profiling in plants.

Nature Protocols, [*s. l.*], v. 1, n. 1, p. 387–396, 2006. Disponível em: https://www.nature.com/articles/nprot.2006.59.

LIU, F. L. *et al.* Chemical Tagging Assisted Mass Spectrometry Analysis Enables Sensitive Determination of Phosphorylated Compounds in a Single Cell. **Analytical Chemistry**, [*s. l.*], v. 93, n. 17, p. 6848–6856, 2021.

LOHAUS, G. *et al.* Is the infiltration-centrifugation technique appropriate for the isolation of apoplastic fluid? A critical evaluation with different plant species. **Physiologia Plantarum**, [*s. l.*], v. 111, n. 4, p. 457–465, 2001.

LONG, J. M.; WIDDERS, I. E. Quantification of apoplastic potassium content by elution analysis of leaf lamina tissue from pea (Pisum sativum L. cv Argenteum). **Plant Physiology**, [*s. l.*], v. 94, n. 3, p. 1040–1047, 1990.

MADSEN, S. R.; NOUR-ELDIN, H. H.; HALKIER, B. A. Collection of Apoplastic Fluids from Arabidopsis thaliana Leaves. *In*: FETT-NETO, A. G.; WALKER, J. M. (org.). **Biotechnology of Plant Secondary Metabolism: Methods and Protocols**. New York, NY: Springer New York, 2016. (Methods in Molecular Biology). v. 1405, p. 35–42. Disponível em: http://link.springer.com/10.1007/978-1-4939-3393-8.

MALINOVA, I. *et al.* Identification of Two Arabidopsis thaliana Plasma Membrane Transporters Able to Transport Glucose 1-Phosphate. **Plant and Cell Physiology**, [*s. l.*], v. 61, n. 2, p. 381–392, 2020. Disponível em: https://academic.oup.com/pcp/article/61/2/381/5625160.

MARENTES, E. *et al.* Proteins accumulate in the apoplast of winter rye leaves during cold acclimation. [*s. l.*], p. 499–508, 1993.

MARTÍNEZ-GONZÁLEZ, A. P. *et al.* What proteomic analysis of the apoplast tells us about plant–pathogen interactions. **Plant Pathology**, [*s. l.*], v. 67, n. 8, p. 1647–1668, 2018. Disponível em: https://bsppjournals.onlinelibrary.wiley.com/doi/10.1111/ppa.12893.

MATSUO, K.; FUKUZAWA, N.; MATSUMURA, T. A simple agroinfiltration method for transient gene expression in plant leaf discs. **Journal of Bioscience and Bioengineering**, [*s. l.*], v. 122, n. 3, p. 351–356, 2016. Disponível em: https://linkinghub.elsevier.com/retrieve/pii/S1389172316000347.

MEDEIROS, D. B. *et al.* Metabolomics for understanding stomatal movements. **Theoretical and Experimental Plant Physiology**, [*s. l.*], v. 31, n. 1, p. 91–102, 2019.

MEDEIROS, D. B. *et al.* Sucrose breakdown within guard cells provides substrates for glycolysis and glutamine biosynthesis during light-induced stomatal opening. **Plant Journal**, [*s. l.*], v. 94, n. 4, p. 583–594, 2018.

MONTANO, J. *et al.* Salmonella enterica Serovar Typhimurium 14028s Genomic Regions Required for Colonization of Lettuce Leaves. **Frontiers in Microbiology**, [*s. l.*], v. 11, 2020. Disponível em: https://www.frontiersin.org/article/10.3389/fmicb.2020.00006/full.

O'LEARY, B. M. *et al.* Early changes in apoplast composition associated with defence and disease in interactions between Phaseolus vulgaris and the halo blight pathogen Pseudomonas

syringae Pv. phaseolicola. **Plant Cell and Environment**, [*s. l.*], v. 39, n. 10, p. 2172–2184, 2016.

O'LEARY, B. M. *et al.* The infiltration-centrifugation technique for extraction of apoplastic fluid from plant leaves using Phaseolus vulgaris as an example. **Journal of Visualized Experiments**, [*s. l.*], n. 94, p. 1–8, 2014.

OUTLAW, W. H.; DE VLIEGHERE-HE, X. Transpiration Rate. An Important Factor Controlling the Sucrose Content of the Guard Cell Apoplast of Broad Bean. **Plant Physiology**, [*s. l.*], v. 126, n. 4, p. 1716–1724, 2001. Disponível em: http://www.plantphysiol.org/lookup/doi/10.1104/pp.126.4.1716.

PARKHURST, D. F. Stereological methods for measuring internal leaf structure variables. **American Journal of Botany**, [*s. l.*], v. 69, n. 1, p. 31–39, 1982.

PEREZ DE SOUZA, L. *et al.* Ultra-high-performance liquid chromatography high-resolution mass spectrometry variants for metabolomics research. **Nature Methods**, [*s. l.*], 2021.

RODRÍGUEZ-CELMA, J. *et al.* Plant fluid proteomics: Delving into the xylem sap, phloem sap and apoplastic fluid proteomes. **Biochimica et Biophysica Acta (BBA) - Proteins and Proteomics**, [*s. l.*], v. 1864, n. 8, p. 991–1002, 2016. Disponível em: https://linkinghub.elsevier.com/retrieve/pii/S1570963916300565.

ROESSNER-TUNALI, U. *et al.* Kinetics of labelling of organic and amino acids in potato tubers by gas chromatography-mass spectrometry following incubation in 13 C labelled isotopes. **The Plant Journal**, [*s. l.*], v. 39, n. 4, p. 668–679, 2004. Disponível em: https://onlinelibrary.wiley.com/doi/10.1111/j.1365-313X.2004.02157.x.

ROHWER, J. M. Kinetic modelling of plant metabolic pathways. **Journal of Experimental Botany**, [*s. l.*], v. 63, n. 6, p. 2275–2292, 2012.

SATTELMACHER, B. The apoplast and its significance for plant mineral nutrition. **New Phytologist**, [*s. l.*], v. 149, n. 2, p. 167–192, 2001. Disponível em: https://nph.onlinelibrary.wiley.com/doi/10.1046/j.1469-8137.2001.00034.x.

SHI, J. *et al.* Phospho enol pyruvate Carboxylase in Arabidopsis Leaves Plays a Crucial Role in Carbon and Nitrogen Metabolism. **Plant Physiology**, [*s. l.*], v. 167, n. 3, p. 671–681, 2015. Disponível em: https://academic.oup.com/plphys/article/167/3/671/6113635.

SMITH, R. R.; CANADY, W. J. Solvation effects upon the thermodynamic substrate activity; correlation with the kinetics of enzyme catalyzed reactions. I. Effects of added reagents such as methanol upon alpha-chymotrypsin. **Biophysical Chemistry**, [*s. l.*], v. 43, n. 2, p. 173–187, 1992. Disponível em: https://linkinghub.elsevier.com/retrieve/pii/030146229280032Z.

STEUDLE, E.; FRENSCH, J. Water transport in plants: Role of the apoplast. **Plant and Soil**, [*s. l.*], v. 187, n. 1, p. 67–79, 1996. Disponível em: http://link.springer.com/10.1007/BF00011658.

YU, Y. *et al.* The effects of organic solvents on the folding pathway and associated thermodynamics of proteins: a microscopic view. **Scientific Reports**, [*s. l.*], v. 6, n. 1, p. 19500, 2016. Disponível em: https://www.nature.com/articles/srep19500.

ZAKHARTSEV, M. *et al.* Metabolic model of central carbon and energy metabolisms of growing Arabidopsis thaliana in relation to sucrose translocation. **BMC Plant Biology**, [*s. l.*], v. 16, n. 1, 2016. Disponível em: http://dx.doi.org/10.1186/s12870-016-0868-3.

Main Figures

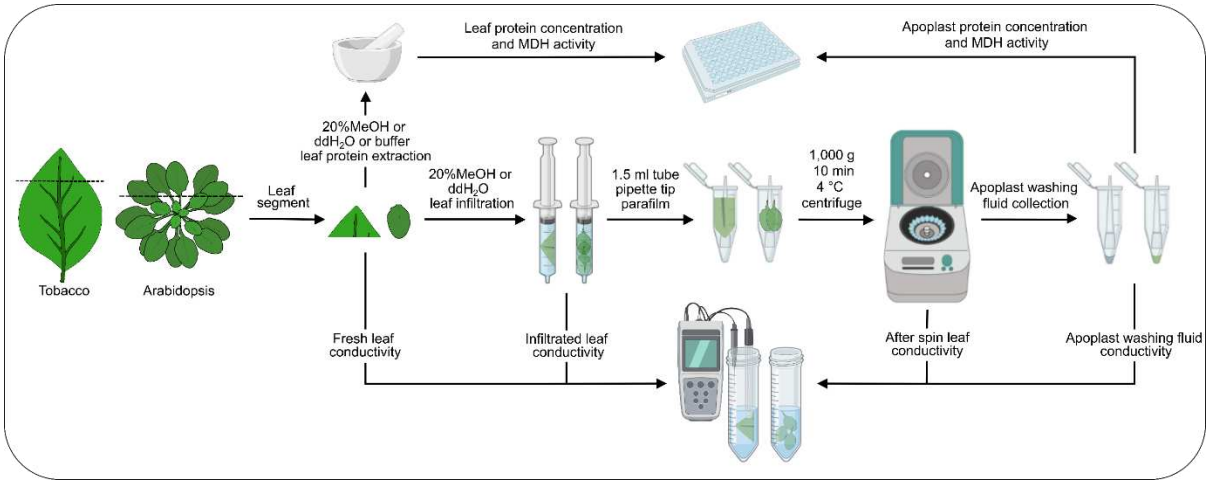

Figure 1. Schematic representation of the procedures to collect the apoplast washing fluid (AWF) from *Nicotiana tabacum* L. and *Arabidopsis thaliana* L. leaves and to measure the AWF purity through conductivity, protein concentration and malate dehydrogenase (MDH) activity analysis in each step of the protocol.

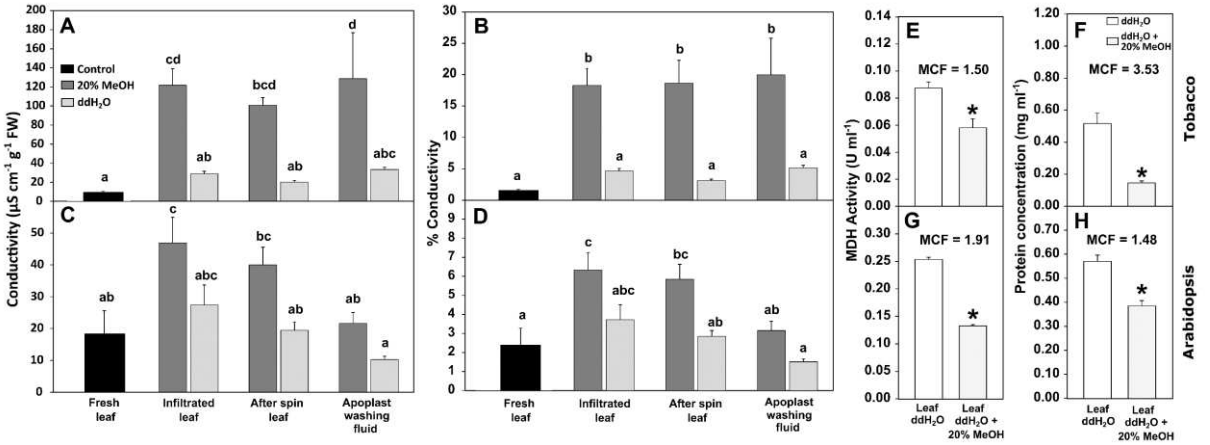

Figure 2. Conductivity analysis and the methanol correction factor (MCF) established for *Nicotiana tabacum* L. and *Arabidopsis thaliana* L. A-D) Absolute (A,C) and relative (percentage) (B,D) conductivity measured in each step of the apoplast washing fluid (AWF) collection from tobacco (upper graphs) and Arabidopsis (lower graphs). E-H) MCF obtained from malate dehydrogenase (MDH) activity (E,G) and protein concentration (F,H) analyses carried out using leaf proteins extracted by using distilled deionized water (ddH_2O) with or without 20% (v/v) methanol (20% MeOH). Bars with different letters differ statistically by ANOVA and Tukey test ($P < 0.05$). Asterisks (*) indicate significant difference between ddH_2O and ddH_2O plus 20% MeOH extracts by Student's *t*-test ($P < 0.05$). Bars represent average values ± standard error (n = 5 ± SE).

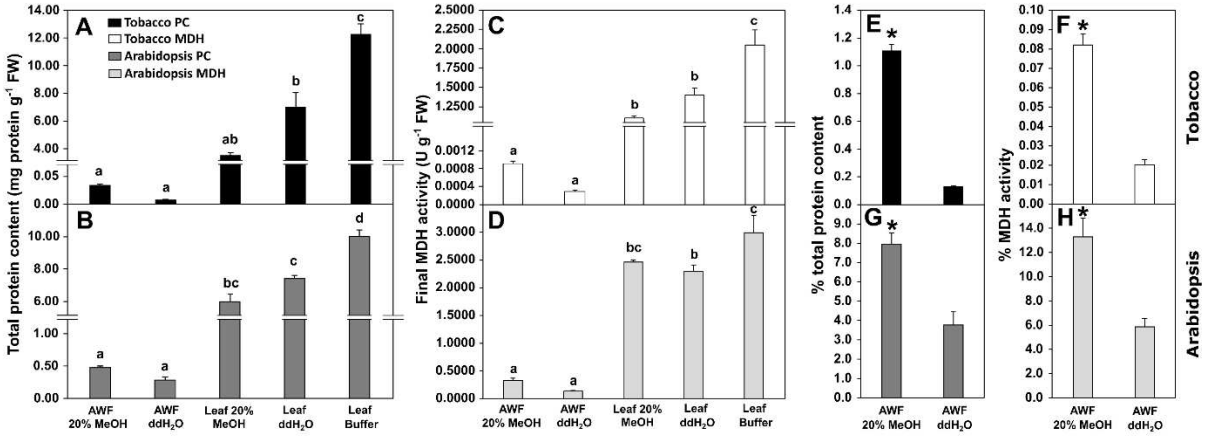

Figure 3. Protein content and malate dehydrogenase (MDH) activity measured in leaves and apoplast washing fluids (AWF) from *Nicotiana tabacum* L. and *Arabidopsis thaliana* L. Total protein content (A-B) and final MDH activity (C-D) were measured in leaves and AWFs from tobacco and Arabidopsis extracted using distilled deionized water (ddH_2O), 20% (v/v) methanol (20% MeOH) or a protein extraction buffer (200 mM HEPES/NaOH pH 8.0, 10 mM $MgCl_2$, 2 mM aminocaproic, 2 mM benzamidine, 1 mM EDTA, 1mM DTT, 0.5 mM PMSF, 10% (v/v) glycerol and 2% (w/v) polyvinylpyrrolidone). Bars with different letters differ statistically by ANOVA and Tukey test ($P < 0.05$). Percentage of the total protein content (E,G) and final MDH activity (F,H) in the AWF from tobacco and Arabidopsis related to the values observed in leaves of these species, which was considered as 100%. Asterisks (*) indicate significant difference between AWFs collected using ddH_2O or 20% MeOH by Student's *t*-test ($P < 0.05$). Bars represent average values ± standard error (n = 5 ± SE).

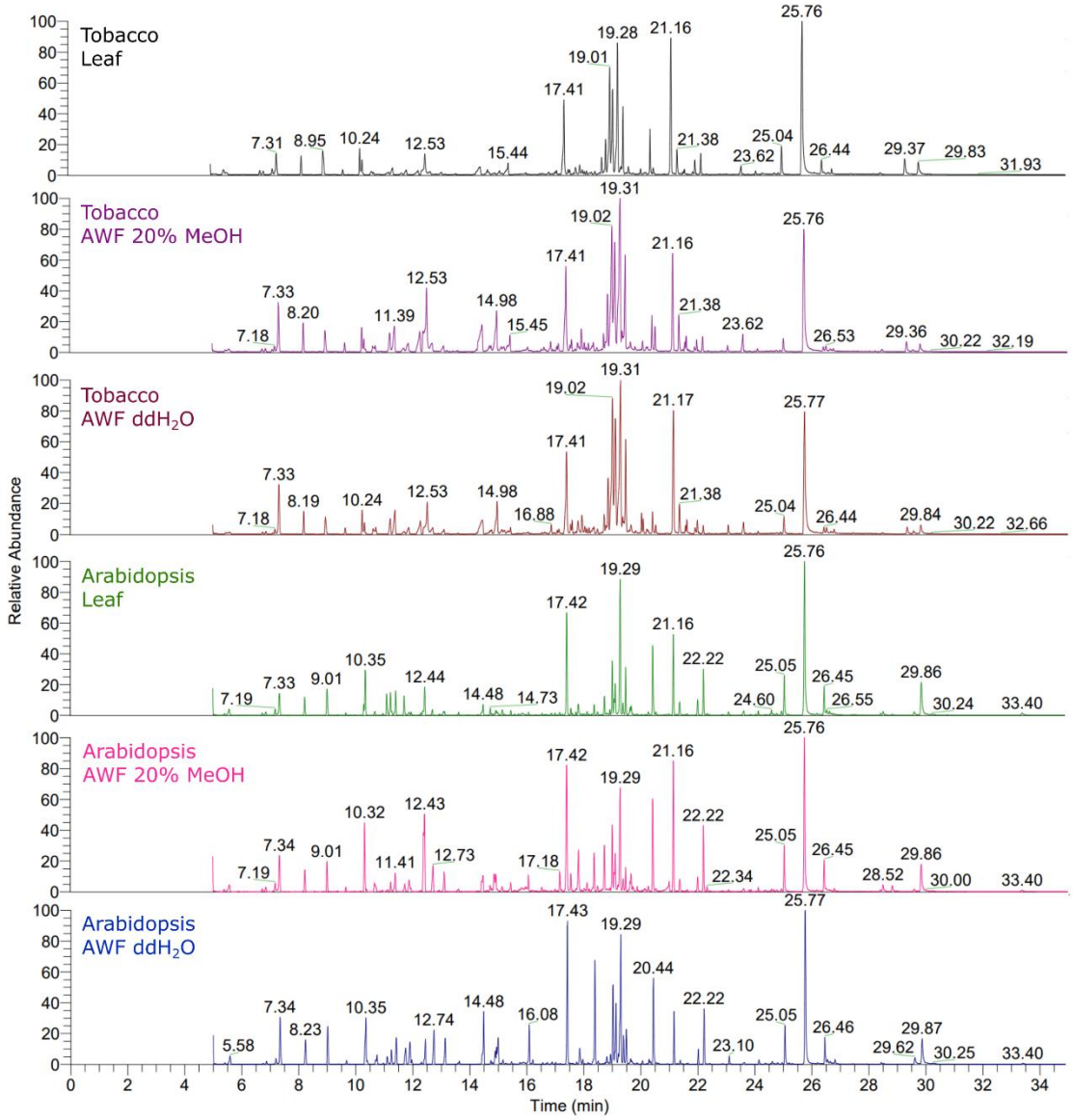

Figure 4. Chromatograms of leaf and apoplast washing fluids (AWF) samples from *Nicotiana tabacum* L. and *Arabidopsis thaliana* L. obtained by gas chromatography coupled to mass spectrometry (GC-MS) analysis. The chromatograms refer to tobacco and Arabidopsis untouched leaf samples and AWF samples collected using either 20% (v/v) methanol (20% MeOH) or distilled deionized water (ddH_2O).

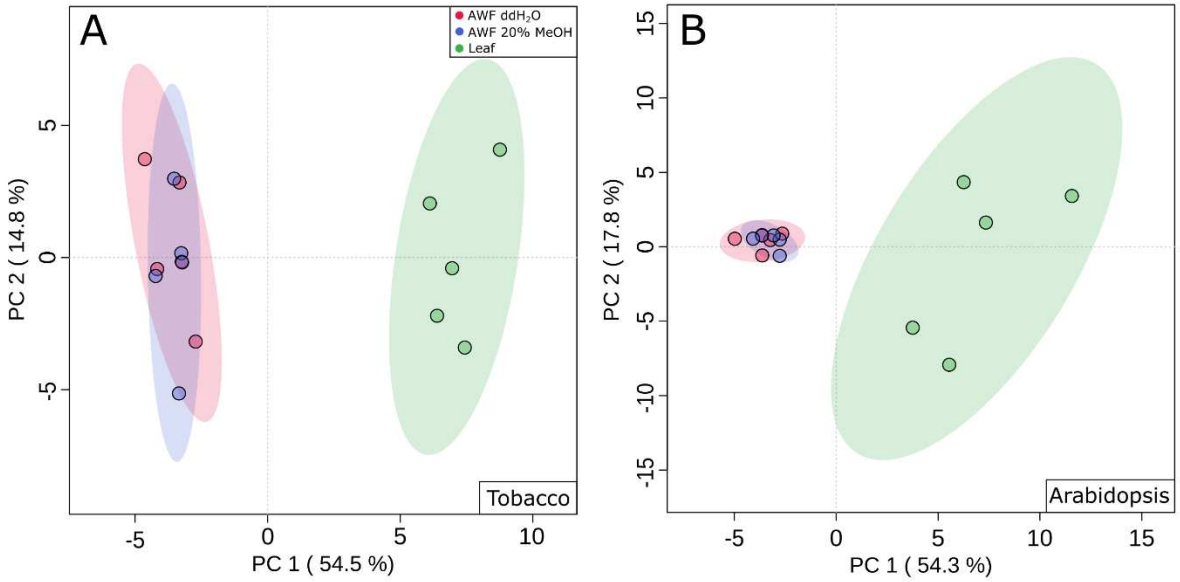

Figure 5. Principal components analysis (PCA) using metabolite profiling data from leaves (green) and leaf apoplast washing fluids (AWF) collected using 20% (v/v) methanol (20% MeOH) (blue) or distilled deionized water (ddH_2O) (red) from *Nicotiana tabacum* L. and *Arabidopsis thaliana* L. The percentage variation explained by the PC1 and PC2 are represented in each axis. These analyses were performed using the MetaboAnalyst platform. (n = 5).

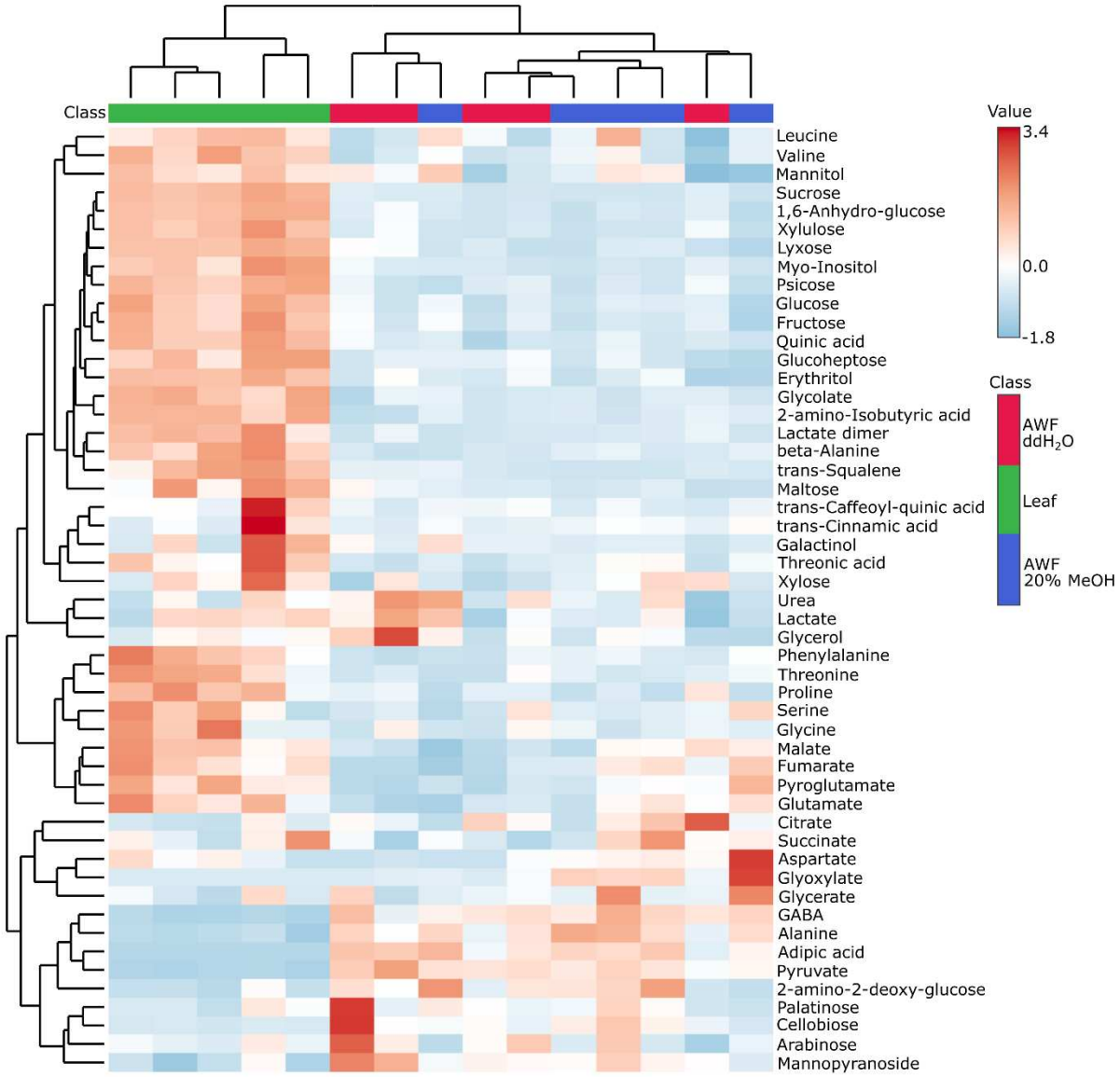

Figure 6. Heatmap representation of gas chromatography mass spectrometry (GC-MS)-based metabolite profiling analysis using leaf and apoplast washing fluids (AWF) samples from *Nicotiana tabacum* L. The classes represent leaf (green) and AWF samples collected using 20% (v/v) methanol (20% MeOH) (blue) or distilled deionized water (ddH_2O) (red). The data were normalized by ribitol, multiplied by vacuum dried volume (µL) and divided by the leaf fresh weight (FW) (in mg). Heatmap and hierarchical clustering analysis were performed using MetaboAnalyst platform using mean-centered normalization (n = 5).

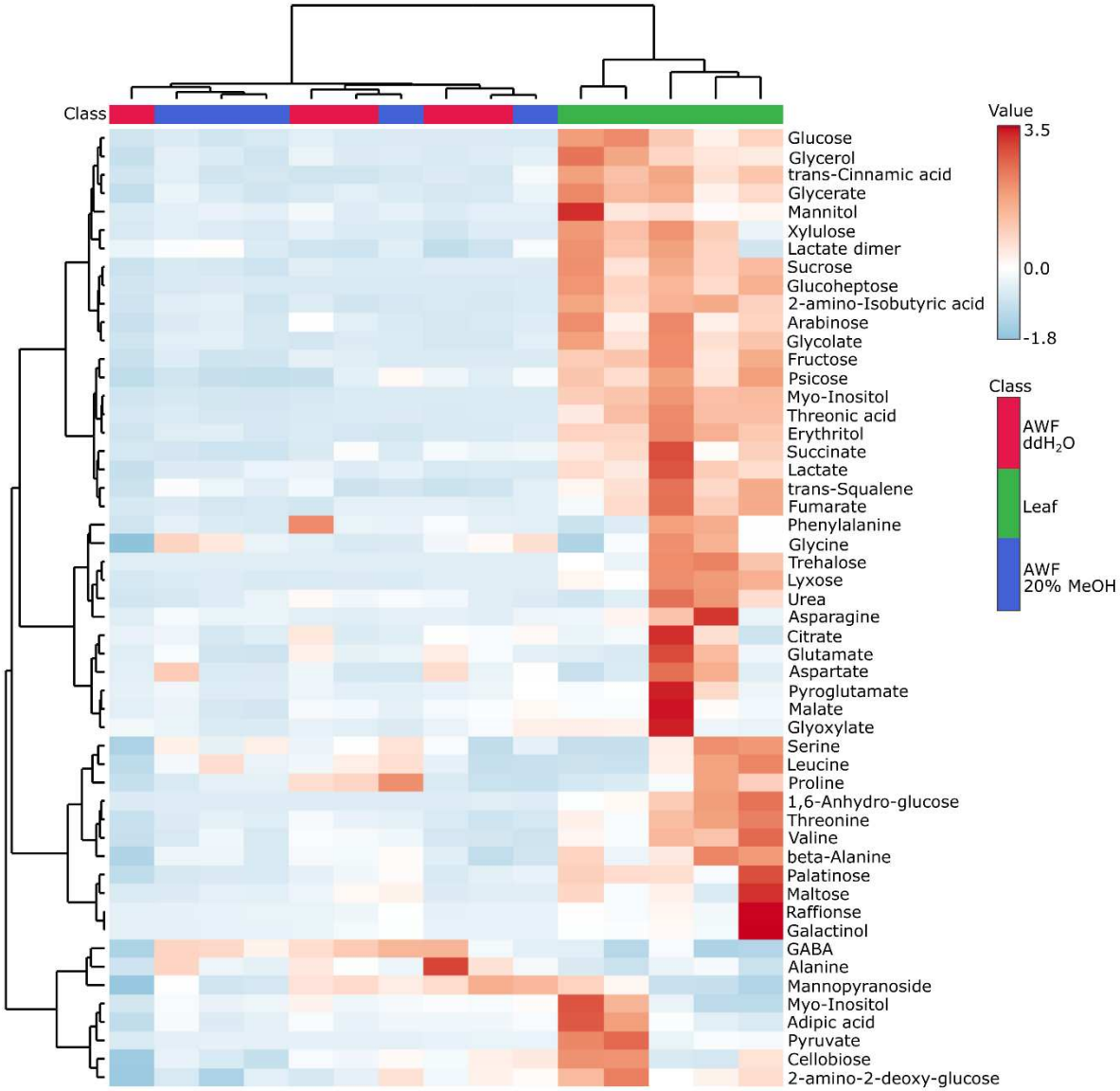

Figure 7. Heatmap representation of gas chromatography mass spectrometry (GC-MS)-based metabolite profiling analysis using leaf and apoplast washing fluids (AWF) samples from *Arabidopsis thaliana* L. The classes represent leaf (green) and AWF samples collected using 20% (v/v) methanol (20% MeOH) (blue) or distilled deionized water (ddH_2O) (red). The data were normalized by ribitol, multiplied by vacuum dried volume (µL) and divided by the leaf fresh weight (FW) (in mg). Heatmap and hierarchical clustering analysis were performed using MetaboAnalyst platform using mean-centered normalization (n = 5).

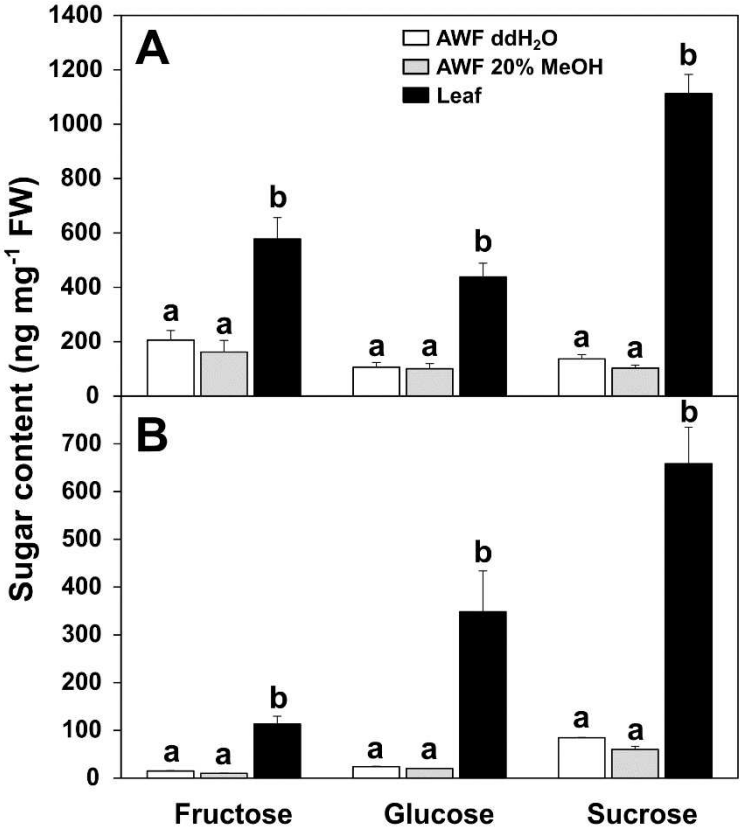

Figure 8. Sugar content in leaves (black bars) and leaf apoplast washing fluids (AWF) collected using 20% (v/v) methanol (20% MeOH) (grey bars) or distilled deionized water (ddH_2O) (white bars) from *Nicotiana tabacum* L. (A) and *Arabidopsis thaliana* L. (B). The content of fructose, glucose and sucrose was determined by gas chromatography mass spectrometry (GC-MS) analysis in leaves and apoplast samples using standard curves of each metabolite and normalized according to the leaf fresh weight (FW) frozen (in the case of leaf) or the FW used for AWF collection. Different letters within each sugar indicate significant differences by ANOVA and Tukey's test ($P < 0.05$). Bars represent average ± standard error (n = 5 ± SE).

Table 1. List of metabolites identified by gas chromatography mass spectrometry (GC-MS) analysis in *Nicotiana tabacum* L. and *Arabidopsis thaliana* L. leaves and apoplast washing fluids (AWF) collected using 20% (v/v) methanol (20% MeOH) or distilled deionized water (ddH_2O). Metabolites found and not found in the respective sample are highlighted in green and red, respectively.

Metabolite	Tobacco			Arabidopsis		
	Leaf	AWF 20% MeOH	AWF ddH_2O	Leaf	AWF 20% MeOH	AWF ddH_2O
2-Aminoisobutyric acid	✓	✓	✓	✓	✓	✓
Lactate	✓	✓	✓	✓	✓	✓
Glycolate	✓	✓	✓	✓	✓	✓
Alanine	✓	✓	✓	✓	✓	✓
Valine	✓	✓	✓	✓	✓	✓
Urea	✓	✓	✓	✓	✓	✓
Pyruvate	✓	✓	✓	✓	✓	✓
Leucine	✓	✓	✓	✓	✓	✓
Glycerol	✓	✓	✓	✓	✓	✓
Proline	✓	✓	✓	✓	✓	✓
Glycine	✓	✓	✓	✓	✓	✓
Succinate	✓	✓	✓	✓	✓	✓
Glycerate	✓	✓	✓	✓	✓	✓
Fumarate	✓	✓	✓	✓	✓	✓
Serine	✓	✓	✓	✓	✓	✓
Threonine	✓	✓	✓	✓	✓	✓
Glyoxylate	✗	✓	✓	✓	✓	✓
beta-Alanine	✓	✓	✓	✓	✓	✓
Malate	✓	✓	✓	✓	✓	✓
Lactate dimer	✓	✓	✓	✓	✓	✓
Erythritol	✓	✓	✓	✓	✓	✓
Aspartate	✓	✓	✓	✓	✓	✓
Pyroglutamate	✓	✓	✓	✓	✓	✓
GABA	✓	✓	✓	✓	✓	✓
Xylulose	✓	✓	✓	✓	✓	✓
Threonic acid	✓	✓	✓	✓	✓	✓
Asparagine	✗	✗	✗	✓	✓	✓
Glutamate	✓	✓	✓	✓	✓	✓
Phenylalanine	✓	✓	✓	✓	✓	✓
Arabinose	✓	✓	✓	✓	✓	✓
Xylose	✓	✓	✓	✓	✓	✓
1,6-anhydro-glucose	✓	✓	✓	✓	✓	✓
Lyxose	✗	✓	✓	✗	✓	✓
Citrate	✓	✓	✓	✓	✓	✓
Mannopyranoside	✓	✓	✓	✓	✓	✓
Psicose	✓	✓	✓	✓	✓	✓
Quinic acid	✓	✓	✓	✗	✗	✗
Adipic acid	✓	✓	✓	✓	✓	✓
Fructose*	✓	✓	✓	✓	✓	✓
Glucose*	✓	✓	✓	✓	✓	✓
2-amino-2-deoxy-glucose	✓	✓	✓	✓	✓	✓
Mannitol	✓	✓	✓	✓	✓	✓
Allo-Inositol	✗	✗	✗	✓	✓	✓
trans-Cinnamic acid	✓	✓	✓	✓	✓	✓
Myo-Inositol	✓	✓	✓	✓	✓	✓
Cellobiose	✓	✓	✓	✓	✓	✓
Glucoheptose	✓	✓	✓	✓	✓	✓
Sucrose*	✓	✓	✓	✓	✓	✓
trans-Squalene	✓	✓	✓	✓	✓	✓
Maltose	✓	✓	✓	✓	✓	✓
Galactinol	✓	✓	✓	✓	✓	✓
trans-Caffeoyl-quinic acid	✓	✓	✓	✗	✗	✗
Trehalose	✗	✗	✗	✓	✗	✗
Palatinose	✓	✓	✓	✓	✓	✓
Raffinose	✗	✗	✗	✓	✓	✓

Supplemental material

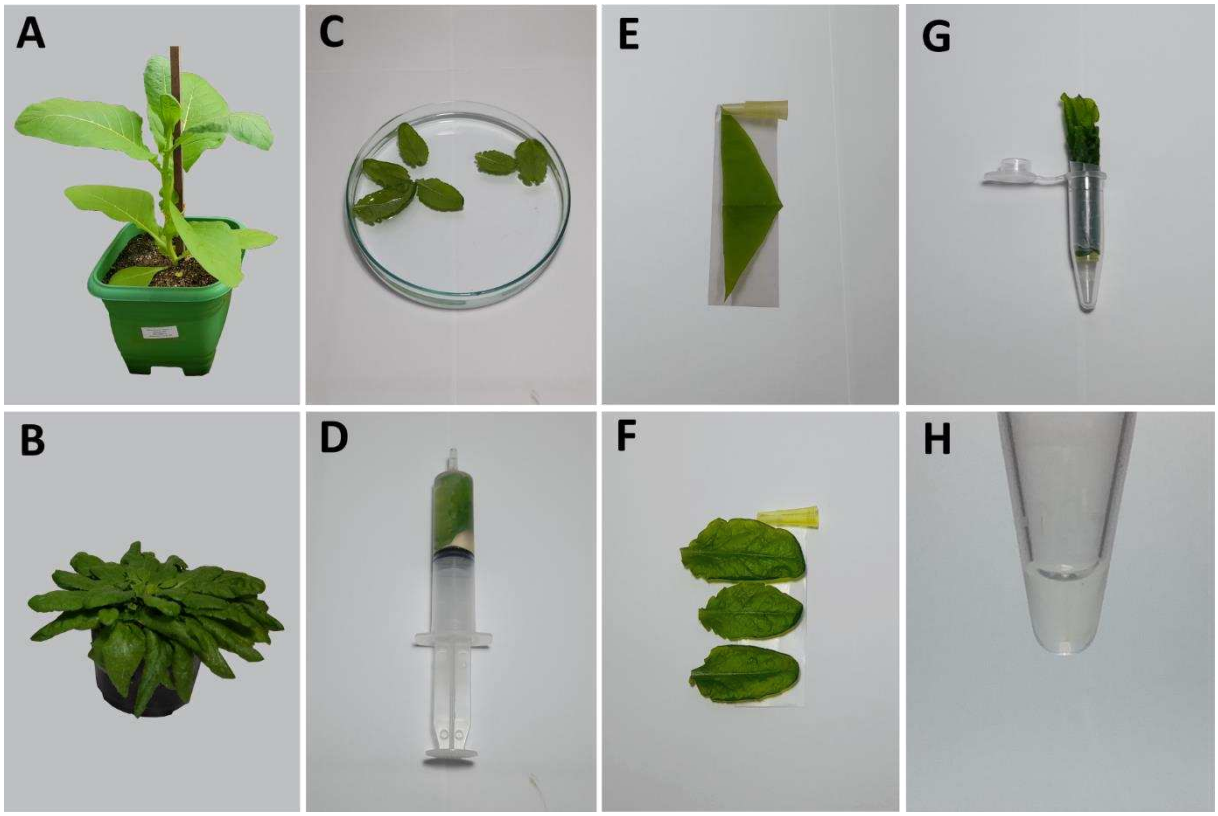

Supplemental Figure S1. Pictures of the steps of the leaf apoplast collection from *Nicotiana tabacum* L. and *Arabidopsis thaliana* L. A-B) Typical tobacco (A) and Arabidopsis (B) plants used for apoplast collection. C) Detached Arabidopsis leaves being washed in distilled deionized water (ddH_2O). D) Infiltration of Arabidopsis leaves in 20% (v/v) methanol (20% MeOH) or ddH_2O using a 20 ml syringe. E-F) Infiltrated tobacco (E) and Arabidopsis (F) leaf segments placed in a parafilm and wrapped in a 200 µl cut pipette tip. G) Infiltrated Arabidopsis leaves inserted in a 1.5 ml tube. H) Apoplast washing fluid (AWF) collected after leaf centrifugation.

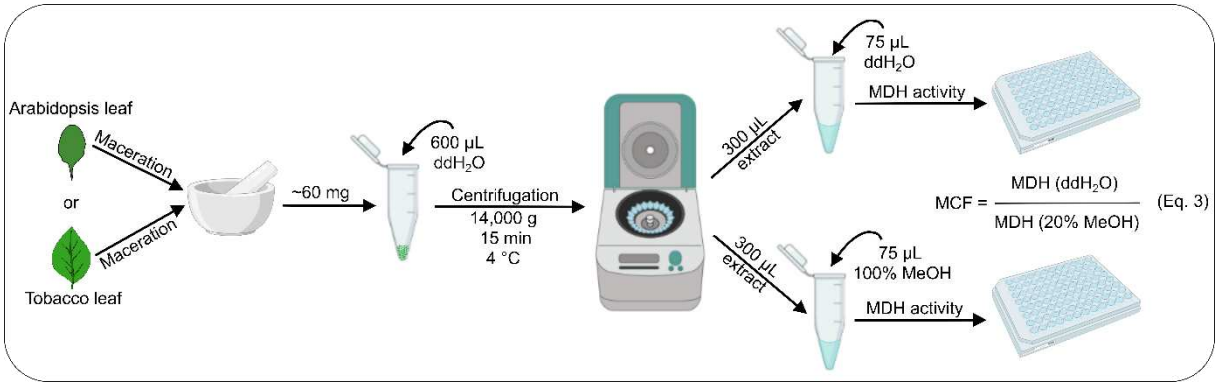

Supplemental Figure S2. Schematic representation of the procedures used to calculate the methanol correction factor (MCF). Leaves from *Nicotiana tabacum* L. and *Arabidopsis thaliana* L were grinded into a powder using mortar and pestle with liquid nitrogen. Leaf proteins were extracted with 600 µl of distilled deionized water (ddH_2O). The MCF was obtained by measuring both protein concentration and malate dehydrogenase (MDH) activity in samples with or without the addition of 75 µl of methanol. For simplification, the figure highlights only the procedures for MDH activity. The same procedure was used to estimate the MCF of the protein concentration.

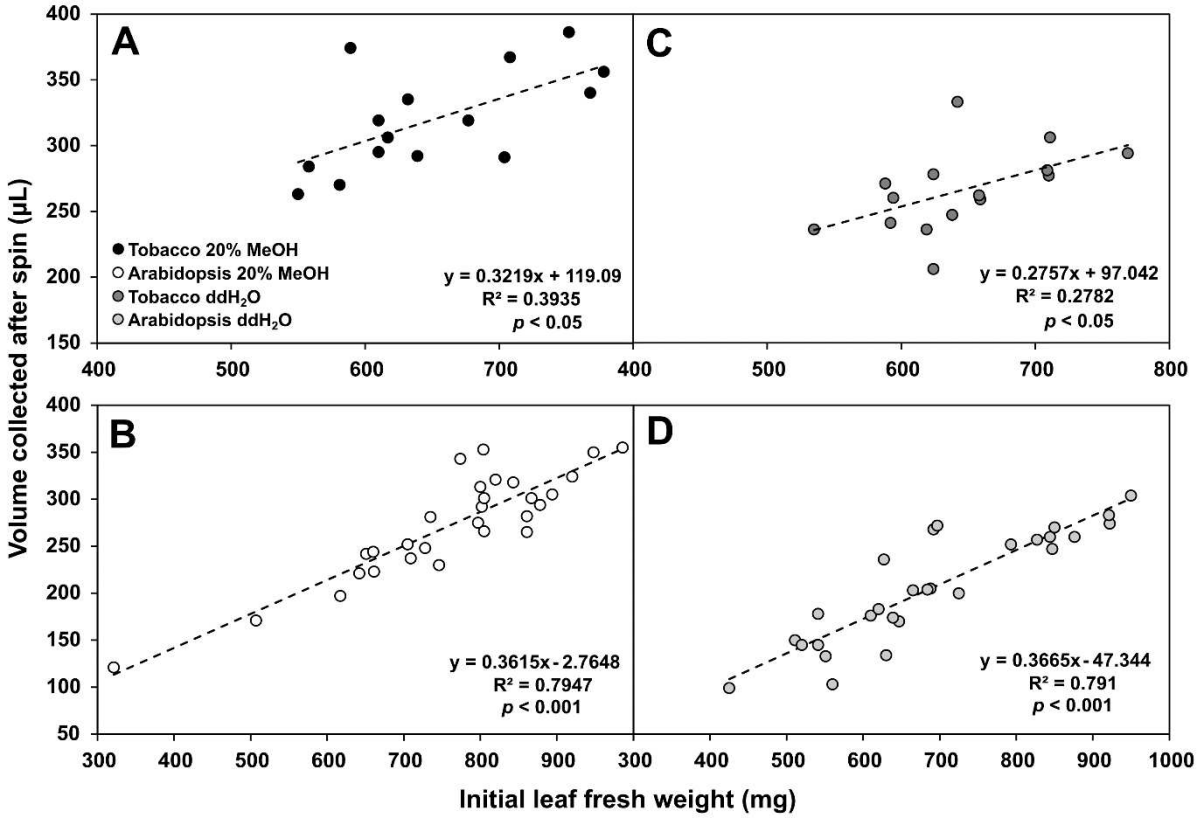

Supplemental Figure S3. Linear regression analysis between the leaf apoplast washing fluid (AWF) volume collected after spin and the initial leaf fresh weight from *Nicotiana tabacum* L. (A,C) and *Arabidopsis thaliana* L. (B,D) leaf AWF collected using 20% (v/v) methanol (20% MeOH) or distilled deionized water (ddH_2O). (n = 15 to 28).

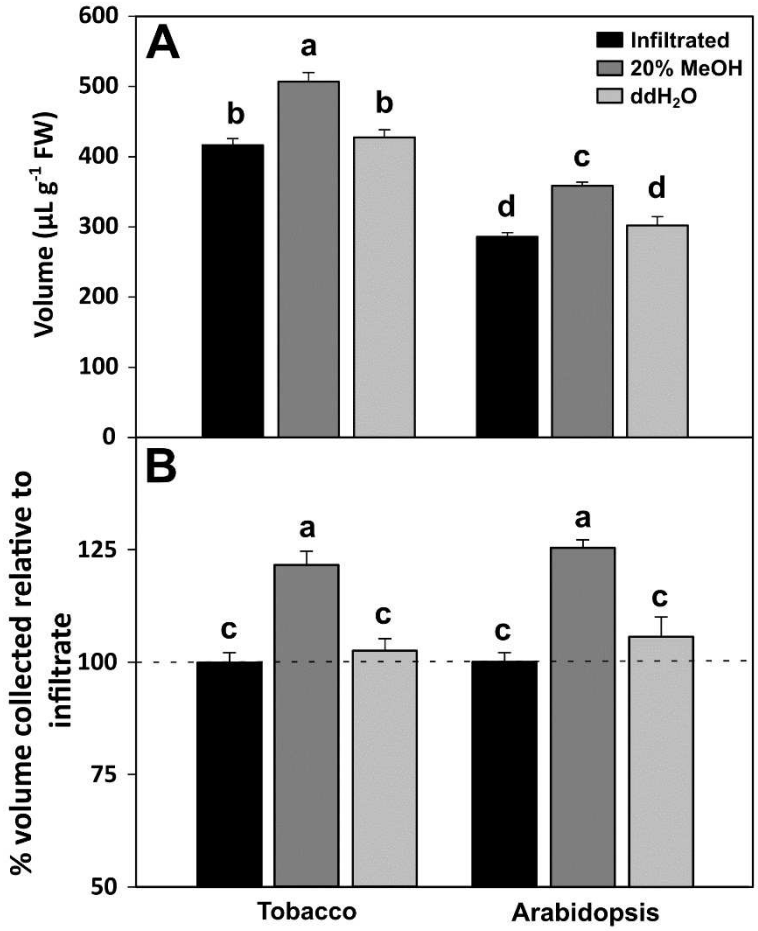

Supplemental Figure S4. Evaluation of leaf apoplast washing fluid (AWF) recovery yield after spin from *Nicotiana tabacum* L. and *Arabidopsis thaliana* L. leaves. A) Leaf AWF volume collected by using 20% (v/v) methanol (20% MeOH) or distilled deionized water (ddH_2O) relative to the leaf fresh weight (FW). B) Percentage volume of AWF collected relative to the infiltrated volume, which was considered as 100% for each species. Bars with different letters differ statistically by ANOVA and Tukey test ($P < 0.05$).

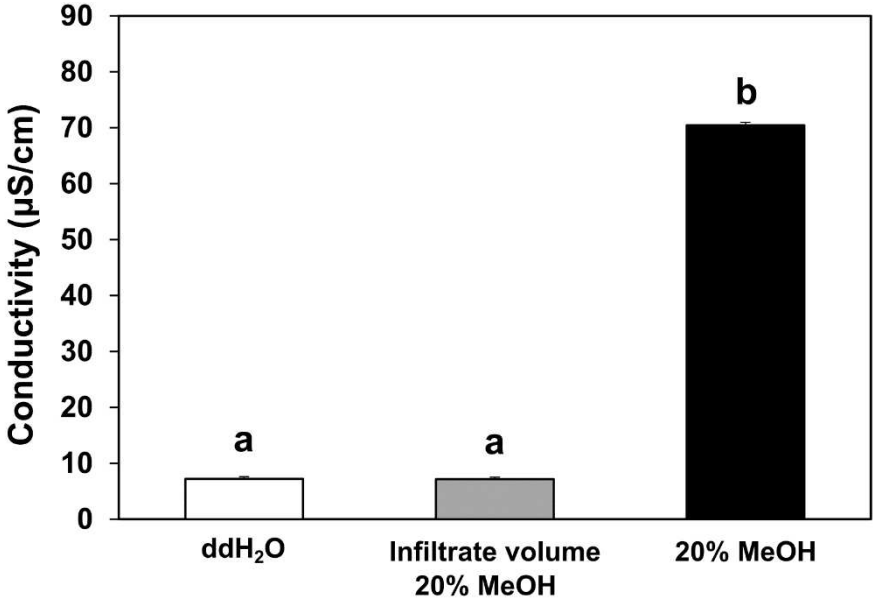

Supplemental Figure S5. Conductivity of distilled deionized water (ddH_2O), the infiltrate volume of 20% (v/v) methanol (20% MeOH) and 20% MeOH. The conductivity of ddH_2O and 20% MeOH was measured in 35 mL of pure solution. The infiltrate volume of 20% MeOH was measured by adding the average of leaf infiltrate volume using 20% MeOH in 35 mL of ddH_2O. The data is represented as average ± standard error (n = 9 ± SE). Bars with different letters differ statistically by ANOVA and Tukey test ($P < 0.05$).

Supplemental Table S1. Conductivity ratio between infiltration fluids used for *Nicotiana tabacum* L. and *Arabidopsis thaliana* L. leaves apoplast washing fluid (AWF) collection. Values from leaf AWF in each apoplast collection step from tobacco and Arabidopsis and the ratio between 20% (v/v) methanol (20% MeOH) and distilled deionized water (ddH_2O) extractions (n = 5 ± SE).

Average	Conductivity (µS cm^{-1} mg^{-1} FW)		% Conductivity	
	Tobacco	Arabidopsis	Tobacco	Arabidopsis
Infiltrated leaf 20% MeOH	0.121 ± 0.017	0.046 ± 0.008	18.26 ± 2.73	6.32 ± 0.92
Infiltrated leaf ddH_2O	0.028 ± 0.002	0.027 ± 0.006	4.63 ± 0.44	3.71 ± 0.78
After spin leaf 20% MeOH	0.100 ± 0.007	0.040 ± 0.005	17.25 ± 2.88	5.84 ± 0.78
After spin leaf ddH_2O	0.020 ± 0.001	0.019 ± 0.002	3.10 ± 0.26	2.84 ± 0.30
AWF 20% MeOH	0.128 ± 0.047	0.021 ± 0.003	19.99 ± 5.82	3.15 ± 0.48
AWF ddH_2O	0.033 ± 0.002	0.010 ± 0.001	5.15 ± 0.40	1.51 ± 0.15
Ratio				
Infiltrated leaf 20% MeOH:ddH_2O	4.23	1.71	3.94	1.70
After spin leaf 20% MeOH:ddH_2O	4.99	2.06	5.56	2.05
AWF 20% MeOH:ddH_2O	3.85	2.12	3.88	2.09

Supplemental Table S2. Malate dehydrogenase (MDH) activity and protein content ratio between infiltration fluids used for *Nicotiana tabacum* L. and *Arabidopsis thaliana* L. leaves apoplast washing fluid (AWF) collection. Values from leaves and leaf AWF collections from tobacco and Arabidopsis and the ratio between 20% (v/v) methanol (20% MeOH) and distilled deionized water (ddH_2O) extractions (n = 5 ± SE).

Average	Final MDH activity (U g^{-1} FW)		Protein content (mg g^{-1} FW)	
	Tobacco	Arabidopsis	Tobacco	Arabidopsis
AWF 20% MeOH	0.00091 ± 0.00006	0.328 ± 0.043	0.039 ± 0.001	0.475 ± 0.034
AWF ddH_2O	0.00028 ± 0.00003	0.135 ± 0.015	0.009 ± 0.000	0.279 ± 0.050
Leaf 20% MeOH	1.11237 ± 0.04197	2.463 ± 0.030	3.538 ± 0.175	5.967 ± 0.462
Leaf ddH_2O	1.40768 ± 0.08904	2.294 ± 0.115	7.013 ± 1.319	7.413 ± 0.189
Leaf Buffer	2.05105 ± 0.19456	2.995 ± 0.308	12.280 ± 1.349	10.027 ± 0.386
Ratio				
Leaf 20% MeOH:ddH_2O	0.79	1.07	0.50	0.80
AWF 20% MeOH:ddH2O	3.18	2.43	4.27	1.70

Supplemental Table S3. Percentage of Malate dehydrogenase (MDH) activity and protein content ratio between infiltration fluids used for *Nicotiana tabacum* L. and *Arabidopsis thaliana* L. leaves apoplast washing fluid (AWF) collection. Values from AWF from tobacco and Arabidopsis and the ratio between 20% (v/v) methanol (20% MeOH) and distilled deionized water (ddH_2O) extractions (n = 5 ± SE).

Average	% MDH activity		% Protein content	
	Tobacco	Arabidopsis	Tobacco	Arabidopsis
AWF 20% MeOH	0.082 ± 0.005	13.295 ± 1.741	1.109 ± 0.043	7.950 ± 0.571
AWF ddH_2O	0.020 ± 0.002	5.882 ± 0.660	0.131 ± 0.004	3.763 ± 0.680
Ratio				
AWF 20% MeOH:ddH_2O	4.03	2.26	8.47	2.11

5. CHAPTER II - Disentangling the role of sucrose for stomatal movement regulation

(Unpublished manuscript)

Disentangling the role of sucrose for stomatal movement regulation

Francisco Bruno S. Freire[1], Eva G. Morais[1], Moaciria S. Lemos[1], Priscila A. Auler[1,#], Werner C. Antunes[2], Jorge Gago[3], Danilo M. Daloso[1*]

[1]LabPlant, Department of Biochemistry and Molecular Biology, Federal University of Ceará. Fortaleza-CE, 60451-970, Brazil.
[2]Department of Biology, State University of Maringá, Maringá-PR, 87020-900, Brazil
[3]Research Group on Plant Biology Under Mediterranean Conditions, Agro-Environmental and Water Economics Institute, University of the Balearic Islands, Palma de Mallorca, Spain.

[#]Current address: University of São Paulo, Luiz de Queiroz College of Agriculture, Department of Genetics versidade de São Paulo, Escola Superior de Agricultura Luiz de Queiroz, Departamento de Genética, Piracicaba-SP, 13418-900, Brazil.

*Author for correspondence
Tel: +55 85 33669821
Email address: daloso@ufc.br

Summary

The role of sucrose for stomatal movement regulation has long been debated, with several controversial studies and theories. Here we demonstrated that sucrose concentration at the leaf apoplast underpin the diel course of tobacco stomatal conductance (g_s), in which the daily stomatal opening and closure were associated with low and high concentration of apoplastic sucrose, respectively. In agreement with this, exogenously applied sucrose increased the speediness of both stomatal opening and closure in a concentration-dependent manner. We further showed that the light-induced stomatal opening is closely associated to the dynamic of sucrose and organic acids within guard cells. Interestingly, these sucrose-mediated stomatal responses were drastically reduced in plants with diminished capacity to import sucrose to their guard cells, highlighting that sucrose importation to these cells is important to modulate the magnitude of both stomatal opening and closure. Our results collectively indicate that sucrose is a master regulator of the daily g_s, being capable of inducing and accelerating both stomatal opening and closure in a concentration and location of accumulation dependent manner.

Keywords: Apoplast, guard cells, photosynthesis, stomata, sugars, water use efficiency.

Introduction

Stomata are microscopic structures composed by two guard cells that surround a pore, which allows the entrance of CO_2 for photosynthesis and the release of water via transpiration (Lima *et al.*, 2018). Stomata are then the master regulators of the water use efficiency (WUE) (Brodribb; Sussmilch; McAdam, 2019), defined as the ratio between the net photosynthetic rate (A) and stomatal conductance (g_s) (A/g_s) or transpiration rate (E) (A/E) at leaf level (Leakey *et al.*, 2019). Stomatal movement is actively regulated by the accumulation of osmolytes and the transport of ions, metabolites and water between guard cells and their surrounding apoplastic space, which modulate the osmotic potential of these compartments and stimulates the influx or efflux of water from guard cells, culminating in stomatal opening or closure, respectively (Lawson; Matthews, 2020). This process is highly influenced by several environmental cues as well as by phytohormones, the circadian clock and metabolites derived from mesophyll cells (Mesophyll-derived sugars are positive regulators of light-driven stomatal openingFlütsch; Santelia, 2021; Hubbard; Webb, 2015; Willmer; Fricker, 1996). Therefore, our understanding on how stomatal movements is regulated depends fundamentally on an integrative view concerning how the metabolisms of the leaf apoplastic space and both mesophyll and guard cells differentially and cooperatively influence stomatal movements.

Among the osmolytes controlling stomatal movements, several theories involving potassium (K^+) and carbohydrates have been proposed (Daloso *et al.*, 2017; Mesophyll-derived sugars are positive regulators of light-driven stomatal openingFlütsch; Santelia, 2021; Granot; Kelly, 2019; Lloyd, 1908; Talbott; Zeiger, 1998). Whilst the mechanisms by which K^+ stimulates stomatal opening is currently relatively well established, the role of sugars for stomatal movement regulation remains unclear, in which several controversial theories have been proposed. This is particularly due, among other reasons, to the intrinsic complexity and plasticity of guard cells, a unique plant cell type in terms of anatomy, morphology and physiology (Zeiger *et al.*, 2002). For instance, guard cells have several characteristics of source and sink as well as C3 and C4/CAM cells (Cockburn, 1983; Daloso *et al.*, 2015; Flütsch; Horrer; Santelia, 2022; Hite; Outlaw; Tarczynski, 1993; Lim *et al.*, 2022; Piro; Flütsch; Santelia, 2023). Furthermore, guard cells are known to have lower photosynthetic activity and higher respiration rate than mesophyll cells (Araújo *et al.*, 2011; Lawson, 2009), indicating a differential rate of synthesis and consumption of sugars within guard cells. Indeed, the apoplastic space and both mesophyll and subsidiary cells are important sources of sugars for guard cells (Mesophyll-derived sugars are positive regulators of light-driven stomatal openingFlütsch; Santelia, 2021;

Outlaw, 2003; Wang *et al.*, 2019). However, although our knowledge on how sucrose regulates stomatal movements has increase substantially recently (Mesophyll-derived sugars are positive regulators of light-driven stomatal openingFlütsch; Santelia, 2021; Granot; Kelly, 2019; Lawson; Matthews, 2020; Lima *et al.*, 2018), the apoplast space has been surprisingly neglected in several stomatal studies and models.

Sucrose is the main photoassimilate transported throughout the plant, being used to support the energetic demand of source cells and to be exported to sink tissues (Fettke; Fernie, 2015). In the route from mesophyll cells toward the phloem, part of the sucrose can reach guard cells through the apoplastic transpiration stream (Outlaw, 2003). Due to the lack of plasmodesmata in most guard cells (Wille; Lucas; Zea, 1984), the importation of sucrose and hexoses to these cells is mainly realized via transporters in the plasma membrane (Outlaw, 1995). In fact, several sugar transporters are highly expressed in guard cells, such as *SUCROSE TRANSPORTER 1* (*SUT1*), *SUGAR TRANSPORTER 1* (*STP1*) and *SUGAR TRANSPORTER 4* (*STP4*) (Daloso; dos Anjos; Fernie, 2016). Antisense inhibition of *SUT1* specifically in tobacco guard cells resulted in less sucrose within guard cells and lower g_s over the diel course (Antunes *et al.*, 2017). Similarly, Arabidopsis plants lacking both *STP1* and *STP4* have disrupted light-induced stomatal opening (Glucose uptake to guard cells via STP transporters provides carbon sources for stomatal opening and plant growthFlütsch *et al.*, 2020). These results highlight that mesophyll-derived sugars are crucial for ordinary stomatal opening in the light, likely due to their energetic and osmotic role developed within guard cells (Daloso *et al.*, 2016; Daubermann *et al.*, 2024; Lima *et al.*, 2023; Robaina-Estévez *et al.*, 2017). However, evidence highlights that high concentration of sucrose can induce stomatal closure in either illuminated leaves or isolated stomata (Cândido-Sobrinho *et al.*, 2022; Kottapalli *et al.*, 2018; Medeiros *et al.*, 2018). These results collectively suggest that sucrose could have a dual role for stomatal movement regulation and could be the elusive link connecting and regulating the A-g_s trade-off over the diel course.

It seems clear that a tinny control may exist between A and g_s to improve the daily WUE. We propose that sucrose is a major signal that modulates g_s according to A and/or the prevailing environmental condition. We hypothesize that the role of sucrose for stomatal movement regulation depends on where, when and how much of this metabolite is accumulated, in which the dynamic of the apoplast sucrose concentration is of paramount importance for the diel course of g_s regulation. To test this hypothesis, we adapted a method to characterize the apoplast metabolome and carried out a thorough physiological and metabolic characterization of

stomatal movements using *Nicotiana tabacum* L. wild type (NtWT) and transgenic plants with reduced expression of the SUT1 transporter (Nt*SUT1*) under control of the KST1 promoter (Antunes *et al.*, 2017), that drives the expression specifically to the guard cells (Kelly *et al.*, 2017).

Material and Methods

Plant material

Two genotypes of *Nicotiana tabacum* L. were used here, namely wild type (NtWT) cv. Havana 425 and antisense to the sucrose transporter 1 (Nt*SUT1*) under the control of the *KST1* promoter (X79779), which drives the expression specifically to the guard cells (Kelly *et al.*, 2017). These plants have been previously characterized in our group (Antunes *et al.*, 2017). Nt*SUT1* was obtained by subcloning the *SUT1* gene into the pBinK vector in the antisense direction and inserted into *E. coli*. After, the gene constructs were inserted by electroporation into *Agrobacterium tumefaciens* LBA 4404 strain and used to transform tobacco plants via T-DNA insertion (Antunes *et al.*, 2017). Several transgenic lines were generated and previously confirmed via PCR of the inserted T-DNA and real-time qPCR target to *SUT1* transcript levels. The transgenic line choose for this work contain 50% less *SUT1* expression in their guard cells with no difference in leaves (Antunes *et al.*, 2017). All the transgenic seeds used in this work are from the homozygous F3 generation.

Plant growth conditions

Tobacco plants were germinated and grown in 5.0 L pots with a substrate composed of a mixture of vermiculite, sand and soil (1:1:1) and kept well irrigated under greenhouse conditions with natural photoperiod (12h/12h light/dark, average of 700 µmol photons m^{-2} s^{-1}, 30 ± 4 ºC and relative humidity 72 ± 20%). Environment parameters such as light intensity, temperature and humidity were recorded every 5 min throughout the entire experiment by a monitoring weather station (Weather Station, WS-1965, Ambient Weather, Chandler, United States) (Fig. S1). All plants were supplemented with Hoagland and Arnon nutrient solution three times a week (Hoagland; Arnon, 1950). 60 days-old plants were used in the experiments.

Diel course of gas exchange and stomatal aperture analyses

Gas exchange analysis was carried out in fully expanded leaves using a portable infrared

gas exchange analyser (IRGA) (LiCor 6400XT, Lincoln, NE, USA). The stomatal conductance (g_s, mol H_2O m^{-2} s^{-1}), net photosynthetic rate (A, μmol m^{-2} s^{-1}), transpiration rate (E, mmol m^{-2} s^{-1}) and the intrinsic water use efficiency (WUE, A/g_s) were estimated from punctual or kinetics analyses (Leakey *et al.*, 2019). The diel course of gas exchange was determined at five different time points, from predawn (ZT 0 - 5 h) until the end of the day (ZT 12) at 5:00 h, 8:00 h, 11:00 h, 14:00 h and 17:00 h. The chamber of the IRGA was set to 1000 μmol of photons m^{-2} s^{-1}, with 10% of blue light, block temperature of 25 ºC and 400 ppm of CO_2.

The stomatal aperture was measured microscopically at the same time points of the gas exchange described above using a well-established method (Scarpeci; Zanor; Valle, 2017). Light-bodied vinylpolysiloxane dental resin (3M ESPE; 3M Dentschland GmbH Dental Products, Neuss, Germany) was applied in the abaxial side of fully expanded leaves until dry (~5 min). The resin impression was then covered with a thin layer of nail polish and after dried the epidermal imprints were placed in a glass slide for photography under an optical microscope with a micrometer ruler for calibration. The measurements of width and length of the stomatal pore were determined using ImageJ software (National Institutes of Health, Bethesda, MD, USA; http://imagej.net/ij/) (Schneider; Rasband; Eliceiri, 2012).

Kinetics of stomatal conductance

Kinetics of stomatal conductance (g_s) in response to exogenous applied compounds were performed in detached leaves, exactly as described previously (Ceciliato *et al.*, 2019). These analyses were carried out using dark (harvested at predawn) and light adapted (harvested 120 min after sunrise) fully expanded wild-type tobacco leaves. The leaves were removed from the plant and immediately placed in a becker containing distilled deionized H_2O, where the petiole was cut to prevent embolism. The compounds were then added to these beckers at the specific time points, according to each experiment (see figure legends). 0.3, 1 or 2.5 mL were taken from stock solution (1 M) to maintain the concentrations of glucose, fructose, sucrose and mannitol (used as osmotic control) equal to 3, 10 or 25 mM in 100 mL beckers. Similarly, ABA was added to a separate becker to keep a final concentration of 5 μM, used here as stomatal closure control. A becker containing H_2O was also used as control. Gas exchange was recorded each 20 seconds for the time indicated in the figures. The condition of the chamber of the IRGA was the same as described above. In order to minimize circadian effects, all measurements were carried out only at the morning period of the day.

Stomatal speediness calculation

Stomatal speediness to opening or closure was estimated by calculating the maximum slope (Sl_{max}) using the linear phase of the g_s kinetic curves (Fig. S9), as previously described (McAusland *et al.*, 2016).

Apoplast wash fluid collection

We adapted a method to collect leaf apoplast wash fluid (AWF) (Gentzel *et al.*, 2019) to perform metabolomics analysis. The collection was performed at the same time points of the gas exchange analysis. Briefly, fully expanded leaves were excised, weighed and inserted into a syringe with 20% (v/v) methanol solution (20% MeOH). After successive pressure movements with the syringe plunger, the leaves were weighed again, wrapped in Parafilm® around a cut 200 µL pipette tip and placed inside a 1.5 mL microcentrifuge tube. The tubes were centrifuged at 1000 *g* for 10 min at 4°C. After, the leaves were weighed, the apoplast wash fluid (AWF) transferred to 2 mL microcentrifuge tube and frozen in liquid nitrogen, as well as leaf section simultaneously harvested and stored at -80 ºC for metabolite extraction. The AWF volume collected was estimated by the difference between leaf weights after infiltration and centrifugation. The purity of the AWF collected by the method use was attested by previous work (Freire et al., 2024, submitted).

Isolation of guard cell-enriched epidermal fragments

Guard cell-enriched epidermal fragments were harvested according to previous protocol optimized for metabolomics analysis (Daloso *et al.*, 2015). Fully expanded tobacco leaves from NtWT and Nt*SUT1* plants were collected at predawn. The first and secondary nervures were removed and the remaining piece of leaves blended with distilled water in a warring blender (Philips, RI 2044 BV Philips International, Amsterdam, Netherlands) with internal filter to remove excess of mesophyll cells and fibers. The filtrate was then filtrated in a 200 µm nylon membrane, washed several times and the retained added in a hyperosmotic solution of 0.5 M Mannitol to maintain the stomata closed until sufficient material was collected. This methodology results in epidermal fragments where at least 95% of the intact cells present are guard cells (Antunes *et al.*, 2017) and has proven efficient to stomatal aperture, metabolite profiling and fluxomics analyses (Daloso *et al.*, 2015, 2016; Lima *et al.*, 2021). The collected guard cells were used in the sugar feeding experiment described below.

Stomatal aperture analysis under exogenous applied sugars

The pool of guard cell-enriched epidermal fragments collected from NtWT and Nt*SUT1* leaves at predawn were filtered, extensively washed to remove the excess of mannitol and transferred to petri dishes containing an opening buffer solution (10 mM MES-Tris, 50 µM $CaCl_2$ and 10 mM KCl, pH 6.15) with or without the addition of sucrose (25 mM). The petri dishes were maintained under light (250 µmol of photons m^{-2} s^{-1}) and harvested after 0, 10, 30, 60 and 180 min. The guard cell-enriched epidermal fragments were collected on the membrane, rapidly washed and dried in a paper and frozen in liquid nitrogen for further metabolomics analysis. In parallel, a drop of the petri dishes solution containing guard cells was added to a glass slide for stomatal aperture analysis.

Metabolic analysis

The extraction of primary metabolites was performed in leaves, AWF and guard cell-enriched epidermal fragments. The extractions were carried out using ~60 mg of grinded leaf powder, ~150 µL of AWF and ~200 mg of grinded epidermal fragments powder. The frozen powder was shaken for 15 min at 350 rpm and 70 °C with methanol containing 0.2 mg mL^{-1} of ribitol as internal quantitative standard. After 10 min of centrifugation at 11000 *g*, the supernatant was collected and added to a new tube with water and chloroform. After 15 min of centrifugation at 11000 *g*, the polar (upper) phase was separated and collected 200 µL, 400 µL and 1000 µL for leaf, AWF and EF samples, respectively. Samples were then dried in a vacuum concentrator. The derivatization and subsequently analysis in gas chromatography coupled to mass spectrometry (GC-MS, QP-PLUS 2010, Shimadzu, Japan) was carried out exactly as described earlier (Lisec *et al.*, 2006). The resulting chromatogram and mass spectral analysis were evaluated using the software Xcalibur® 2.1 (Thermo Fisher Scientific, Waltham, MA, EUA) and the metabolite identification was performed by using the Golm Metabolome Database (http://gmd.mpimp-golm.mpg.de/) (Kopka *et al.*, 2005).

The absolute quantification of sugars was carried out using linear calibration curves of authentic standards of sucrose, glucose and fructose (i.e., >99% purity; e.g., Sigma-Aldrich) (Fig. M1) ran in the GC-MS (Jayasinghe *et al.*, 2018; Rosado-Souza *et al.*, 2019). The volume used to calculate the concentration in the apoplast was previously recorded during the AWF collection and the volume present in the leaves was estimated by the difference between leaf fresh and dry weight for each individual sample. The real apoplast sugar concentrations for each genotype and time point was corrected by the calculation of the dilution factor according to a previous protocol (O'Leary *et al.*, 2014).

Statistical analysis

All the data are represented as average ± standard error (SE). Significant differences among three or more factors were determined by analysis of variance one-way ANOVA and Tukey's test ($P < 0.05$), while the differences between two factors were determined by Student's *t*-test ($P < 0.05$). All statistical and regression analysis were performed using Microsoft Excel software (Microsoft, Redmond, WA, USA), SigmaPlot 14 (Systat Software Inc., San Jose, CA, USA) or Minitab 17 statistical software (Minitab Inc., State College, PA, USA). The metabolomics data were analysed using the MetaboAnalyst platform (Chong *et al.*, 2018).

Results

NtSUT1 plants have reduced stomatal conductance throughout the diel course

A rapid increase in A, g_s, E and stomatal aperture was observed at the first hours of light in both NtWT and Nt*SUT1* tobacco plants, but in a lower magnitude in the transgenic ones (Figs. 1a-c; S2a-c). This dynamic resembles those from plants grown under tropical conditions (see Fig. S1 and Table S1 for the climate conditions of the day of analysis). The intrinsic WUE (A/g_s) increased linearly over the day in both genotypes (Fig. 1d), which is associated to a reduction in g_s from 08:00h to 14:00h while A was maintained relatively stable during this period, especially in the NtWT. These analyses highlight that disruption in the capacity to import sucrose to the guard cells reduces stomatal opening over the diel course, with clear consequences for carbon assimilation.

Guard cell SUT1-downregulation altered the dynamic and the concentration of sugars in the apoplast, but not in leaves

The content (ng mg^{-1} fresh weight) and the concentration (mM) of apoplastic sucrose was lower in Nt*SUT1* plants than the WT at 14h and 17h, respectively. Interestingly, whilst the highest content of apoplastic sucrose was observed at 11:00h in both NtWT and Nt*SUT1* plants, when then it decreased until 17:00h, the concentration of this metabolite increased throughout the day in NtWT and did not change in Nt*SUT1* (Figs. 1e-f). The diel course of glucose and fructose accumulation/degradation was drastically altered in the apoplast of Nt*SUT1* plants, as compared to the NtWT (Figs. 1g-j). For instance, the highest content of apoplastic hexoses was observed at 8:00h and 11:00h in NtWT and Nt*SUT1* plants, respectively. Furthermore, the content of hexoses was maintained high among 08:00h and 14:00h in NtWT, while the peak of

hexose observed at 11:00h was followed by a drastic reduction from 11:00h to 14:00h in Nt*SUT1* (Figs. 1g,i). By contrast to the differences observed at the apoplast, neither the dynamic nor the content or concentration of leaf sucrose was altered in Nt*SUT1* plants (Figs. S3a-b). The highest content and concentration of glucose was observed at 08:00h and 14:00h in leaves of NtWT and Nt*SUT1* plants, respectively (Figs. S3c-d). The dynamic of fructose was similar to glucose in leaves of NtWT, while Nt*SUT1* showed an exquisite dynamic with two peaks of leaf fructose accumulation over the diel course (Figs. S3e-f). These results indicate that antisense inhibition of guard cell *SUT1* substantially alters the apoplastic sugar dynamic, with slight impact on leaf sucrose and hexoses accumulation, suggesting that the differences in the diel course of g_s observed between NtWT and Nt*SUT1* is mostly due to changes in sugar metabolism in the apoplast rather than in leaves.

The dynamic of the apoplast sucrose concentration is negatively associated with g_s

K-means cluster analysis using data from both NtWT and Nt*SUT1* plants highlights an opposite dynamic between g_s and the concentration of sucrose at the apoplast. For instance, the increase in g_s from 05:00h to 08:00h, which corresponds to the dark-to-light transition of the diel course, was accompanied by a reduction in the concentration of sucrose. By contrast, the reduction in g_s from 08:00h to 11:00h and from 14:00h to 17:00h was followed by an increase in sucrose concentration at the apoplast (Fig. 2a). These trends were not observed between g_s and the content of sucrose at the apoplast (which do not consider the volume of the apoplast) (Fig. 2a) as well as between g_s and the concentration and content of leaf sucrose (Fig. 2b). The light-induced stomatal opening observed between 05:00h to 08:00h was positively associated with the concentration of sugars in leaves and at the apoplast, with exception of the apoplastic sucrose concentration that was negatively associated to g_s (Figs. 3a-f). Leaf sugars plus the apoplastic concentration of hexoses were also positively correlated with *A*, *E* and WUE while apoplastic sucrose concentration was negatively correlated with both g_s and *E* during the dark-to-light transition (Figs. 3g-h). Additionally, glucose concentration from both apoplast and leaf was positively correlated with *A*, *E* and WUE while sucrose from both apoplast and leaf was not correlated with these parameters and g_s from 14:00h to 17:00h, the period with strong reduction in g_s (Figs. 3i-j).

These results indicate that the diel course of g_s is regulated by a differential accumulation of sucrose and hexoses between leaves and the apoplast, supporting the idea that

the transport of sucrose among mesophyll cells, leaf apoplast space and guard cells is a key mechanism for stomatal movement regulation.

Beyond sucrose: the accumulation of sugars, sugar alcohols and TCA cycle related metabolites at the apoplast is also important to modulate g_s

We next carried out an unprecedented metabolite profiling analysis of the apoplast harvested over the diel course. Partial least square discriminant analysis (PLS-DA) showed that the primary metabolism differed between leaves and the apoplast as well as between NtWT and Nt*SUT1* plants at most time points of the day (Figs. S4-6). The level of 31 and 25 metabolites was significantly altered in at least one time point in the apoplast and leaves of Nt*SUT1*, respectively, as compared to the NtWT (Figs. S7a-b). The level of several of these metabolites was lower at the apoplast of Nt*SUT1*, while a higher level of certain sugars and sugar alcohols was observed in leaves of Nt*SUT1*, when compared to NtWT (Figs. S7a-b). Interestingly, the level of several sugars and sugar alcohols from the apoplast were positively correlated with g_s from 05:00h to 08:00h and 14:00h to 17:00h (Figs. S8a-b). By contrast, few leaf sugars and sugar alcohols were positively correlated with g_s in these time intervals (Figs. S8c-d), strengthening the idea that sugar accumulation at the apoplast is a major factor underpinning g_s regulation.

K-means clustering analysis revealed that, beyond the concentration of sucrose, the diel course of several metabolites of, or associated to, the tricarboxylic acid (TCA) cycle such as aspartate, beta-alanine, proline, glutamate, citrate, fumarate, succinate and malate had an opposite trend in the apoplast than g_s (see Clusters 4 and 5; Fig. 2c) and were negatively correlated with g_s (Fig. 3k). By contrast, several sugars, sugar alcohols plus pyruvate, serine and *trans*-cinnamic acid from the apoplast were clustered together with A, g_s and E (Fig. 2c). These trends were not observed in leaves and none of the TCA cycle related metabolites from leaves were significantly correlated with g_s (Figs. 2d; 3l). It is noteworthy that only fructose, glucose, maltose and 2-amino-2-deoxy glucose from both leaves and apoplast were clustered together with A, g_s and E (Figs. 2c,d), being thus good markers of the dynamic of the leaf gas exchange despite their accumulation in leaves or at the apoplast. These analyses collectively indicate that the dynamic of other primary metabolites at the apoplast, especially those associated with the TCA cycle, may be also involved in the A-g_s trade-off regulation.

The concentration of exogenously applied sucrose determines the rate and the speed of stomatal opening and closure

We next investigated the effect of exogenous application of different concentrations of sucrose, glucose and fructose on stomatal kinetics in dark or light-adapted WT leaves (Figs. S9a-b), comparing with stomatal kinetics under H_2O (general control), mannitol (osmotic control), and ABA (stomatal closure control) (Figs. S10a-n and S11a-n). The kinetics of stomatal opening differ substantially according to the sugar concentration applied in dark-adapted leaves. Whilst the kinetic under H_2O follows a typical sigmoid model observed during the dark-to-light transition, increasing the concentration of exogenously applied sugars leads to a gaussian model, with a peak of g_s approximately 30 min after light imposition followed by a strong decrease in g_s (Figs. 4a-d). This response was also observed under mannitol, but the speed of stomatal opening (Sl_{max}) was higher under sucrose 25 mM than all the other treatments (Fig. 4e). In contrast, the speed of stomatal closure of several treatments including ABA and the highest concentration of mannitol, glucose, fructose and sucrose differed from the H_2O control (Fig. 4f). The concentration of exogenously applied mannitol, glucose, fructose and sucrose was positively associated to the speed of both stomatal opening and closure, but the effect on the speed of stomatal opening is much higher when sucrose is applied (Figs. 4g-n).

In light-acclimated leaves, in which g_s was at steady state when sugars were applied (Fig. S9b), the addition of H_2O did not change g_s while ABA application induced a rapid stomatal closure as expected (Fig. 5a). The magnitude of the sugar-induced stomatal closure was concentration dependent. However, hexoses and sucrose, but not mannitol, slightly increased g_s before the closure when 10 mM and especially 25 mM were applied (Figs. 5b-d). Furthermore, only 10 and 25 mM of hexoses and sucrose increased the speed of stomatal opening (Fig. 5e), although regression analysis suggests that only the concentration of hexoses have a linear and significant relationship with Sl_{max} (Figs. 5g-j). The stomata rapidly closed after approximately 15 min of exogenous application of 10 or 25 mM of all metabolites, with no difference in the speed of stomatal closure among these compounds (Fig. 5f). In this case, the Sl_{max} was linearly related to the concentration of the compound applied, except in fructose (Figs. 5k-n). These results collectively indicate that an osmotic coupled to a sucrose-mediated and concentration-dependent mechanisms determine the rate and the speed of stomatal movements in either dark or light acclimated leaves.

The role of sucrose for stomatal opening and closure depends on its importation to the guard cells

We next harvested guard cell enriched epidermal fragments (GCEFs) from NtWT and Nt*SUT1* plants at predawn and subjected them to an opening buffer solution containing (OBS) or not (OB) 25 mM of sucrose. After 0, 10, 30, 60 and 180 min under white light, stomatal aperture was measured and the GCEFs were frozen for metabolomics analysis. The dynamic of stomatal aperture showed a hyperbolic increase over time in OB, whilst OBS showed a maximum of stomatal aperture at 30 and 10 min in NtWT and Nt*SUT1*, respectively, when then it drastically reduced in the NtWT, but not in Nt*SUT1*, until 180 min (Figs. 6a,e). This dynamic was similar to the g_s one observed previously, demonstrating the feasibility of the approach using GCEFs (Figs. S12a-b). Light-induced stomatal opening was higher in NtWT than Nt*SUT1* and higher under OBS than OB in each genotype (Figs. 6a,e; S13a). This analysis reinforces the idea that the role of sucrose for stomatal opening depends partially on its importation to the guard cells.

Stomatal aperture is modulated by the dynamic of accumulation/degradation of sucrose and TCA cycle metabolites within guard cells

Metabolite profiling analysis revealed that guard cell metabolism of both NtWT and Nt*SUT1* changed over time, as indicated by the separation of the samples harvested at 10, 30, 60 and 180 min from the time 0 min by the PC1 of the PLS-DA's (Figs. S14a-d). This analysis further indicates that the metabolism of NtWT and Nt*SUT1* guard cells differed mainly under OB, as evidenced by the separation of these genotypes under OB but not under OBS (Figs. S14e-f). The content of sucrose, glucose and fructose from the OBS treatment followed the same gaussian-like model of stomatal aperture in NtWT, but the highest sugar content and stomatal aperture were observed at 10 and 30 min, respectively (Figs. 6b-d). However, the content of these sugars decreased linearly from 10 to 60 min, when then slightly increased until 180 min. None of these trends were observed under OB in NtWT, in which sucrose decreased linearly while hexoses slightly changed over time (Figs. 6b-d). The content of all sugars decreased in Nt*SUT1* OB and increased until a plateau in Nt*SUT1* OBS over time (Fig. 6f-h).

Sucrose and glucose content were negatively correlated with stomatal aperture in NtWT under OB from 0 to 10 min after light imposition. This was neither observed in NtWT OB in the other time intervals nor in Nt*SUT1* OB in all time intervals (Figs. 15a-h). By contrast, glucose and fructose content was positively correlated with stomatal aperture in Nt*SUT1* OB during the dark-to-light transition (i.e. from 0 to 10 and 10 to 30 min) (Figs. 15e-f). The exogenously application of sucrose leads to a positive correlation between sucrose and hexoses

with stomatal aperture in NtWT OBS during the dark-to-light transition (Fig. S15i). Nonetheless, between one to three hours (from 60 to 180 min) of exposure to 25 mM of sucrose, this correlation was negative (Fig. S15l). In Nt*SUT1* OBS, only sucrose from 0 to 10 min was (positively) correlated with stomatal aperture (Figs. S15m-p). These results highlight that sucrose importation and its degradation within guard cells is important to modulate stomatal opening during the dark-to-light transition as well as that the excess of sucrose imported to the guard cells end up stimulating stomatal closure.

Stomatal aperture was clustered with sucrose and the TCA cycle metabolites malate, citrate and succinate in NtWT (see Clt3; Fig. S16a). The dynamic of accumulation/degradation of the metabolites of the Clt4 showed an opposite trend than the Clt3, while Clt1 and Clt5 decreased and Clt2 was invariable over time (Fig. S16a). In Nt*SUT1*, stomatal aperture (Clt3) was neither clustered with sucrose nor with TCA cycle metabolites. The level of the metabolites found in Clt4 in NT*SUT1* decreased over time, which includes several sugars, organic acids and amino acids (Fig. S16b), which might a compensatory mechanism to release more carbon to the metabolism given the lower capacity of Nt*SUT1* guard cells in importing sucrose.

Discussion

Sucrose has been historically pointed as a key metabolite for stomatal movements regulation. However, the exact mechanism by which sucrose regulates stomatal movements diverge among the theories created in the last >100 years (discussed here in through the name of the main author of the most representative works). Initially, the sucrose-starch theory (Lloyd's "theory") proposed that sugar and starch synthesis within guard cells would be a mechanism to stimulate stomatal opening and closure, respectively (Lloyd, 1908). This idea was later supported by findings showing that guard cell starch content was quantitatively related to stomatal aperture (Outlaw; Manchester, 1979) and that sucrose was supposed to be the main osmolyte accumulated within guard cells to maintain stomatal opening in the afternoon period of the day (Zeiger's "theory") (Amodeo; Talbott; Zeiger, 1996; Talbott; Zeiger, 1996). Later, several works proposed that the transport of sucrose from mesophyll cells to the guard cell apoplast would be a mechanism to induce stomatal closure in periods of high photosynthetic rate ("Outlaw's "theory") (Kang, Yun *et al.*, 2007; Kang, YUN *et al.*, 2007; Lu *et al.*, 1995, 1997). These ideas were recently complemented by studies showing that: (i) sucrose can induce stomatal closure when applied at high concentrations (Kelly *et al.*, 2013; Medeiros *et al.*, 2018), including in basal lineage of plants (Cândido-Sobrinho *et al.*, 2022; Kottapalli *et al.*, 2018), (ii)

the sucrose-mediated stomatal closure depends on hexokinase and involves ABA signalling pathway within guard cells (Granot's "theory") (Kelly *et al.*, 2013, 2019; Lugassi *et al.*, 2015), (iii) the role of guard cell sucrose for stomatal opening is primarily energetic (Daloso's "theory") (Daloso *et al.*, 2015, 2016; Freire *et al.*, 2021; Lima *et al.*, 2023; Medeiros *et al.*, 2018; Ni, 2012; Robaina-Estévez *et al.*, 2017), and (iv) starch is degraded within guard cells during the blue light-induced stomatal opening (Santelia's "theory") (Azoulay-Shemer *et al.*, 2016; Guard cell starch degradation yields glucose for rapid stomatal opening in ArabidopsisFlütsch *et al.*, 2020; Horrer *et al.*, 2016). These studies collectively highlight that guard cell carbohydrate metabolism is crucial for the regulation of stomatal movements, but no consensus concerning the mechanisms behind it was achieved after more than 100 years of studies.

Although several of these works seem to contradict each other, these ideas/theories were built on well-performed experiments, good analytical results, using different species and well-established metabolic principles. This suggests that none of these theories are absolutely wrong and could thus coexist. For instance, although several recent works showed that sucrose is degraded within guard cells during the dark-to-light transition (Daloso *et al.*, 2015, 2016; Lima *et al.*, 2023; Medeiros *et al.*, 2018; Robaina-Estévez *et al.*, 2017), partially contradicting Zeiger's theory (Amodeo; Talbott; Zeiger, 1996; Zeiger1; Zhu, 1998), transgenic and mutant plants with reduced capacity to import sucrose to the guard cells have lower g_s (Antunes *et al.*, 2017; Glucose uptake to guard cells via STP transporters provides carbon sources for stomatal opening and plant growthFlütsch *et al.*, 2020), as showed here (Fig. 1b). The lower g_s and stomatal aperture in Nt*SUT1* plants was strongly associated to the lower capacity of these plants to import sucrose to their guard cells. In turn, lower sucrose within guard cells could compromise both osmotic regulation and energy production within these cells, given support to both Zeiger and Daloso's theories. Additionally, although Granot and Outlaw's theories seem controversial regarding the mechanisms by which sucrose induce stomatal closure, which relies on whether sucrose is accumulated at the apoplast or imported to the guard cells during stomatal closure, we hypothesized that these mechanisms could occur simultaneously (Lima *et al.*, 2018). Indeed, our results demonstrated that the diel course of g_s is underpinned mainly by the concentration of sucrose and other metabolites at the apoplast (Fig. 2a), but this and other stomatal responses observed here were reduced in Nt*SUT1* plants (Figs. 1b and 6a,e). This indicates that the role of sucrose for stomatal closure is strongly associated to its level at the

apoplast and partially depends on its importation to the guard cells, supporting both Granot and Outlaw's theories.

Our results further suggest that sucrose availability determines the rate and the speed of stomatal movements, which tightly connects g_s regulation with *A*. The concentration of leaf sugars (sucrose, glucose and fructose) was positively correlated with *A*, g_s and WUE during the dark-to-light transition (Figs. 2c,f). This is rather than expected, given that sugars are the major photoassimilates produced in leaves (Fettke; Fernie, 2015) and that the *A*-g_s relationship is linear in the first hours of light, especially in plants grown under tropical conditions (Lima *et al.*, 2019). Thus, high *A* leads to high sucrose production in mesophyll cells, which is transported, imported and degraded within guard cells during the dark-to-light transition. Evidence supporting this idea is several fold: (i) both the rate and the speed of stomatal opening were higher as the concentration of exogenously applied sucrose increased (Figs. 4b-j; 6a,e), (ii) the increase in stomatal aperture mediated by sucrose exogenous application was lower in Nt*SUT1* plants (Figs. 6a,e), (iii) sucrose was degraded within guard cells under OB treatment (Figs. 6d,h), and (iv) g_s was negatively correlated with sucrose concentration at the apoplast during the dark-to-light transition (Figs. 2c,f). These results are further supported by findings showing that plants with reduced capacity to import or degrade sugars within guard cells have lower g_s (Antunes *et al.*, 2017; Glucose uptake to guard cells via STP transporters provides carbon sources for stomatal opening and plant growthFlütsch *et al.*, 2020; Freire *et al.*, 2021; Kelly *et al.*, 2013; Lugassi *et al.*, 2015; Ni, 2012), while plants with increased sucrose degradation capacity within guard cells have higher g_s (Antunes *et al.*, 2012; Daloso *et al.*, 2016). This mechanism aids to explain the evolution of g_s regulation, given that plants with higher *A* have higher accumulation of primary metabolites (including sucrose) and higher g_s (Carriquí *et al.*, 2015; Gago *et al.*, 2019; Lima *et al.*, 2019; Tosens *et al.*, 2016).

Beyond stomatal opening, our results highlight that sucrose is a master regulator of the stomatal closure. For example, the decreases in g_s were accompanied by increases in sucrose concentration at the apoplast over the diel course (Fig. 2a). Moreover, sucrose exogenous application induced stomatal closure in a concentration-dependent manner (Figs. 4b-d; 5b-d). These results suggest that sucrose is a metabolite that reduce g_s in periods of high *A*. Interestingly, sucrose exogenously application induced stomatal opening before the closure in a concentration-dependent manner in either previously dark or light-adapted leaves (Figs. 4a-d; 5a-d). Thus, photosynthetic-derived sucrose acts as a signalling mechanism to open the stomata likely until sufficient photoassimilates are produced, when then the stomata close, as a

mechanism to improve WUE under non-source limited conditions, as previously proposed (Outlaw's theory) (Outlaw, 2003). In fact, g_s reduced while *A* was maintained stable from 08:00h to 14:00h (Figs. 1a-b), which leads to a linear increase of WUE in NtWT throughout the day (Fig. 1d). It is noteworthy that the sucrose-induced stomatal closure was less prominent in Nt*SUT1* plants (Figs. 6a,e), suggesting that its importation to the guard cells is also important for stomatal closure, given support to Granot's theory. Indeed, the concentration of sucrose within guard cells was up to ~2-fold higher in NtWT than Nt*SUT1* under OBS treatment, which explain the differences in stomatal opening and closure observed between these genotypes. Recent results showed that ABA-unresponsive ferns can close the stomata under exogenous application of sucrose, but in a lower speed when compared to angiosperms (Cândido-Sobrinho *et al.*, 2022). Thus, the sucrose-induced stomatal closure mechanism described here could explain the origin of stomatal closure control in land plants. However, further studies are needed to prove whether this hypothesis holds true or not.

Beyond sugars, TCA cycle related metabolites have also historically been implicated with stomatal movement regulation. Evidence suggests that malate accumulation at the apoplast and withing guard cells plays an important role for stomatal movement regulation (Araújo *et al.*, 2011; Daloso *et al.*, 2015; Hedrich; Marten, 1993; Nunes-Nesi *et al.*, 2007). Here, the apoplastic level of malate, succinate and citrate plus proline, aspartate, beta-alanine and glutamate, that are closely associated to the TCA cycle, were negatively correlated with g_s during the dark-to-light transition (Figs. 3k-l). Furthermore, the level of malate, citrate and succinate within guard cells was clustered with sucrose and stomatal aperture in NtWT but not in Nt*SUT1* plants during the dark-to-light transition (Fig. S16a). This highlights that sucrose importation to the guard cells is crucial for guard cell metabolism homeostasis and, as consequence, for the regulation of stomatal movements. Indeed, PLS-DA showed that the primary metabolism is substantially different between NtWT and Nt*SUT1* guard cells, but this difference disappears in guard cells fed with sucrose (Figs. S14e-f). These results collectively indicate that guard cell sugars and organic acids are tightly regulated as well as that, beyond sugars, the accumulation of organic acids at the apoplast and within guard cells is important for the regulation of stomatal opening.

In summary, our results provide compelling evidence highlighting that sucrose can induce and speed up both stomatal opening and closure in a concentration and location of accumulation dependent manner, given support to Zeiger, Daloso, Granot and Outlaw's theories. It is noteworthy that scientific theories are built on the continue search for improving

methods, experimental approaches and theoretical knowledge to test and validate (or not) old and new hypothesis. Therefore, the model proposed here for the role of sucrose for stomatal movement regulation was only made possible by the contribution of each of these and several other works carried out in the last >100 years.

Acknowledgments

This work was partially supported by the National Institute of Science and Technology in Plant Physiology under Stress Conditions (INCT Plant Stress Physiology – Grant: 406455/2022–8) and the National Council for Scientific and Technological Development (CNPq, grants 404817/2021–1). The authors gratefully acknowledge the CNPq for the PhD fellowship to F.B.S.F. (Grant 141043/2020-2), for the PostDoc fellowship to P.A.A. (Grant 150277/2020-2) and the research fellowship to D.M.D. (Grant 306870/2023-1). We also thank the scholarship granted by the Brazilian Federal Agency for Support and Evaluation of Graduate Education (CAPES-Brazil) to E.G.M. and M.S.L.

Author contributions

F.B.S.F. and D.M.D. designed the research and experiments; F.B.S.F., E.G.M., M.S.L., P.A.A. and D.M.D. performed the experiments; all authors contributed to write the final manuscript; D.M.D. obtained funding.

Funding

This work was partially supported by the National Institute of Science and Technology in Plant Physiology under Stress Conditions (INCT Plant Stress Physiology – Grant: 406455/2022-8) and the National Council for Scientific and Technological Development (CNPq, Grant No. 404817/2021-1).

Conflict of interest

The authors declare no conflict of interest.

References

AMODEO, G.; TALBOTT, L. D.; ZEIGER, E. Use of potassium and sucrose by onion guard cells during a daily cycle of osmoregulation. **Plant and Cell Physiology**, [*s. l.*], v. 37, n. 5, p. 575–579, 1996.

ANTUNES, W. C. *et al.* Changes in stomatal function and water use efficiency in potato

plants with altered sucrolytic activity. **Plant, Cell and Environment**, [*s. l.*], v. 35, n. 4, p. 747–759, 2012.

ANTUNES, W. C. *et al.* Guard cell-specific down-regulation of the sucrose transporter SUT1 leads to improved water use efficiency and reveals the interplay between carbohydrate metabolism and K+ accumulation in the regulation of stomatal opening. **Environmental and Experimental Botany**, [*s. l.*], v. 135, p. 73–85, 2017. Disponível em: http://dx.doi.org/10.1016/j.envexpbot.2016.12.004.

ARAÚJO, W. L. *et al.* Antisense Inhibition of the Iron-Sulphur Subunit of Succinate Dehydrogenase Enhances Photosynthesis and Growth in Tomato via an Organic Acid–Mediated Effect on Stomatal Aperture. **The Plant Cell**, [*s. l.*], v. 23, n. 2, p. 600–627, 2011. Disponível em: http://www.plantcell.org/lookup/doi/10.1105/tpc.110.081224.

AZOULAY-SHEMER, T. *et al.* Starch Biosynthesis in Guard Cells But Not in Mesophyll Cells Is Involved in CO2-Induced Stomatal Closing. **Plant physiology**, [*s. l.*], v. 171, n. 2, p. 788–798, 2016.

BRODRIBB, T. J.; SUSSMILCH, F.; MCADAM, S. A. M. From Reproduction to Production, Stomata are the Master Regulators. **The Plant Journal**, [*s. l.*], p. tpj.14561, 2019.

CÂNDIDO-SOBRINHO, S. A. *et al.* Metabolism-mediated mechanisms underpin the differential stomatal speediness regulation among ferns and angiosperms. **Plant, Cell & Environment**, [*s. l.*], v. 45, n. 2, p. 296–311, 2022. Disponível em: https://onlinelibrary.wiley.com/doi/10.1111/pce.14232.

CARRIQUÍ, M. *et al.* Diffusional limitations explain the lower photosynthetic capacity of ferns as compared with angiosperms in a common garden study. **Plant, Cell and Environment**, [*s. l.*], v. 38, n. 3, p. 448–460, 2015.

COCKBURN, W. Stomatal mechanism as the basis of the evolution of CAM and C4 photosynthesis. **Plant, Cell & Environment**, [*s. l.*], v. 6, n. 4, p. 275–279, 1983.

DALOSO, D. M. *et al.* Guard cell-specific upregulation of sucrose synthase 3 reveals that the role of sucrose in stomatal function is primarily energetic. **New Phytologist**, [*s. l.*], v. 209, n. 4, p. 1470–1483, 2016.

DALOSO, D. M. *et al.* Metabolism within the specialized guard cells of plants. **New Phytologist**, [*s. l.*], v. 216, n. 4, p. 1018–1033, 2017.

DALOSO, D. M. *et al.* Tobacco guard cells fix CO2 by both Rubisco and PEPcase while sucrose acts as a substrate during light-induced stomatal opening. **Plant Cell and Environment**, [*s. l.*], v. 38, n. 11, p. 2353–2371, 2015.

DALOSO, D. M.; DOS ANJOS, L.; FERNIE, A. R. Roles of sucrose in guard cell regulation. **New Phytologist**, [*s. l.*], v. 211, n. 3, p. 809–818, 2016.

DAUBERMANN, A. G. *et al.* Novel guard cell sink characteristics revealed by a multi-species/cell-types meta-analysis of 13C-labelling experiments. **Theoretical and Experimental Plant Physiology**, [*s. l.*], n. 0123456789, 2024. Disponível em: https://doi.org/10.1007/s40626-023-00299-9.

FETTKE, J.; FERNIE, A. R. Intracellular and cell-to-apoplast compartmentation of carbohydrate metabolism. **Trends in Plant Science**, [*s. l.*], v. 20, n. 8, p. 490–497, 2015.

FLÜTSCH, S. *et al.* Glucose uptake to guard cells via STP transporters provides carbon sources for stomatal opening and plant growth. **EMBO reports**, [*s. l.*], v. 21, n. 8, 2020. Disponível em: https://onlinelibrary.wiley.com/doi/abs/10.15252/embr.201949719.

FLÜTSCH, S. *et al.* Guard cell starch degradation yields glucose for rapid stomatal opening in Arabidopsis. **Pant Cell, in press**, [*s. l.*], 2020.

FLÜTSCH, S.; HORRER, D.; SANTELIA, D. Starch biosynthesis in guard cells has features of both autotrophic and heterotrophic tissues. **Plant Physiology**, [*s. l.*], p. 541–556, 2022.

FLÜTSCH, S.; SANTELIA, D. Mesophyll-derived sugars are positive regulators of light-driven stomatal opening. **New Phytologist**, [*s. l.*], v. 230, n. 5, p. 1754–1760, 2021.

FLÜTSCH, S.; SANTELIA, D. Mesophyll-derived sugars are positive regulators of light-driven stomatal opening. **New Phytologist**, [*s. l.*], v. 230, n. 5, p. 1754–1760, 2021. Disponível em: https://onlinelibrary.wiley.com/doi/10.1111/nph.17322.

FREIRE, F. B. S. *et al.* Mild reductions in guard cell sucrose synthase 2 expression leads to slower stomatal opening and decreased whole plant transpiration in Nicotiana tabacum L. **Environmental and Experimental Botany**, [*s. l.*], v. 184, n. October 2020, 2021.

GAGO, J. *et al.* Photosynthesis Optimized across Land Plant Phylogeny. **Trends in Plant Science**, [*s. l.*], v. 73, p. 1–12, 2019.

GRANOT, D.; KELLY, G. Evolution of Guard-Cell Theories: The Story of Sugars. **Trends in Plant Science**, [*s. l.*], v. 24, n. 6, p. 507–518, 2019. Disponível em: https://doi.org/10.1016/j.tplants.2019.02.009.

HEDRICH, R.; MARTEN, I. Malate-induced feedback regulation of plasma membrane anion channels could provide a CO2 sensor to guard cells. **The EMBO journal**, [*s. l.*], v. 12, n. 3, p. 897–901, 1993.

HITE, D. R. C.; OUTLAW, W. H.; TARCZYNSKI, M. C. Elevated levels of both sucrose-phosphate synthase and sucrose synthase in Vicia guard cells indicate cell-specific carbohydrate interconversions. **Plant physiology**, [*s. l.*], v. 101, n. 4, p. 1217–1221, 1993.

HORRER, D. *et al.* Blue light induces a distinct starch degradation pathway in guard cells for stomatal opening. **Current Biology**, [*s. l.*], v. 26, n. 3, p. 362–370, 2016.

HUBBARD, K. E.; WEBB, A. A. R. Circadian Rhythms in Stomata: Physiological and Molecular Aspects. *In*: RHYTHMS IN PLANTS. Cham: Springer International Publishing, 2015. p. 231–255. Disponível em: http://link.springer.com/10.1007/978-3-319-20517-5_9.

KANG, YUN *et al.* Guard-cell apoplastic sucrose concentration – a link between leaf photosynthesis and stomatal aperture size in the apoplastic phloem loader Vicia faba L. **Plant, Cell & Environment**, [*s. l.*], v. 30, n. 5, p. 551–558, 2007. Disponível em: http://doi.wiley.com/10.1111/j.1365-3040.2007.01635.x.

KANG, Yun *et al.* Guard cell apoplastic photosynthate accumulation corresponds to a

phloem-loading mechanism. **Journal of Experimental Botany**, [*s. l.*], v. 58, n. 15–16, p. 4061–4070, 2007.

KELLY, G. *et al.* Guard-Cell Hexokinase Increases Water-Use Efficiency Under Normal and Drought Conditions. **Frontiers in plant science**, [*s. l.*], v. 10, p. 1499, 2019. Disponível em: https://www.frontiersin.org/article/10.3389/fpls.2019.01499/full.

KELLY, G. *et al.* Hexokinase mediates stomatal closure. **Plant Journal**, [*s. l.*], v. 75, n. 6, p. 977–988, 2013.

KELLY, G. *et al.* The Solanum tuberosum KST1 partial promoter as a tool for guard cell expression in multiple plant species. **Journal of Experimental Botany**, [*s. l.*], v. 68, n. 11, p. 2885–2897, 2017.

KOTTAPALLI, J. *et al.* Sucrose-induced stomatal closure is conserved across evolution. **PLoS ONE**, [*s. l.*], v. 13, n. 10, p. 1–17, 2018.

LAWSON, T. Guard cell photosynthesis and stomatal function. **New Phytologist**, [*s. l.*], v. 181, n. 1, p. 13–34, 2009. Disponível em: http://doi.wiley.com/10.1111/j.1469-8137.2008.02685.x.

LAWSON, T.; MATTHEWS, J. Guard Cell Metabolism and Stomatal Function. **Annual Review ofPlant Biology**, [*s. l.*], v. 71, p. 273–302, 2020.

LEAKEY, A. D. B. *et al.* Water Use Efficiency as a Constraint and Target for Improving the Resilience and Productivity of C 3 and C 4 Crops. **Annual Review of Plant Biology**, [*s. l.*], v. 70, n. 1, p. 781–808, 2019. Disponível em: https://www.annualreviews.org/doi/10.1146/annurev-arplant-042817-040305.

LIM, S.-L. *et al.* Arabidopsis guard cell chloroplasts import cytosolic ATP for starch turnover and stomatal opening. **Nature Communications**, [*s. l.*], v. 13, n. 1, p. 652, 2022. Disponível em: https://www.nature.com/articles/s41467-022-28263-2.

LIMA, V. F. *et al.* The sucrose-to-malate ratio correlates with the faster CO2 and light stomatal responses of angiosperms compared to ferns. **New Phytologist**, [*s. l.*], v. 223, n. 4, p. 1873–1887, 2019. Disponível em: https://onlinelibrary.wiley.com/doi/abs/10.1111/nph.15927.

LIMA, V. F. *et al.* Toward multifaceted roles of sucrose in the regulation of stomatal movement. **Plant Signaling and Behavior**, [*s. l.*], v. 13, n. 8, p. 1–8, 2018. Disponível em: https://doi.org/10.1080/15592324.2018.1494468.

LIMA, V. F. *et al.* Unveiling the dark side of guard cell metabolism. **Plant Physiology and Biochemistry**, [*s. l.*], p. 107862, 2023. Disponível em: https://doi.org/10.1016/j.plaphy.2023.107862.

LLOYD, F. . E. The physiology of stomata. **Publications of the Carnegie Institution of Washington**, [*s. l.*], v. 82, p. 1–42, 1908.

LU, P. *et al.* A New Mechanism for the Regulation of Stomatal Aperture Size in Intact Leaves (Accumulation of Mesophyll-Derived Sucrose in the Guard-Cell Wall of Vicia faba). **Plant Physiology**, [*s. l.*], v. 114, n. 1, p. 109–118, 1997. Disponível em:

https://academic.oup.com/plphys/article/114/1/109/6071024.

LU, P. *et al.* Sucrose: a solute that accumulates in the guard-cell apoplast and guard-cell symplast of open stomata. **FEBS Letters**, [*s. l.*], v. 362, n. 2, p. 180–184, 1995. Disponível em: http://doi.wiley.com/10.1016/0014-5793%2895%2900239-6.

LUGASSI, N. *et al.* Expression of Arabidopsis Hexokinase in Citrus Guard Cells Controls Stomatal Aperture and Reduces Transpiration. **Frontiers in Plant Science**, [*s. l.*], v. 6, n. December, p. 1–11, 2015. Disponível em: http://journal.frontiersin.org/Article/10.3389/fpls.2015.01114/abstract.

MEDEIROS, D. B. *et al.* Sucrose breakdown within guard cells provides substrates for glycolysis and glutamine biosynthesis during light-induced stomatal opening. **Plant Journal**, [*s. l.*], v. 94, n. 4, p. 583–594, 2018.

NI, D. A. Role of vacuolar invertase in regulating Arabidopsis stomatal opening. **Acta Physiologiae Plantarum**, [*s. l.*], v. 34, n. 6, p. 2449–2452, 2012. Disponível em: http://link.springer.com/10.1007/s11738-012-1036-5.

NUNES-NESI, A. *et al.* Deficiency of mitochondrial fumarase activity in tomato plants impairs photosynthesis via an effect on stomatal function. **The Plant Journal**, [*s. l.*], v. 50, n. 6, p. 1093–1106, 2007. Disponível em: http://doi.wiley.com/10.1111/j.1365-313X.2007.03115.x.

OUTLAW, W. H. J. Integration of Cellular and Physiological Functions of Guard Cells. **Critical Reviews in Plant Sciences**, [*s. l.*], v. 22, n. 6, p. 503–5229, 2003.

OUTLAW, W. H. J. Sucrose and stomata: a full circle. *In*: MADORE, M. A.; LUCUS, W. J. (org.). **Carbon Partitioning and Source–Sink Interactions in Plants**. Rockville, MD, USA: American Society of Plant Physiologists, 1995. p. 56–67.

OUTLAW, W. H.; MANCHESTER, J. Guard cell starch concentration quantitatively related to stomatal aperture. **Plant physiology**, [*s. l.*], v. 64, p. 79–82, 1979.

PIRO, L.; FLÜTSCH, S.; SANTELIA, D. Arabidopsis Sucrose Synthase 3 (SUS3) regulates starch accumulation in guard cells at the end of day. **Plant Signaling and Behavior**, [*s. l.*], v. 18, n. 1, p. 4–8, 2023.

ROBAINA-ESTÉVEZ, S. *et al.* Resolving the central metabolism of Arabidopsis guard cells. **Scientific Reports**, [*s. l.*], v. 7, n. 1, p. 1–13, 2017.

TALBOTT, L. D.; ZEIGER, E. Central roles for potassium and sucrose in guard-cell osmoregulation. **Plant Physiology**, [*s. l.*], v. 111, n. 4, p. 1051–1057, 1996.

TALBOTT, L. D.; ZEIGER, E. The role of sucrose in guard cell osmoregulation. **Journal of Experimental Botany**, [*s. l.*], v. 49, n. Special, p. 329–337, 1998. Disponível em: https://academic.oup.com/jxb/article-lookup/doi/10.1093/jxb/49.Special_Issue.329.

TOSENS, T. *et al.* The photosynthetic capacity in 35 ferns and fern allies: Mesophyll CO2diffusion as a key trait. **New Phytologist**, [*s. l.*], v. 209, n. 4, p. 1576–1590, 2016.

WANG, H. *et al.* A Subsidiary Cell-Localized Glucose Transporter Promotes Stomatal

Conductance and Photosynthesis. **The Plant cell**, [*s. l.*], v. 31, n. 6, p. 1328–1343, 2019.

WILLE, A. C.; LUCAS, W. J.; ZEA, L. Ultrastructural and histochemical studies on guard cells. **Planta**, [*s. l.*], v. 160, n. 2, p. 129–142, 1984. Disponível em: http://link.springer.com/10.1007/BF00392861.

WILLMER, C.; FRICKER, M. **Stomata**. 2. ed. Dordrecht: Springer Netherlands, 1996. Disponível em: http://link.springer.com/10.1007/978-94-011-0579-8.

ZEIGER, E. *et al.* The guard cell chloroplast: a perspective for the twenty-first century. **New Phytologist**, [*s. l.*], v. 153, n. 3, p. 415–424, 2002. Disponível em: http://doi.wiley.com/10.1046/j.0028-646X.2001.NPH328.doc.x.

ZEIGER1, E.; ZHU, J. Role of zeaxanthin in blue light photoreception and the modulation of light–CO 2 interactions in guard cells. **Journal of Experimental Botany**, [*s. l.*], v. 49, n. March, p. 433–442, 1998.

Main Figures

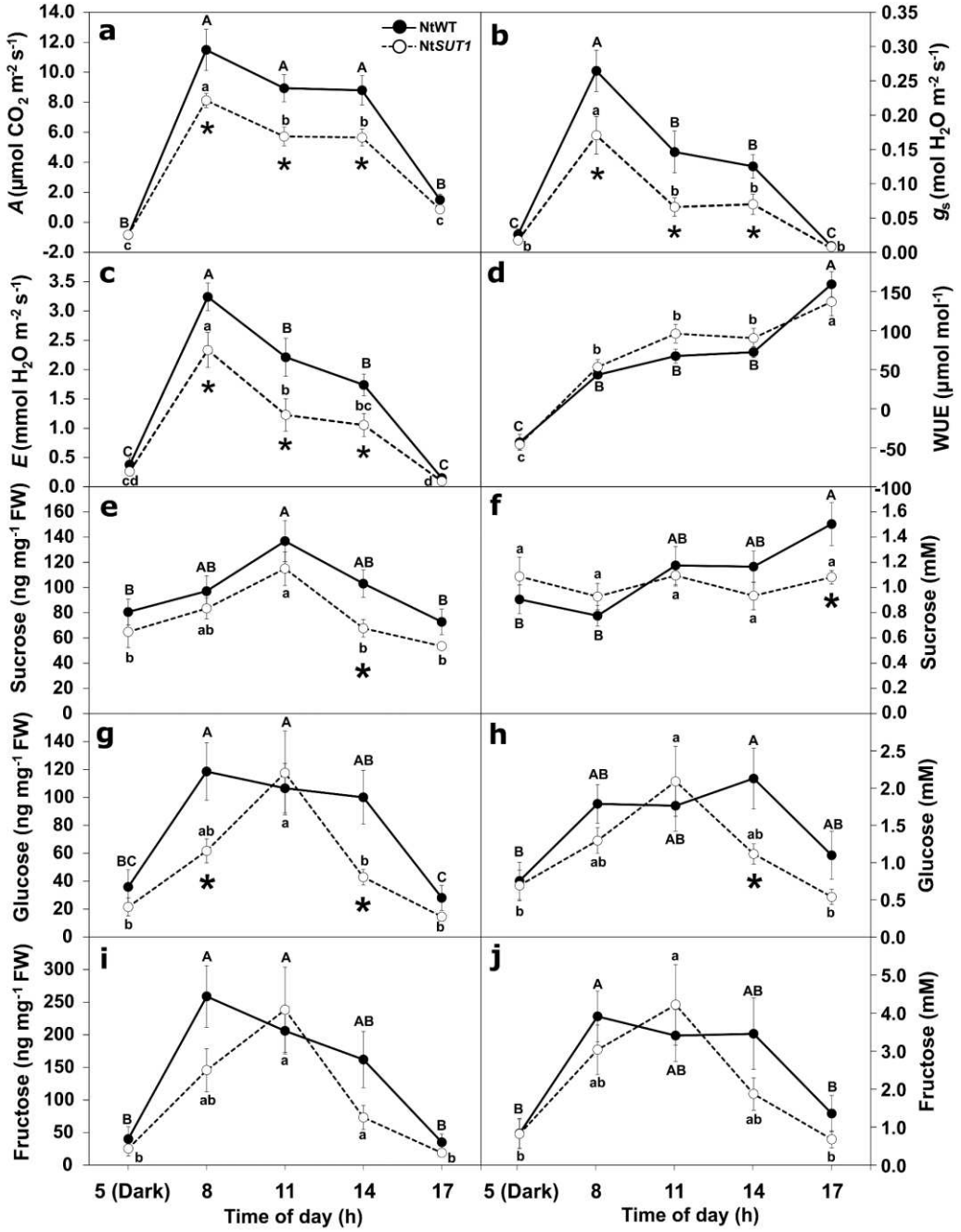

Figure 1. Diel course of gas exchange and concentration of sugars at the apoplast of *Nicotiana tabacum* wild type (NtWT) and the transgenic line antisense to the *SUT1* gene (Nt*SUT1*). The diel course of photosynthetic rate (*A*) (**a**), stomatal conductance (g_s) (**b**), transpiration rate (*E*) (**c**) and water use efficiency (WUE) (**d**) was determined using an infrared gas exchange analyser. The concentration of the apoplastic sucrose, glucose and fructose were determined by the leaf fresh weight (FW) (**e**, **g**, **i**) and at molar level (**f**, **h**, **j**). These analyses were carried out in fully expanded leaves from plants grown under greenhouse and well-watered conditions. Different uppercase and lowercase letters indicate significant differences between time-points of NtWT and Nt*SUT1* genotype, respectively, by ANOVA and Tukey's test ($P < 0.05$). Asterisks (*) indicate significant difference between NtWT and Nt*SUT1* in each time-point by Student's *t* test ($P < 0.05$). The data are represented as average ± standard error (n = 5 ± SE).

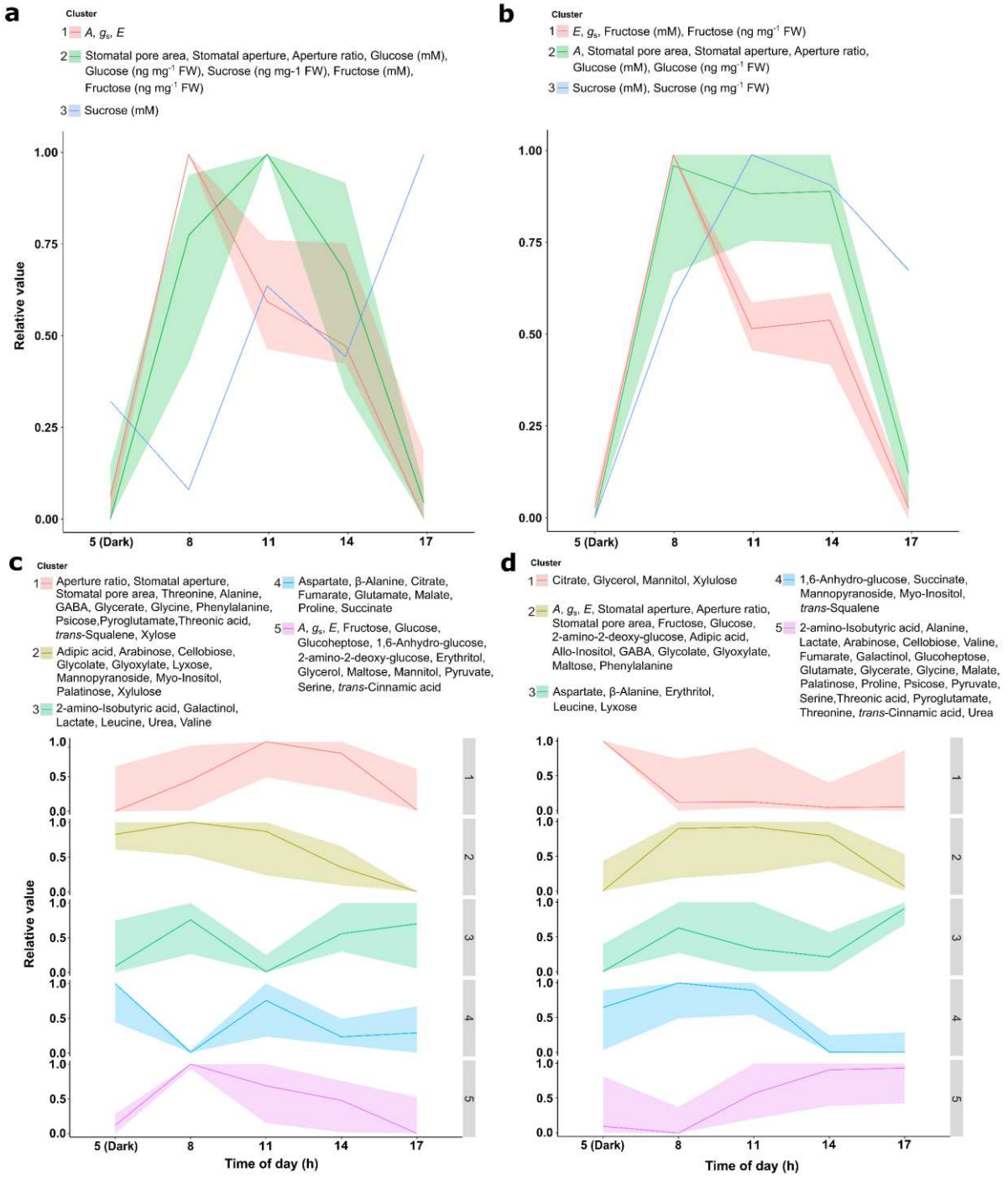

Figure 2. K-means clustering analysis of metabolite profile, gas exchange, stomatal aperture and the concentration of sugars from apoplast (**a**, **c**) and leaf (**b**, **d**) of *Nicotiana tabacum* wild type (NtWT) with the transgenic line antisense to the *SUT1* gene (Nt*SUT1*). The analysis was performed using concentration of sugars (**a**-**b**) or metabolite profile (**c**-**d**) combined with gas exchange and stomatal aperture data through the diel course. The k-means clustering analyses data were subjected to a maximum-minimum transformation within each variable (f(x) = xi - min(x) / max(x) - min(x), where xi is an observation of a variable) and performed using the MetaboAnalyst platform (n = 10).

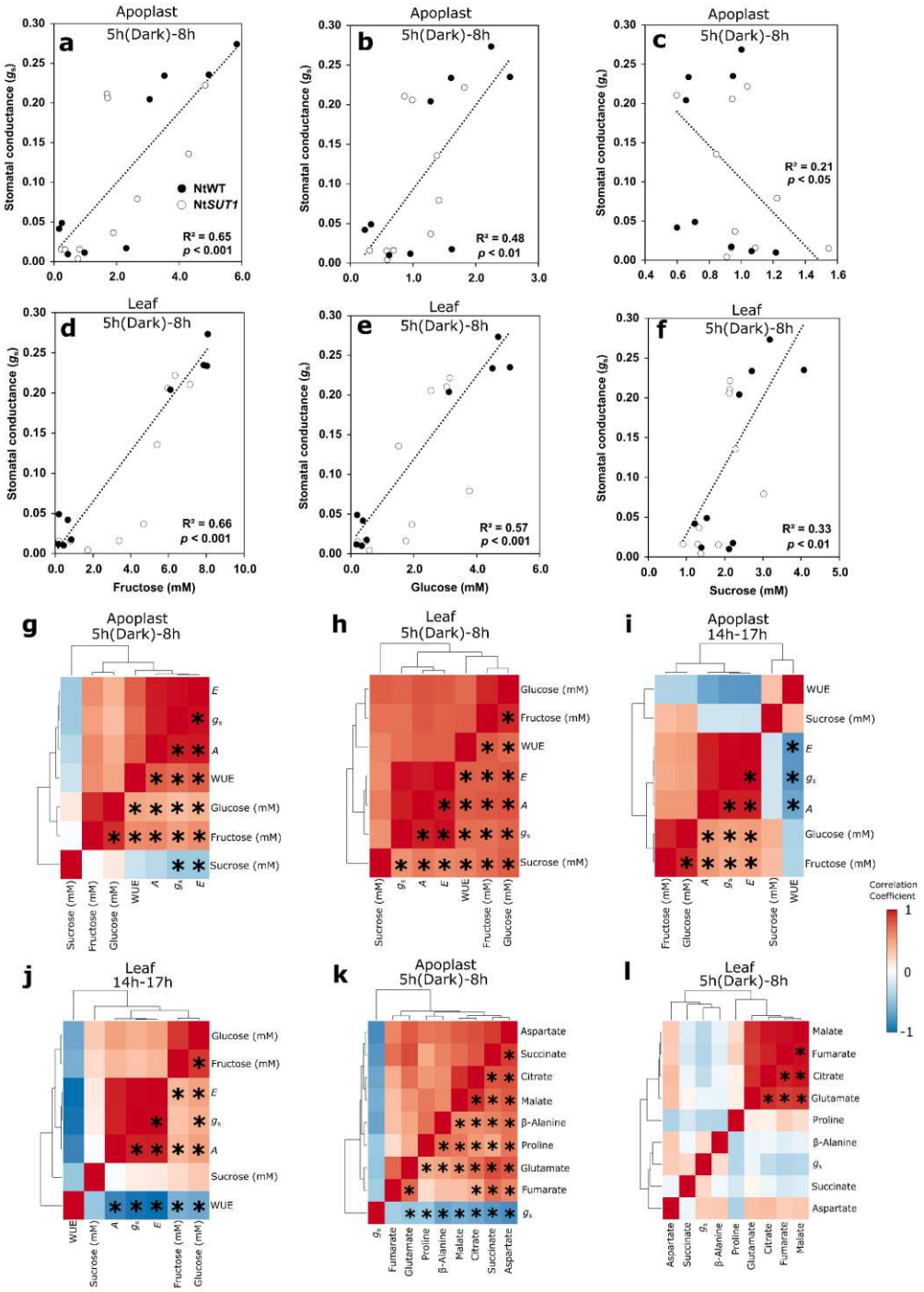

Figure 3. Linear regression and Pearson correlation analysis of metabolite profile, gas exchange and stomatal aperture from apoplast and leaf of *Nicotiana tabacum* wild type (NtWT) with the transgenic line antisense to the *SUT1* gene (Nt*SUT1*). Linear regression between g_s and each apoplast (**a**-**c**) and leaf (**d**-**f**) sugar concentration during dark-to-light transition. The correlation of photosynthetic rate (*A*), stomatal conductance (g_s), transpiration rate (*E*) and water use efficiency (WUE) with apoplast and leaf sugar concentrations is demonstrated per time point transitions from 5h to 8h and 14h to 17h (**g-j**). The correlation of g_s with apoplast (**k**) and leaf (**l**) amino acids and organic acids relative content is demonstrated at dark-to-light transition. All analysis combined the data from both tobacco (NtWT and Nt*SUT1*) genotypes. Asterisks (*) indicate significant Pearson's correlation coefficient (*r*) ($P < 0.05$).

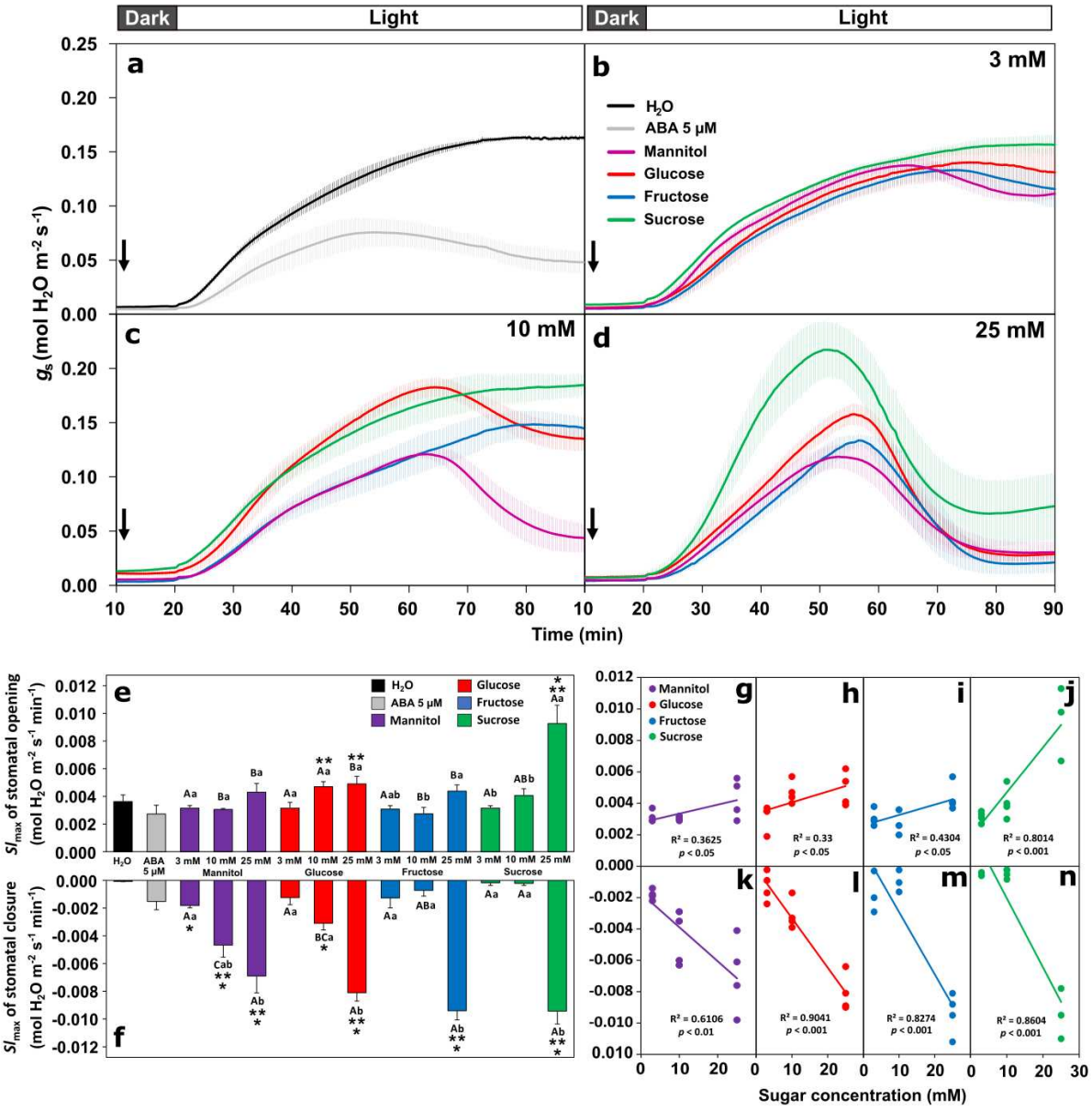

Figure 4. Kinetic of stomatal response of dark-adapted *Nicotiana tabacum* leaves under dark-to-light transition and influence of ABA (abscisic acid) and different concentrations of sugar. Time series of stomatal conductance (g_s) responses of dark-adapted wild type tobacco (NtWT) detached leaves under dark-to-light transition (0-1000 µmol photons m^{-2} s^{-1}) with only H_2O (general control) and 5 µM ABA (stomatal closure control) (**a**), Mannitol (osmotic control), Glucose, Fructose and Sucrose at 3 (**b**), 10 (**c**) and 25 mM (**d**). Black arrows represent the time point which each solute was added. This data is represented as average (n = 4). Maximum slope (Sl_{max}) of the linear region of the g_s response curves for stomatal opening (**e**) and closure (**f**). This data is represented as average ± standard error (n = 4 ± SE). Linear regression analysis of maximum slope (Sl_{max}) and increasing sugar concentrations for stomatal opening (**g**-**j**) and closure (**k**-**n**). See Fig. S13a. Different uppercase and lowercase letters indicate significant differences between metabolites within each concentration and concentrations within each metabolite, respectively, by ANOVA and Tukey's test ($P < 0.05$). One (*) and two asterisks (**) indicate significant difference from H_2O and ABA, respectively, by Student's *t* test at 5% of probability ($P < 0.05$).

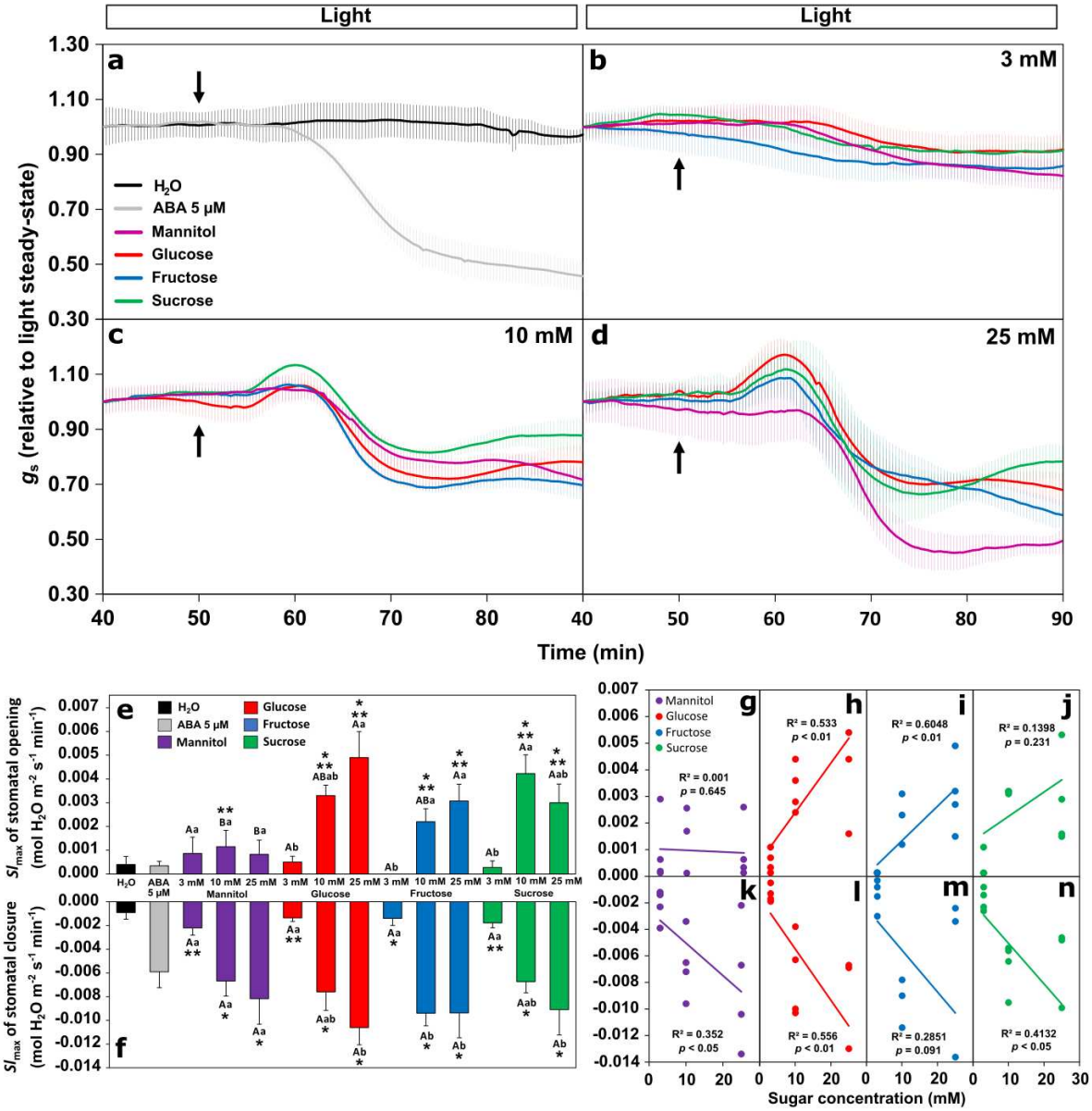

Figure 5. Kinetic of stomatal response of light-adapted *Nicotiana tabacum* leaves under light and influence of ABA (abscisic acid) and different concentrations of sugar. Time series of stomatal conductance (g_s) responses of light-adapted wild type tobacco (NtWT) detached leaves relative to steady-state (average of 10 readings before 10 min of the application of the compounds) at light (1000 µmol photons m^{-2} s^{-1}) with only H_2O (general control) and 5 µM ABA (stomatal closure control) (**a**), Mannitol (osmotic control), Glucose, Fructose and Sucrose at 3 (**b**), 10 (**c**) and 25 mM (**d**). Black arrows represent the time point which each solute was added. This data is represented as average (n = 4). Maximum slope (Sl_{max}) of the linear region of the g_s response curves for stomatal opening (**e**) and closure (**f**). This data is represented as average ± standard error (n = 4 ± SE). Linear regression analysis of maximum slope (Sl_{max}) and increasing sugar concentrations for stomatal opening (**g**-**j**) and closure (**k**-**n**). See Fig. S13b. Different uppercase and lowercase letters indicate significant differences between metabolites within each concentration and concentrations within each metabolite, respectively, by ANOVA and Tukey's test ($P < 0.05$). One (*) and two asterisks (**) indicate significant difference from H_2O and ABA, respectively, by Student's *t* test at 5% of probability ($P < 0.05$).

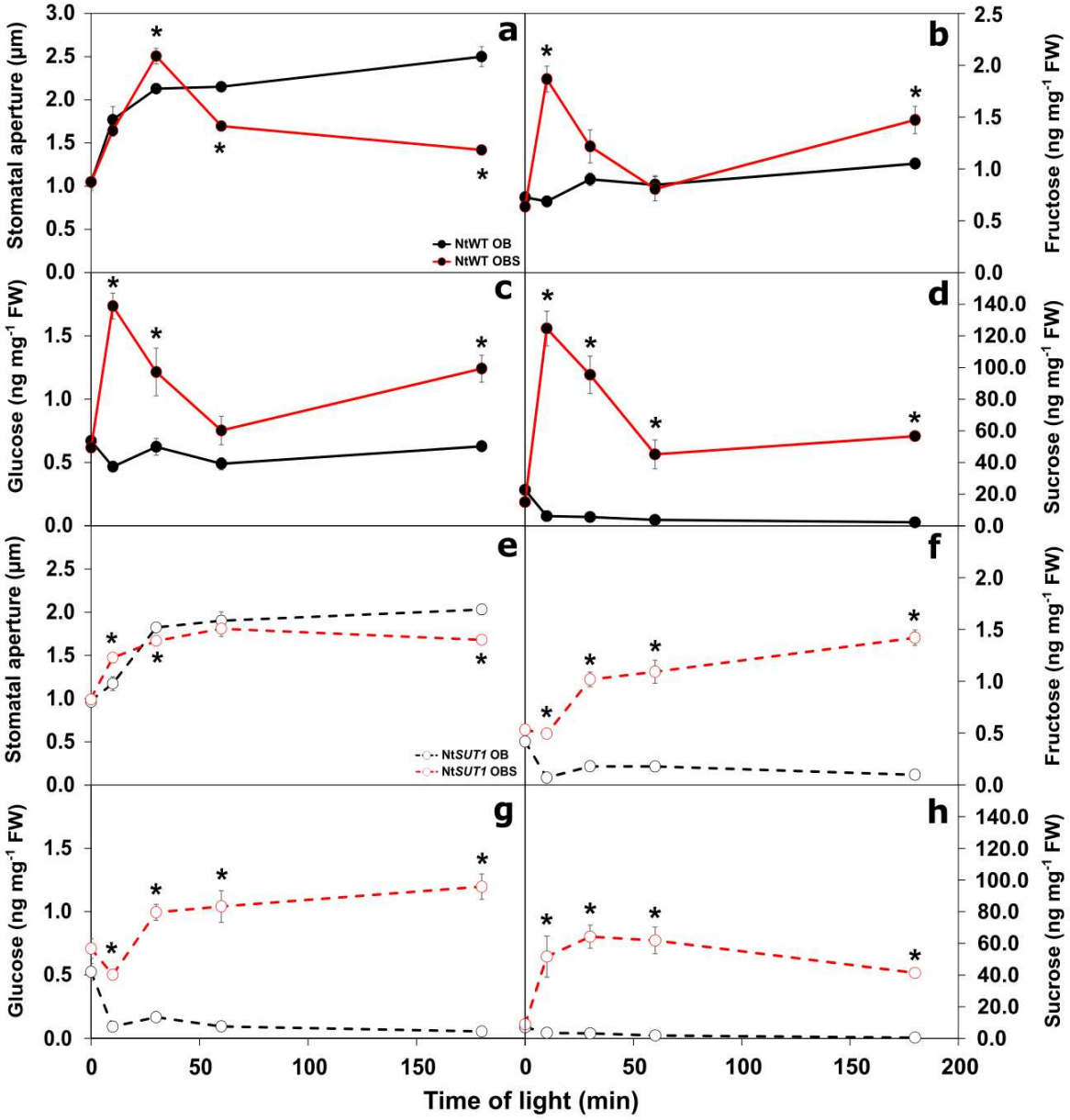

Figure 6. Stomatal aperture and content of sugars in guard cell enriched epidermal fragments (GCEF) of *Nicotiana tabacum* wild type (NtWT) and the transgenic line antisense to *SUT1* gene (Nt*SUT1*) under light and exogenous application of a buffer or the buffer plus sucrose (25 mM). GCEFs were harvested at pre-dawn and submitted to light (250 µmol photons m^{-2} s^{-1}) in an opening buffer solution containing 10 mM MES-Tris + 50 µM $CaCl_2$ + 10 mM KCl (OB) or opening buffer + 25 mM Sucrose (OBS). The measurements were taken at 0, 10, 30, 60 and 180 min after transition to the light. Time 0 indicates samples analysed immediately after collecting the GCEF. Stomatal aperture (**a,e**) and the concentration of fructose (**b,f**), glucose (**c,g**) and sucrose (**d,h**) by the GCEF fresh weight (FW) of NtWT (**a-d**) and Nt*SUT1* (**e-h**) at light in opening buffer with and without 25 mM Sucrose. The aperture data represents average of at least 60 stomata per time point ± standard error (n = 60 ± SE). The content data are represented as average ± standard error (n = 4 ± SE). Asterisks (*) indicate significant difference between OB and OBS in each time-point for each genotype by Student's *t* test ($P < 0.05$).

Materials and Methods Figures

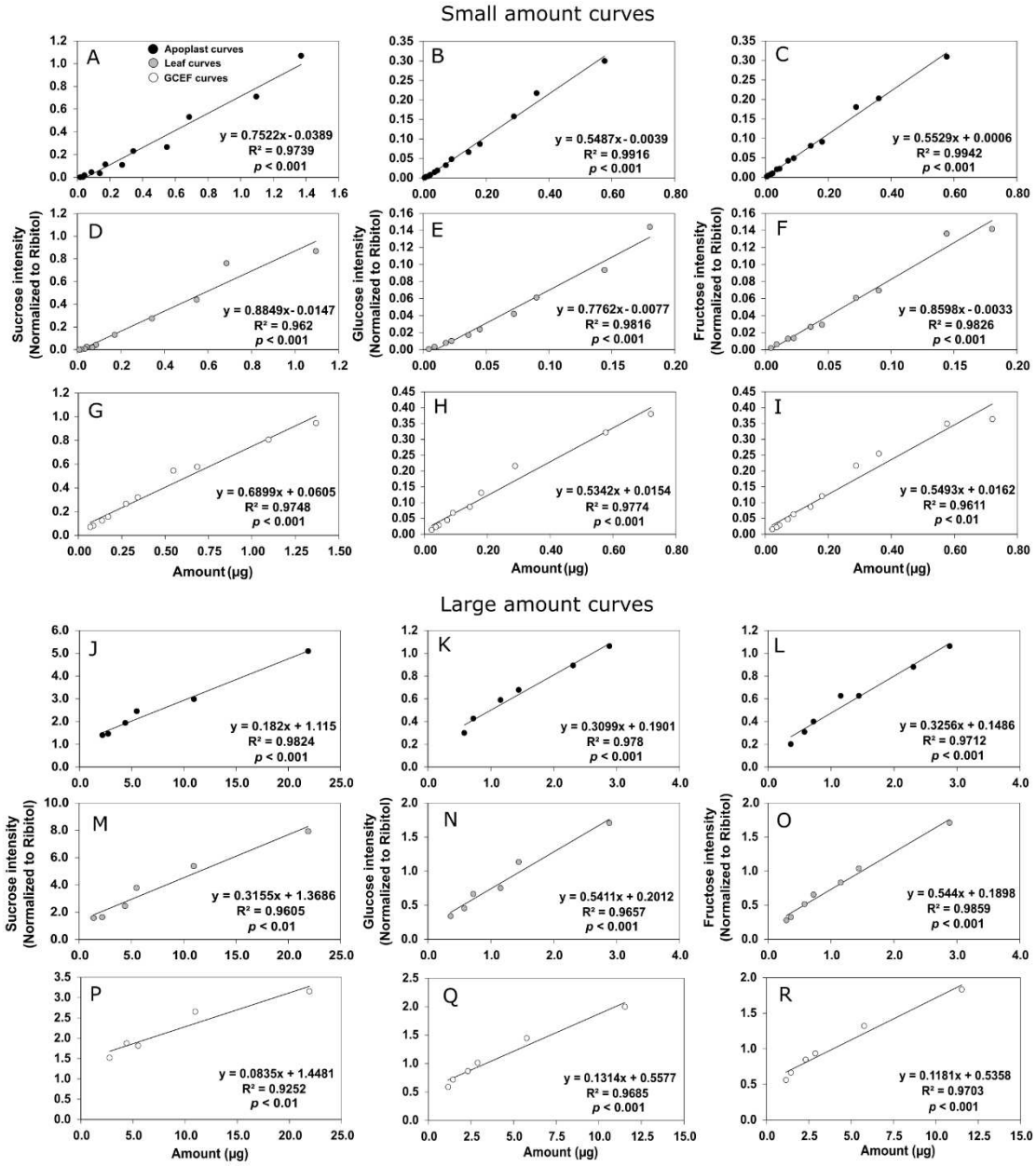

M&M Figure M1. Linear regression curves for sugar absolute quantification. Curves for small (**a-i**) and large (**j-r**) quantities of sucrose, glucose and fructose for apoplast, leaf and guard cell enriched epidermal fragments (GCEF). Linear regression was carried out using the sugar standard intensities found in GC-MS analysis normalized by the ribitol intensity for each, apoplast and leaf samples.

Supplemental material

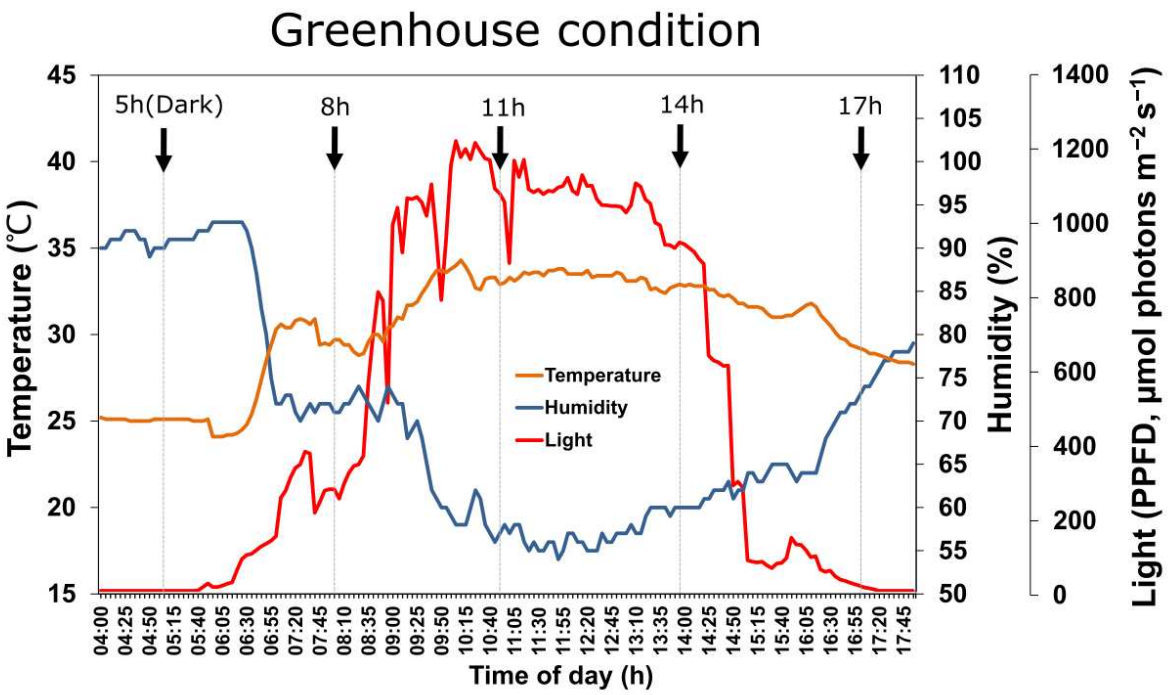

Supplemental Figure S1. Microclimate of growth conditions for *Nicotiana tabacum*. Light (µmol photons m^{-2} s^{-1}), temperature (ºC) and humidity (%) variation at the precisely day of experiment in greenhouse conditions. Black arrows represent the data and sample collection time points.

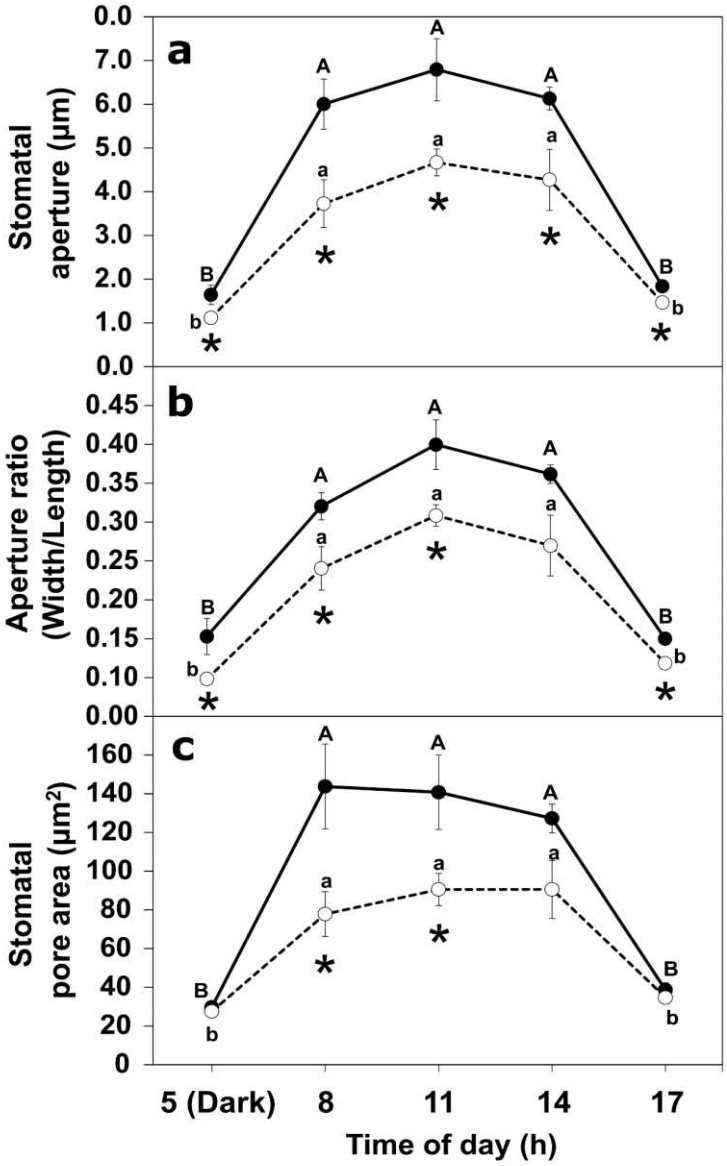

Supplemental Figure S2. Diel course of stomatal aperture of *Nicotiana tabacum* wild type (NtWT) and the transgenic line antisense to the *SUT1* gene (Nt*SUT1*). The diel course of stomatal aperture (**a**), aperture ratio (**b**) and stomatal pore area (**c**) were determined microscopically. These analyses were carried out in fully expanded leaves from plants grown under greenhouse and well-watered conditions. Different uppercase and lowercase letters indicate significant differences between time-points of NtWT and Nt*SUT1* genotype, respectively, by ANOVA and Tukey's test ($P < 0.05$). Asterisks (*) indicate significant difference between NtWT and Nt*SUT1* in each time-point by Student's *t* test ($P < 0.05$). The data are represented as average ± standard error (n = 5 ± SE).

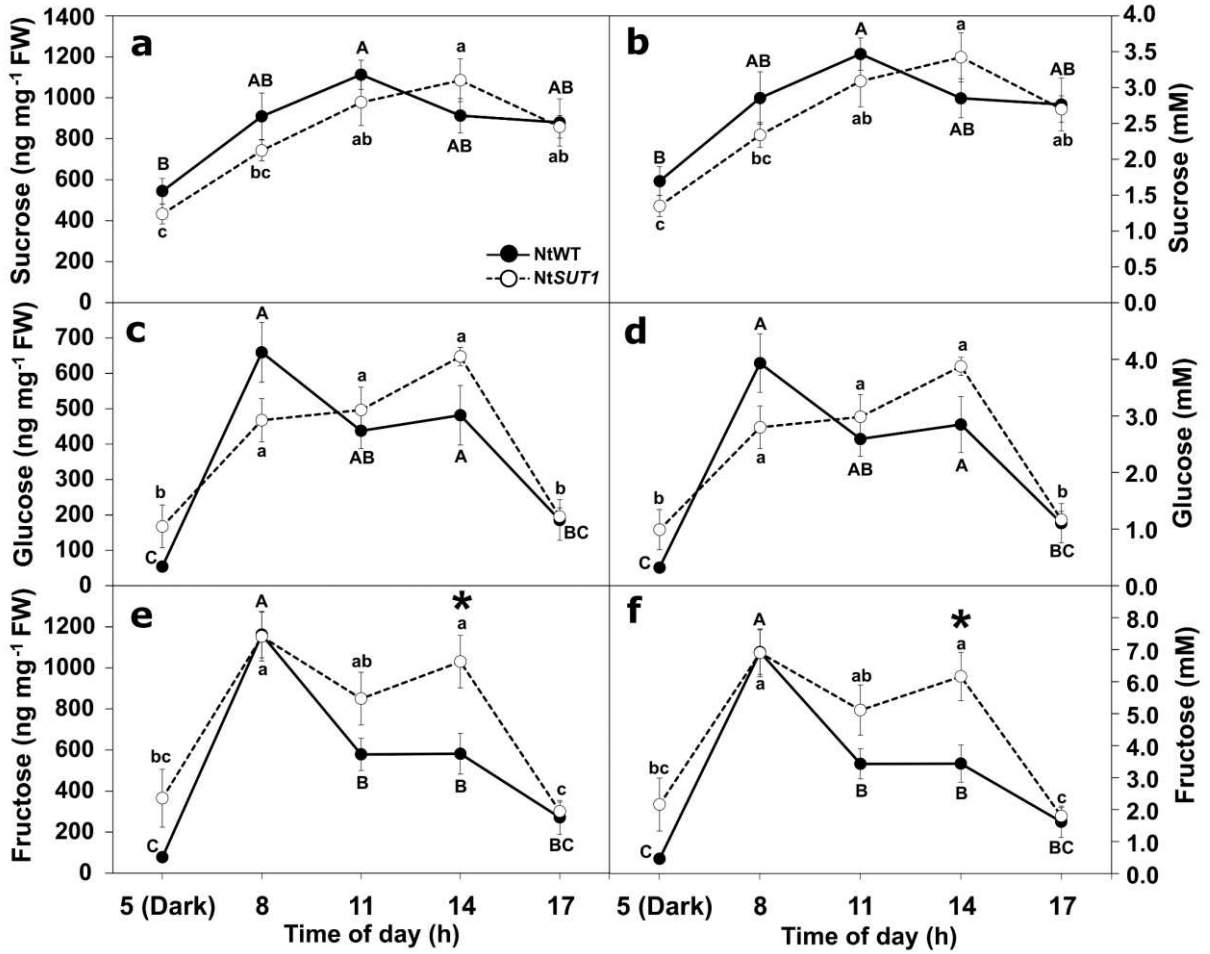

Supplemental Figure S3. Diel course of the concentration of sugars in leaves of *Nicotiana tabacum* wild type (NtWT) and the transgenic line antisense to *SUT1* gene (Nt*SUT1*). The concentration of the leaf sucrose, glucose and fructose were determined by the leaf fresh weight (FW) (**a**, **c**, **e**) and at molar level (**b**, **d**, **f**). Different uppercase and lowercase letters indicate significant differences between time-points of NtWT and Nt*SUT1* genotype, respectively, by ANOVA and Tukey's test ($P < 0.05$). Asterisks (*) indicate significant difference between NtWT and Nt*SUT1* in each time-point by Student's *t* test ($P < 0.05$). The data are represented as average ± standard error (n = 4 ± SE).

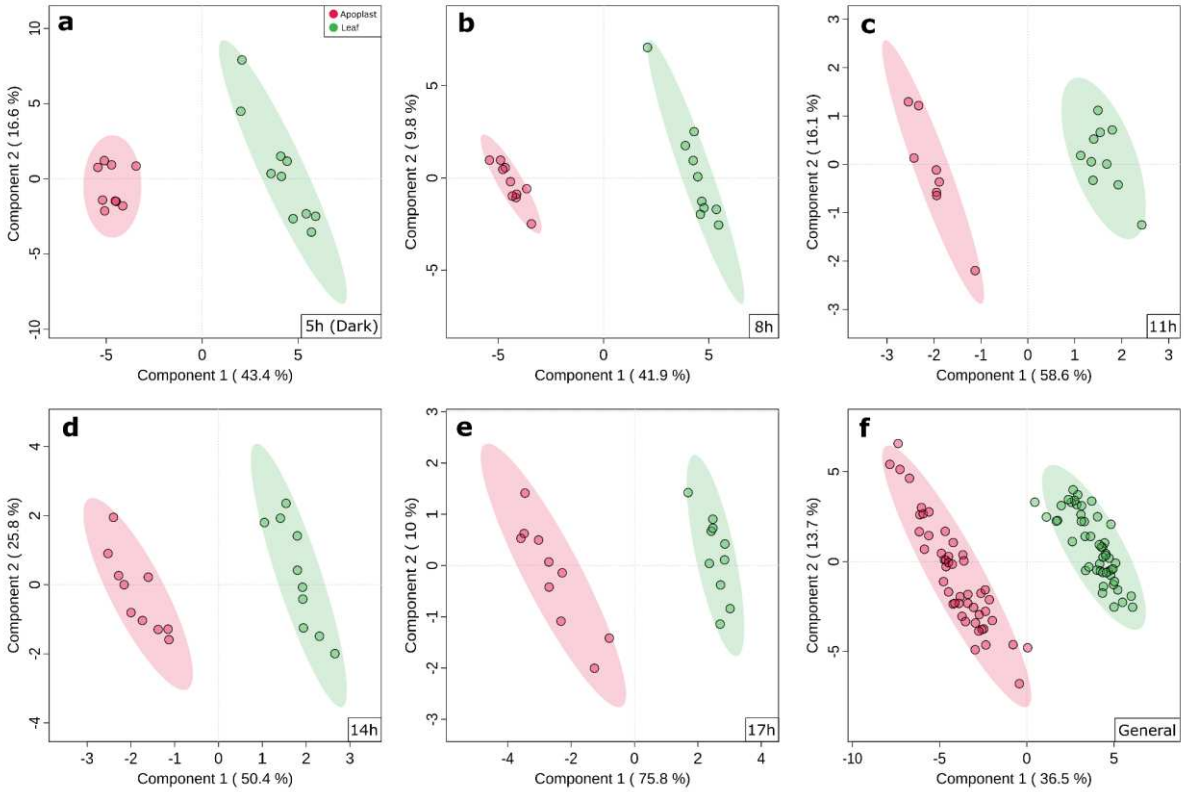

Supplemental Figure S4. Multivariate analysis of diel course metabolite profile of leaves (in green) and the apoplast (in red) from *Nicotiana tabacum* wild type (NtWT) and the transgenic line antisense to the *SUT1* gene (Nt*SUT1*). Partial least square discriminant analysis (PLS-DA) using leaf and apoplast metabolite profile data from each time point of the diel course (5h, 8h, 11h, 14h and 17h) (**a**-**e**) and using all time points together (general) (**f**). These analyses were performed using the MetaboAnalyst platform.

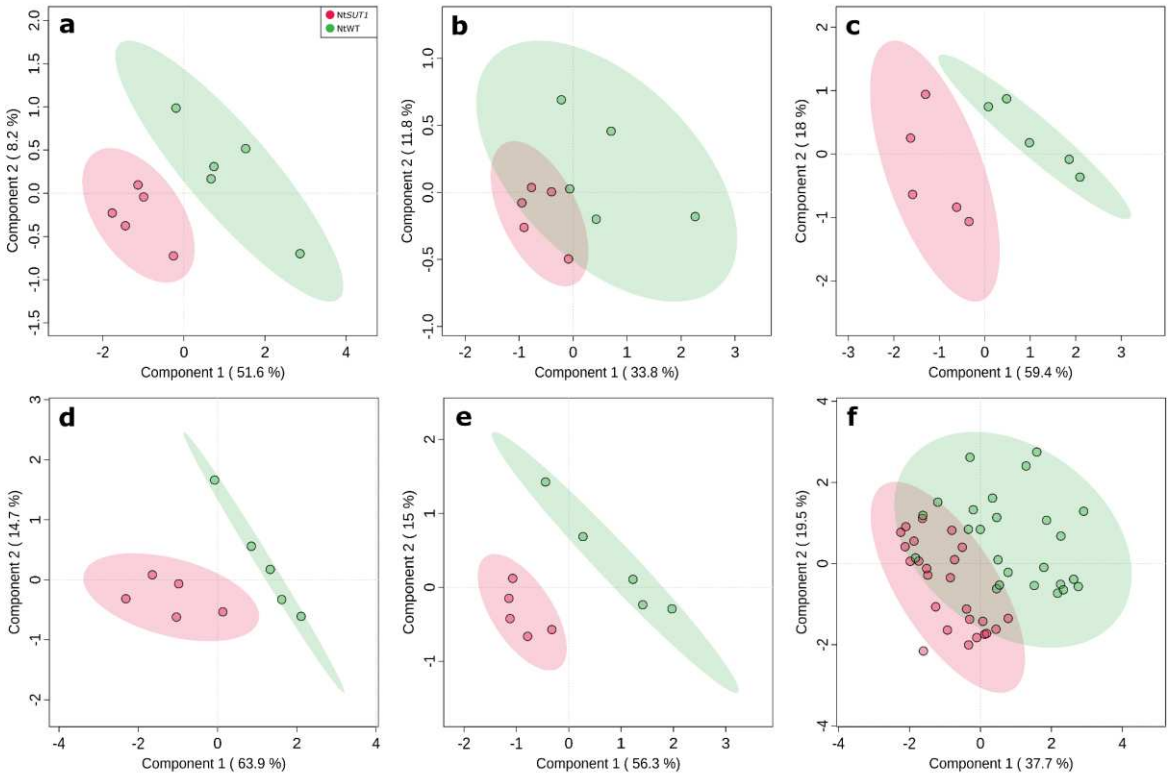

Supplemental Figure S5. Partial least square discriminant analysis (PLS-DA) analysis of diel course metabolite profile of the apoplast (**a**-**f**) comparing *Nicotiana tabacum* wild type (NtWT) (in green) with the transgenic line antisense to the *SUT1* gene (Nt*SUT1*) (in red). The multivariate analysis was performed using metabolite profile data from each time point of the diel course (5h, 8h, 11h, 14h and 17h) and using all time points together (general) from apoplast (**a**-**f**). These analyses were performed using the MetaboAnalyst platform.

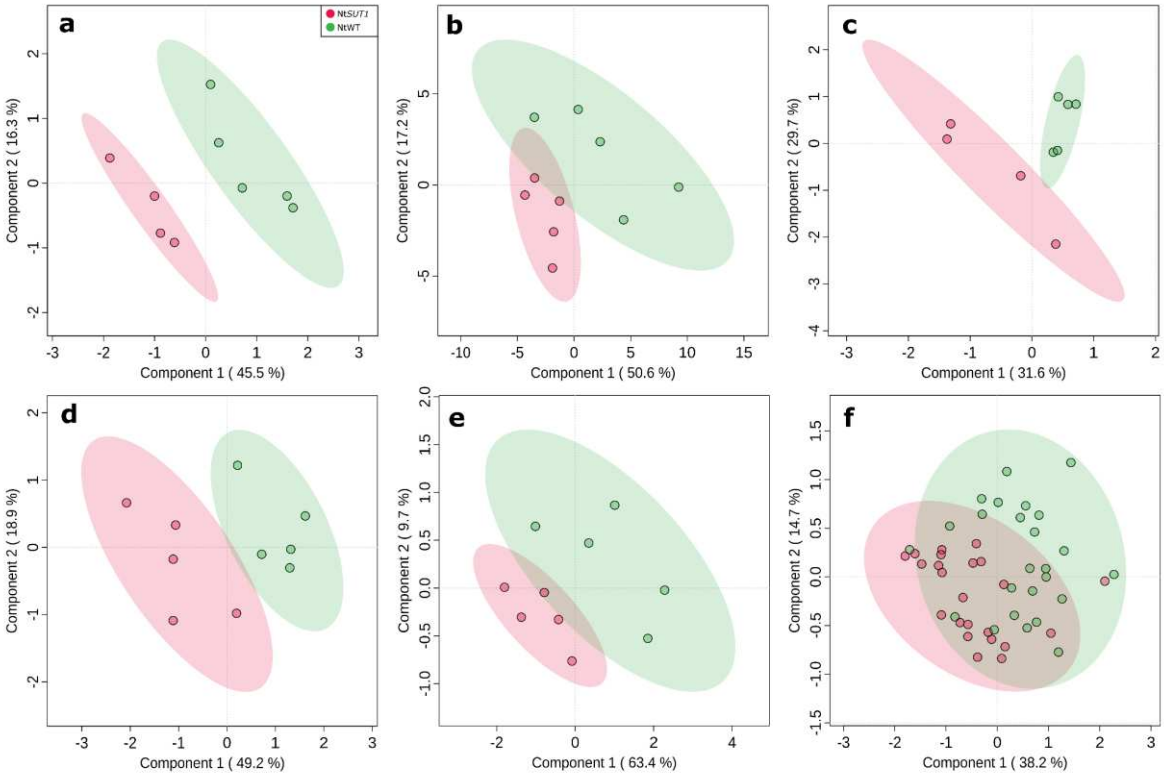

Supplemental Figure S6. Partial least square discriminant analysis (PLS-DA) analysis of diel course metabolite profile of leaves (**a**-**f**) comparing *Nicotiana tabacum* wild type (NtWT) (in green) with the transgenic line antisense to the *SUT1* gene (Nt*SUT1*) (in red). The multivariate analysis was performed using metabolite profile data from each time point of the diel course (5h, 8h, 11h, 14h and 17h) and using all time points together (general) from leaf (**a**-**f**). These analyses were performed using the MetaboAnalyst platform.

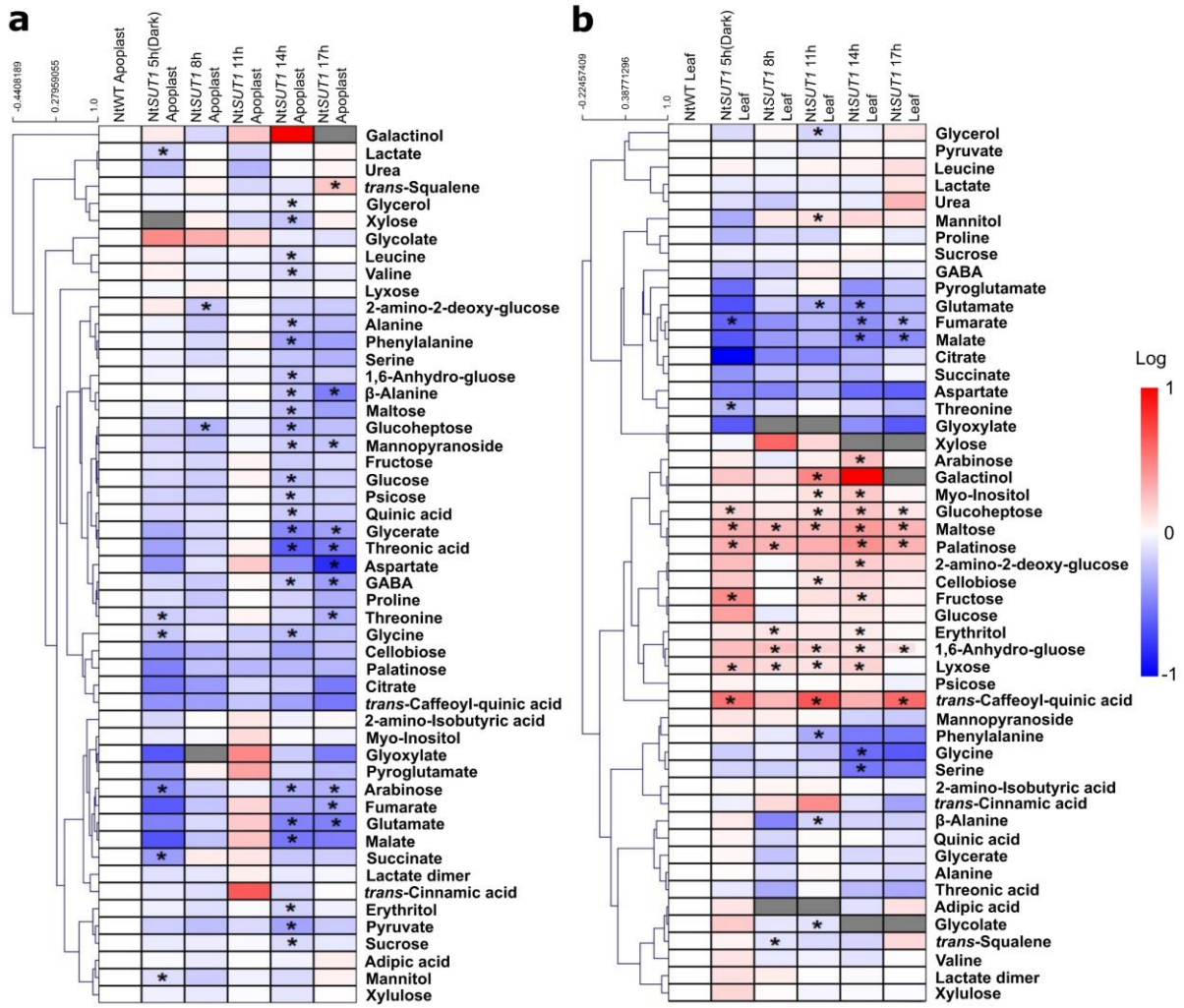

Supplemental Figure S7. Heat map representation of the differences in the diel course of the apoplast (**a**) and leaf (**b**) metabolite profile between *Nicotiana tabacum* L. wild type (NtWT) and the transgenic line antisense to *SUT1* gene (Nt*SUT1*). The heat maps were created by normalizing the absolute values of Nt*SUT1* according to the average of NtWT values at each time point and then log2 transformed. Asterisks (*) indicate significant difference between NtWT and Nt*SUT1* in each time point by Student's *t* test ($P < 0.05$) (n = 5).

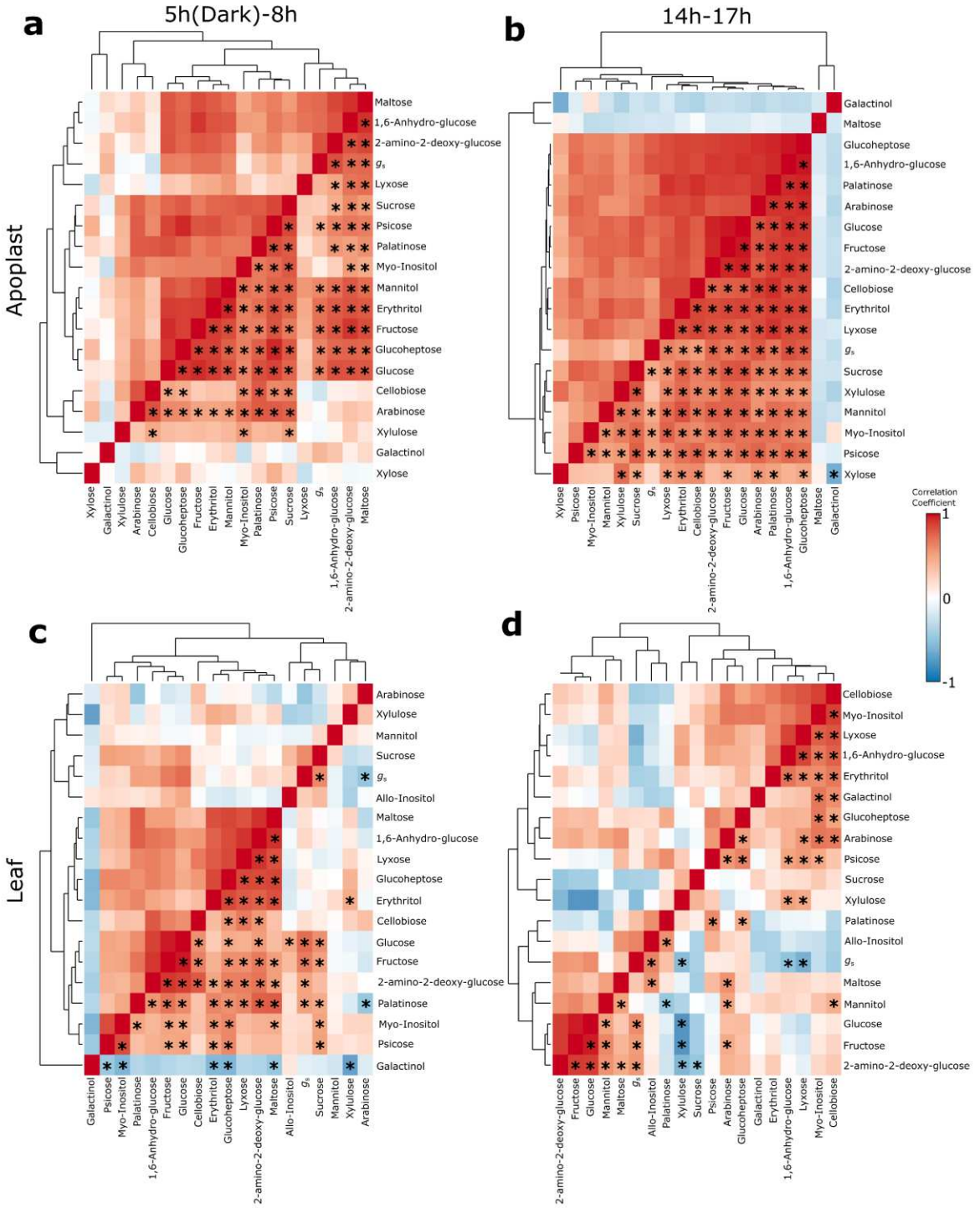

Supplemental Figure S8. Pearson correlation analysis carried out using the diel course data of stomatal conductance (g_s) and sugar and sugar alcohol relative content of the apoplast (**a-b**) and leaf (**c-d**) of *Nicotiana tabacum* L. wild type (NtWT) and the transgenic line antisense to *SUT1* gene (Nt*SUT1*). The correlation is demonstrated per time point transition from 5h to 8h (**a**, **c**) and 14h to 17h (**b**, **d**) for apoplast and leaf combining the data from both tobacco genotypes (NtWT and Nt*SUT1*). The metabolite relative contents used for correlation were normalized by ribitol, multiplied by vacuum dried volume µL and divided by mg^{-1} FW, leaves fresh weight. Asterisks (*) indicate significant Pearson's correlation coefficient (r) values ($P < 0.05$). These analyses were performed using MetaboAnalyst (n = 50).

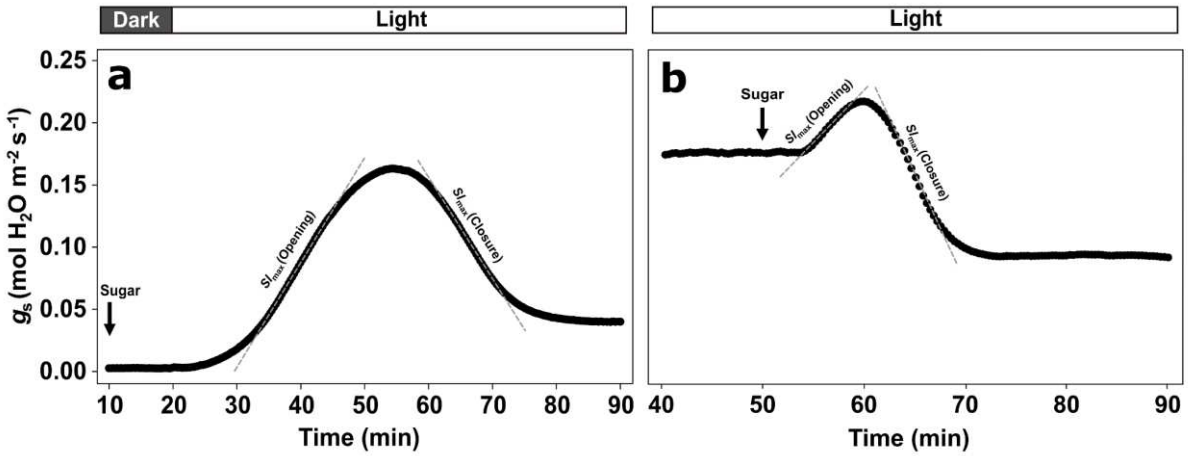

Supplemental Figure S9. Experimental set up to analyse the stomatal conductance (g_s) kinetic at light in function of sugar concentration. Schematic representation of changes in g_s kinetic in response under dark-to-light transition (**a**) and light (**b**) to the addition of external sugar (vertical black arrow) in dark-adapted and light-adapted leaves from *Nicotiana tabacum* L., respectively. Sl_{max} describes the maximum slope of the linear region of the g_s response curves for opening or closure.

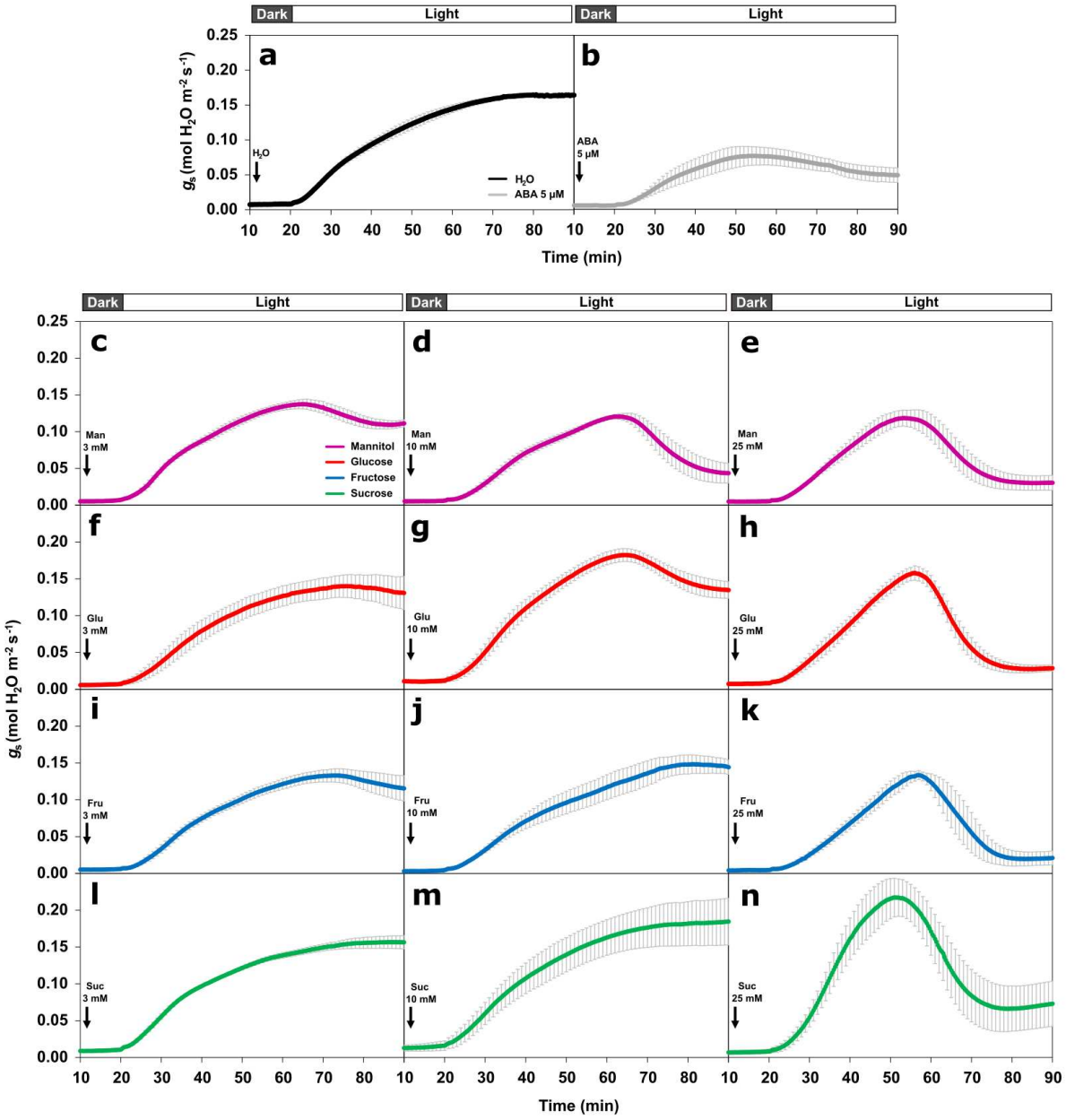

Supplemental Figure S10. Kinetics of stomatal conductance (g_s) during the dark-to-light transition under exogenous application of water (H_2O), abscisic acid (ABA) and different sugar concentrations. Detached and dark-adapted wild type *Nicotiana tabacum* L. leaves were placed in beckers of 100 ml containing H_2O (control) (**a**), ABA (5 µM) (**b**) or 3, 10 or 25 mM of mannitol (used as an osmotic control) (**c**-**e**), glucose (**f**-**h**), fructose (**i**-**k**) or sucrose (**l**-**n**). Time series of g_s were recorded every 20 sec for 20 min in the dark and 70 min in the light (1000 µmol photons m^{-2} s^{-1}) using an infra-red gas analyser (IRGA). Black arrows represent the time point which each compound was added. The data represents average ± standard error (n = 4 ± SE).

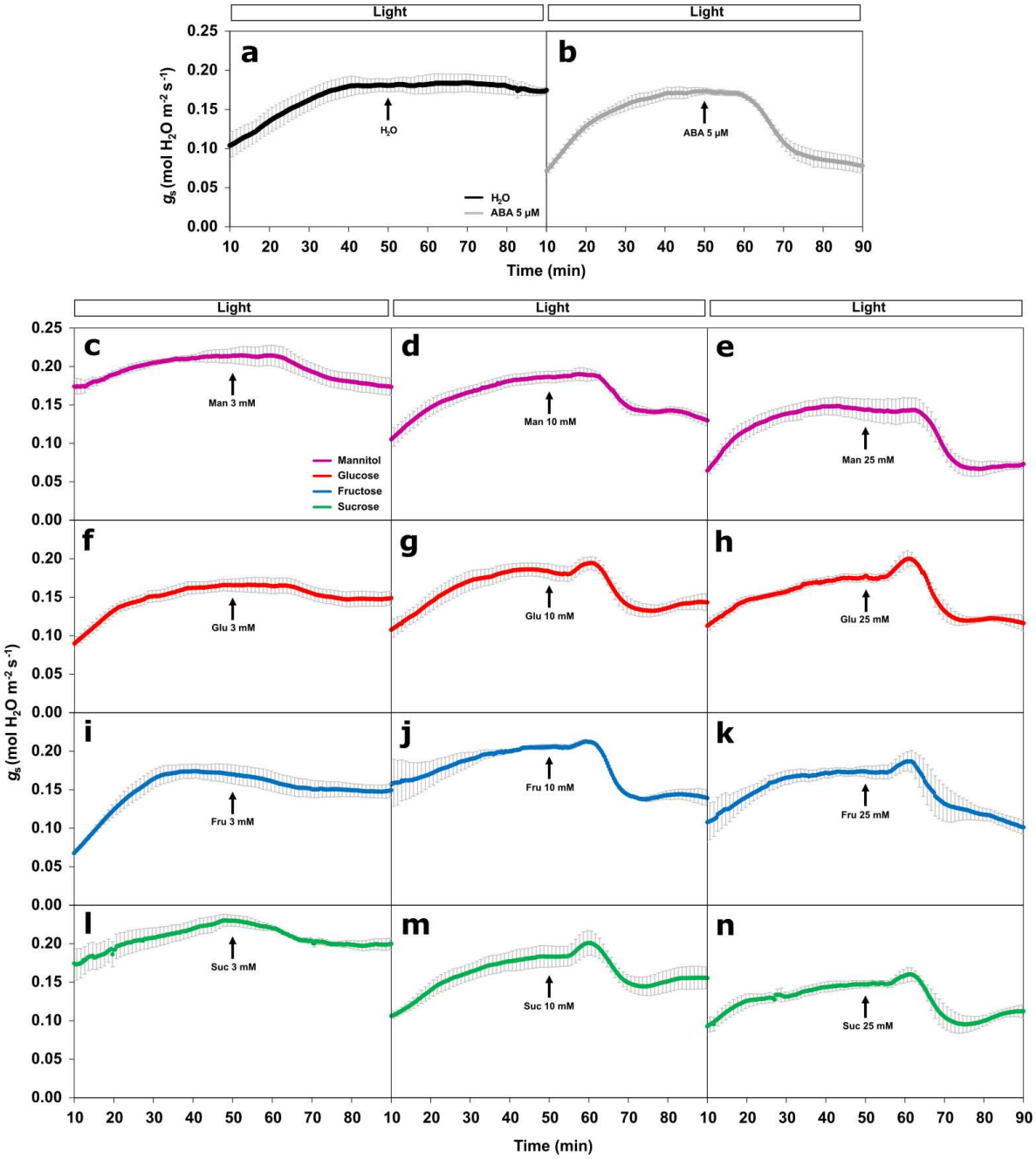

Supplemental Figure S11. Kinetics of stomatal conductance (g_s) in the light under exogenous application of water (H_2O), abscisic acid (ABA) and different sugar concentrations. Detached and light-adapted wild type *Nicotiana tabacum* L. leaves were placed in beckers of 100 ml containing H_2O (control) (**a**), ABA (5 µM) (**b**) or 3, 10 or 25 mM of mannitol (used as an osmotic control) (**c**-**e**), glucose (**f**-**h**), fructose (**i**-**k**) or sucrose (**l**-**n**). Time series of g_s were recorded every 20 sec for 50 min before and 40 min after the addition of the compound in the light (1000 µmol photons m^{-2} s^{-1}) using an infra-red gas analyser (IRGA). Black arrows represent the time point which each compound was added. The data represents average ± standard error (n = 4 ± SE).

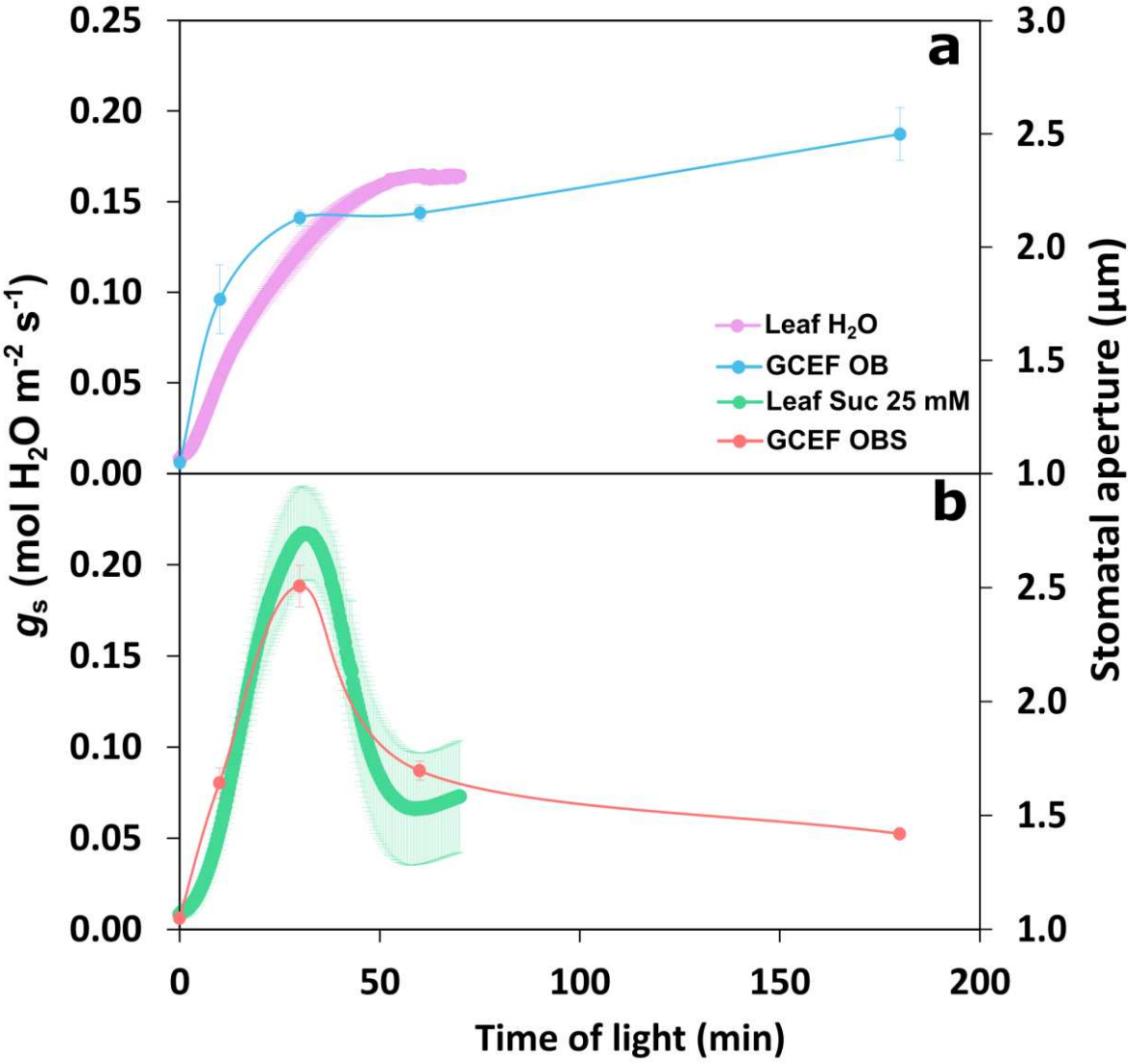

Supplemental Figure S12. Stomatal dynamics of leaf and guard cell enriched epidermal fragments (GCEF) of *Nicotiana tabacum* wild type (NtWT) under light and exogenous application of sucrose (25 mM). Detached and dark-adapted NtWT leaves were placed in beckers of 100 ml containing H_2O (control) or 25 mM of sucrose. GCEFs were harvested at pre-dawn and submitted to light (250 µmol photons m^{-2} s^{-1}) in an opening buffer solution containing 10 mM MES-Tris + 50 µM $CaCl_2$ + 10 mM KCl (OB) or opening buffer + 25 mM Sucrose (OBS). Time series of g_s were recorded every 20 sec for 70 min in the light (1000 µmol photons m^{-2} s^{-1}) using an infra-red gas analyser (IRGA). The aperture measurements were taken at 0, 10, 30, 60 and 180 min after transition to the light. Kinetics of g_s and stomatal aperture in H_2O/OB (**a**) and 25 mM Sucrose/OBS (**b**). Kinetics of g_s of detached leaves and stomatal aperture of EF in 25 mM Sucrose and OBS, respectively (b). The g_s data represents average ± standard error (n = 4 ± SE). The aperture data represents average of at least 60 stomata per time point ± standard error (n = 60 ± SE).

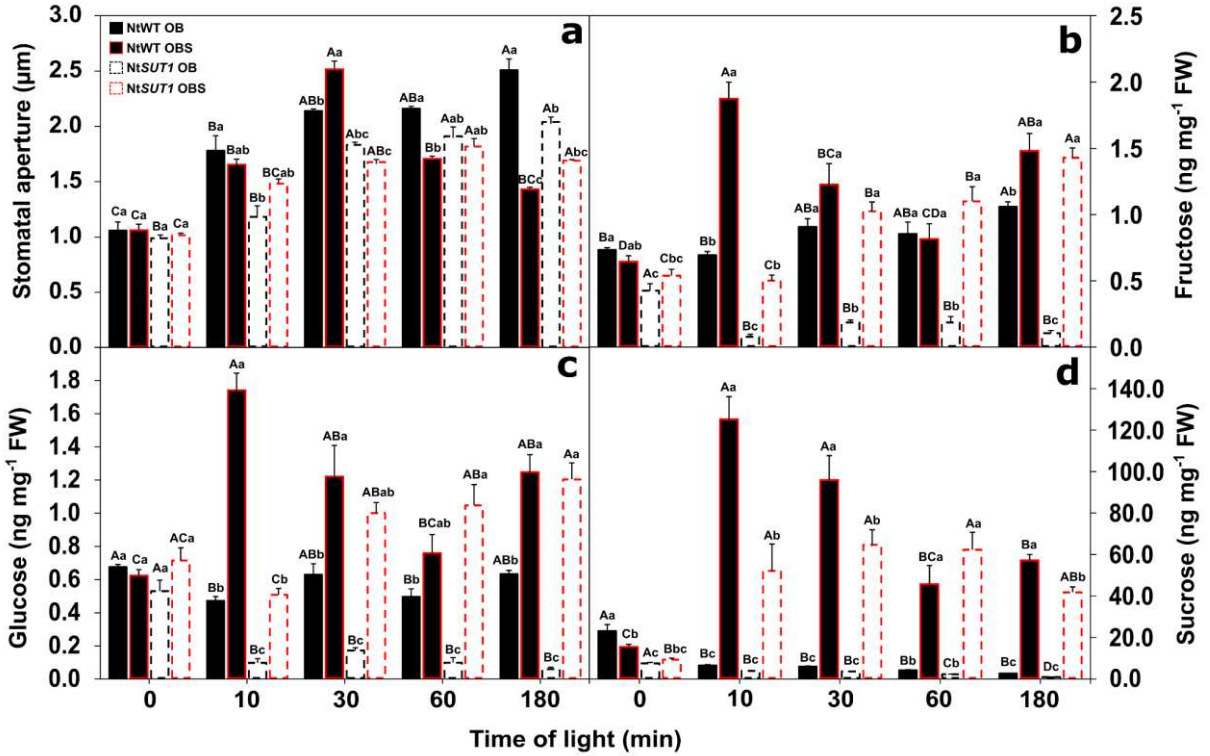

Supplemental Figure S13. Comparing stomatal aperture and concentration of sugars in guard cell enriched epidermal fragments (GCEF) of *Nicotiana tabacum* wild type (NtWT) and the transgenic line antisense to *SUT1* gene (Nt*SUT1*) under light and exogenous application of a buffer or the buffer plus sucrose (25 mM). GCEFs were harvested at pre-dawn and submitted to light (250 µmol photons m^{-2} s^{-1}) in an opening buffer solution containing 10 mM MES-Tris + 50 µM $CaCl_2$ + 10 mM KCl (OB) or opening buffer + 25 mM Sucrose (OBS). The measurements were taken at 0, 10, 30, 60 and 180 min after transition to the light. Time 0 indicates samples analysed immediately after collecting the GCEF. Stomatal aperture (**a**) and the concentration of fructose (**b**), glucose (**c**) and sucrose (**d**) by the GCEF fresh weight (FW) of NtWT and Nt*SUT1* at light in opening buffer with and without 25 mM Sucrose. The aperture data represents average of at least 60 stomata per time point ± standard error (n = 60 ± SE). The concentration data are represented as average ± standard error (n = 4 ± SE). Different uppercase and lowercase letters indicate significant differences between time points within each genotype/treatment and genotype/treatments within each time point, respectively, by ANOVA and Tukey's test ($P < 0.05$).

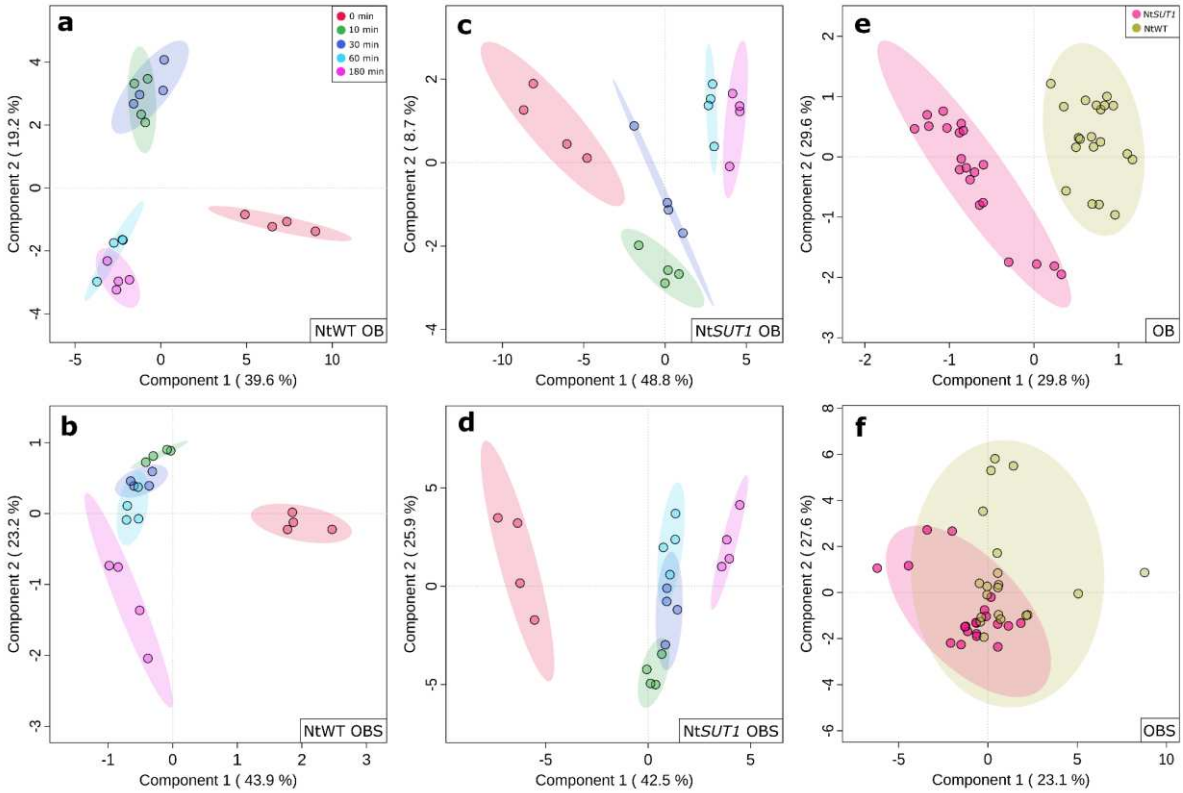

Supplemental Figure S14. Partial least square discriminant analysis (PLS-DA) analysis of metabolite profile of guard cell enriched epidermal fragments (GCEF) of *Nicotiana tabacum* wild type (NtWT) and the transgenic line antisense to *SUT1* gene (Nt*SUT1*) under light and exogenous application of a buffer or the buffer plus sucrose (25 mM). GCEFs were harvested at pre-dawn and submitted to light (250 µmol photons m^{-2} s^{-1}) in an opening buffer solution containing 10 mM MES-Tris + 50 µM $CaCl_2$ + 10 mM KCl (OB) or opening buffer + 25 mM Sucrose (OBS). The measurements were taken at 0, 10, 30, 60 and 180 min after transition to the light. Time 0 indicates samples analysed immediately after collecting the GCEF. The multivariate analysis was performed using metabolite profile data from each time point at 0, 10, 30, 60 and 180 min after transition to the light of NtWT (**a-b**) and Nt*SUT1* (**c-d**) GCEFs in both conditions and using all time points together for each genotype in OB (**e**) and OBS (**f**). These analyses were performed using the MetaboAnalyst platform.

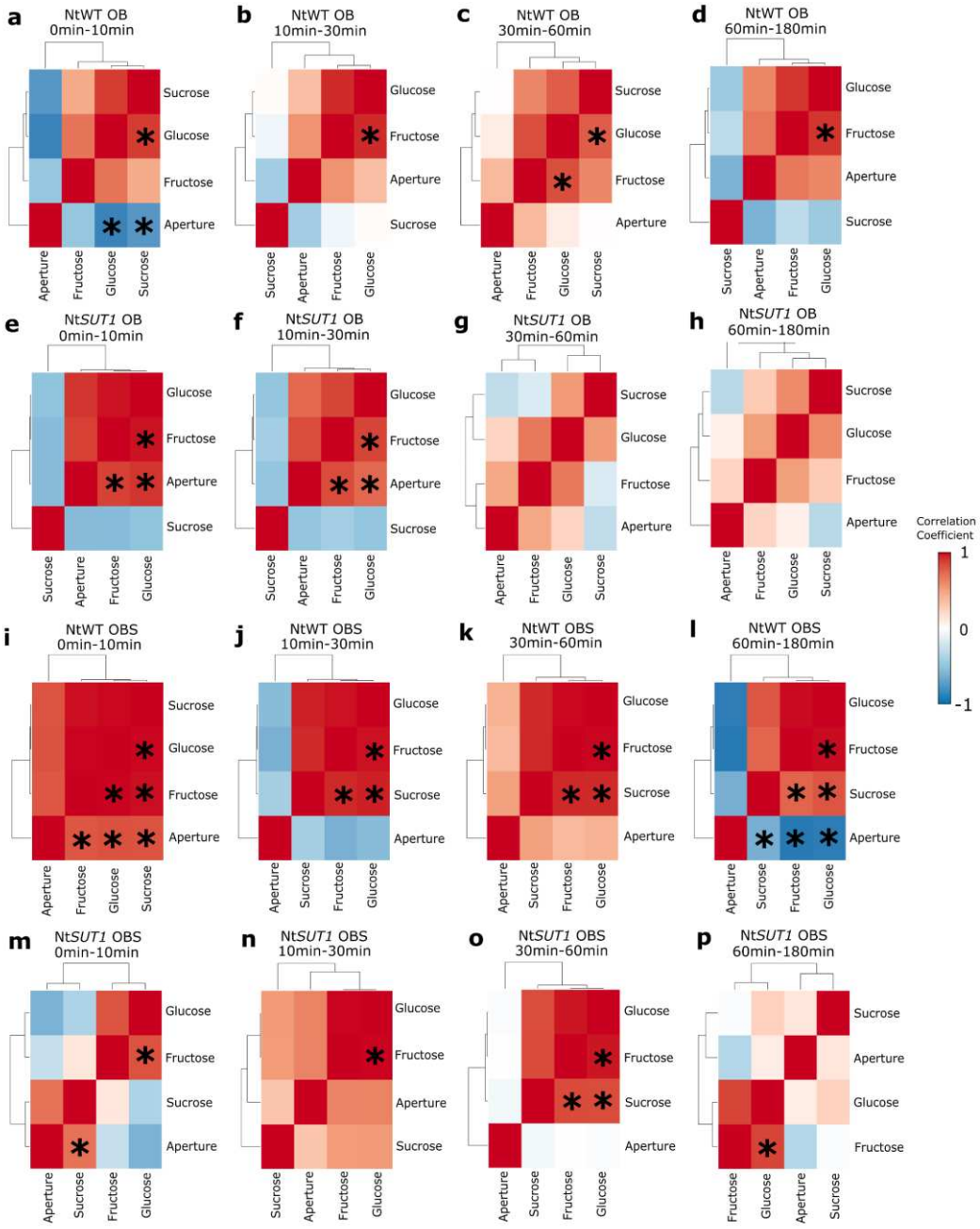

Supplemental Figure S15. Pearson correlation analysis carried out using sugar concentration and stomatal aperture from guard cell enriched epidermal fragments (GCEF) of *Nicotiana tabacum* L. wild type (NtWT) and the transgenic line antisense to *SUT1* gene (Nt*SUT1*) under light and exogenous application of a buffer or the buffer plus sucrose (25 mM). GCEFs were harvested at pre-dawn and submitted to light (250 µmol photons m^{-2} s^{-1}) in an opening buffer solution containing 10 mM MES-Tris + 50 µM $CaCl_2$ + 10 mM KCl (OB) or opening buffer + 25 mM Sucrose (OBS). The sugar concentration data used is represented as ng by mg^{-1} of GCEF fresh weight. The correlation is demonstrated per time point transition from 0 min to 10 min, 10 min to 30 min, 30 min to 60 min and 60 min to 180 min for both tobacco genotypes, NtWT and Nt*SUT1*, and conditions, OB (**a-h**) and OBS (**i-p**). Asterisks (*) indicate significant Pearson's correlation coefficient (r) values ($P < 0.05$). These analyses were performed using MetaboAnalyst (n = 50).

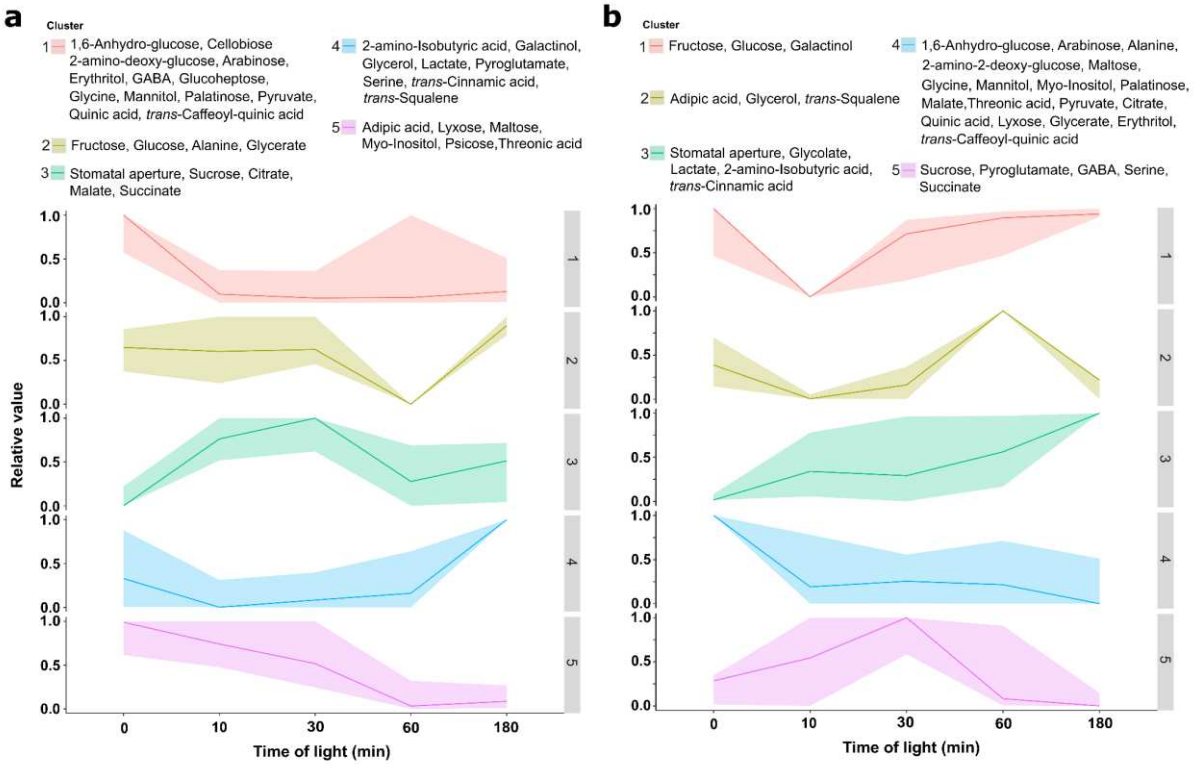

Supplemental Figure S16. K-means clustering analysis of metabolite profile and stomatal aperture from guard cell enriched epidermal fragments (GCEF) of *Nicotiana tabacum* wild type (NtWT) and the transgenic line antisense to the *SUT1* gene (Nt*SUT1*) under light and exogenous application of a buffer or the buffer plus sucrose (25 mM). GCEFs were harvested at pre-dawn and submitted to light (250 µmol photons m^{-2} s^{-1}) in an opening buffer solution containing 10 mM MES-Tris + 50 µM $CaCl_2$ + 10 mM KCl (OB) or opening buffer + 25 mM Sucrose (OBS). The analysis was performed using metabolite profile combined with stomatal aperture of GCEF of NtWT (**a**) and Nt*SUT1* (**b**) data through the diel course. The k-means clustering analyses data were subjected to a maximum-minimum transformation within each variable (f(x) = xi - min(x) / max(x) - min(x), where xi is an observation of a variable) and performed using the MetaboAnalyst platform (n = 10).

Supplemental Table S1. Greenhouse environment parameters at experiment time intervals of sample collection. Temperature, humidity and light intensity were recorded every 5 minutes by a weather station. The parameters are represented as average ± standard error (n = 14 ± SE).

Greenhouse conditions				
Time point	Time interval (hr)	Temperature (℃)	Humidity (%)	Light (PPFD, µmol photons m^{-2} s^{-1})
5h(Dark)	04:45-05:50	25.06 ± 0.01	90.86 ± 0.23	2.22 ± 1.55
8h	07:45-08:50	29.46 ± 0.10	71.93 ± 0.27	378.44 ± 47.93
11h	10:45-11:50	33.41 ± 0.07	56.21 ± 0.33	1084.35 ± 17.36
14h	13:45-14:50	32.61 ± 0.07	60.79 ± 0.30	770.62 ± 54.41
17h	16:45-17:50	28.88 ± 0.11	75.21 ± 0.68	7.22 ± 2.53

Supplemental Table S2. Diel course of apoplast sucrose, glucose and fructose content and concentration of *Nicotiana tabacum* wild type (NtWT) and the transgenic line antisense to *SUT1* gene (Nt*SUT1*). The parameters are represented as average ± standard error (n = 4 ± SE).

Apoplast		(ng mg^{-1} FW)			(mM)		
		Sucrose	Glucose	Fructose	Sucrose	Glucose	Fructose
5h(Dark)	NtWT	81 ± 10	36 ± 12	40 ± 19	0.90 ± 0.11	0.75 ± 0.25	0.84 ± 0.39
	Nt*SUT1*	65 ± 12	22 ± 7	25 ± 12	1.08 ± 0.15	0.69 ± 0.20	0.83 ± 0.38
8h	NtWT	97 ± 12	119 ± 21	259 ± 47	0.77 ± 0.08	1.78 ± 0.26	3.92 ± 0.67
	Nt*SUT1*	83 ± 8	62 ± 9*	146 ± 33	0.92 ± 0.10	1.29 ± 0.16	3.04 ± 0.65
11h	NtWT	137 ± 16	107 ± 18	206 ± 35	1.17 ± 0.15	1.76 ± 0.34	3.41 ± 0.68
	Nt*SUT1*	115 ± 13	118 ± 30	238 ± 65	1.09 ± 0.09	2.09 ± 0.46	4.22 ± 1.06
14h	NtWT	103 ± 11	100 ± 19	162 ± 43	1.16 ± 0.12	2.12 ± 0.40	3.46 ± 0.94
	Nt*SUT1*	68 ± 7*	43 ± 6*	73 ± 19	0.93 ± 0.11	1.11 ± 0.13*	1.88 ± 0.43
17h	NtWT	73 ± 10	28 ± 9	35 ± 13	1.50 ± 0.17	1.09 ± 0.32	1.36 ± 0.47
	Nt*SUT1*	54 ± 2	15 ± 3	19 ± 7	1.08 ± 0.05*	0.53 ± 0.10	0.69 ± 0.22

Asterisks (*) indicate significant difference from NtWT in each respective time-point by Student's *t* test at 5% of probability ($P < 0.05$).

Supplemental Table S3. Diel course of leaf sucrose, glucose and fructose content and concentration of *Nicotiana tabacum* wild type (NtWT) and the transgenic line antisense to *SUT1* gene (Nt*SUT1*). The parameters are represented as average ± standard error (n = 4 ± SE).

Leaf		(ng mg^{-1} FW)			(mM)		
		Sucrose	Glucose	Fructose	Sucrose	Glucose	Fructose
5h(Dark)	NtWT	544 ± 62	54 ± 10	78 ± 22	1.69 ± 0.20	0.32 ± 0.06	0.45 ± 0.13
	Nt*SUT1*	433 ± 48	167 ± 60	365 ± 141	1.34 ± 0.15	0.99 ± 0.36	2.15 ± 0.83
8h	NtWT	909 ± 114	659 ± 84	1162 ± 113	2.85 ± 0.37	3.93 ± 0.52	6.92 ± 0.70
	Nt*SUT1*	743 ± 51	468 ± 61	1153 ± 119	2.33 ± 0.17	2.79 ± 0.38	6.90 ± 0.75
11h	NtWT	1113 ± 71	438 ± 51	578 ± 78	3.46 ± 0.22	2.59 ± 0.31	3.42 ± 0.47
	Nt*SUT1*	978 ± 113	497 ± 64	850 ± 128	3.08 ± 0.35	2.98 ± 0.39	5.10 ± 0.78
14h	NtWT	913 ± 84	482 ± 84	582 ± 99	2.84 ± 0.27	2.84 ± 0.49	3.43 ± 0.58
	Nt*SUT1*	1085 ± 104	648 ± 26	1030 ± 128*	3.42 ± 0.34	3.87 ± 0.16	6.16 ± 0.75*
17h	NtWT	879 ± 115	186 ± 58	271 ± 83	2.76 ± 0.37	1.11 ± 0.34	1.61 ± 0.49
	Nt*SUT1*	859 ± 55	195 ± 25	301 ± 45	2.69 ± 0.18	1.17 ± 0.15	1.79 ± 0.27

Asterisks (*) indicate significant difference from NtWT in each respective time-point by Student's *t* test at 5% of probability ($P < 0.05$).

6. CONCLUSIONS

In summary, the apoplast collection method established here is appropriate for metabolomics analysis and sucrose is, in fact, a master regulator of the stomatal movements, inducing stomatal opening and closure depending on its concentration and location of accumulation. Our results suggest that methanol can be used as infiltration fluid for the collection of apoplast for GC-MS-based metabolomics analysis from tobacco leaves, but ddH_2O is more recommended as it does not increase symplast contamination and is non-toxic. However, a methanol correction factor is proposed to adjust the values from symplastic enzyme activity, when used as purity parameter. The results of the role of sucrose in controlling g_s demonstrate that, through the diel course, the stomatal movement was negatively associated with apoplastic sucrose level. Also, we observed that light-induced stomatal opening is closely associated with the dynamics of sucrose and organic acids within guard cells. Furthermore, the speed of stomatal opening and closure was positively and negatively correlated with the sucrose concentration in illuminated leaves, respectively. Additionally, exogenously applied sucrose reduced the stomatal movement response in plants with less capacity to import sucrose from the apoplast to within guard cells, which highlights the importation of sucrose into these cells as an important modulator of the magnitude of stomatal movement. Overall, our findings add more steps toward understanding the regulation of stomatal movements and indicate that engineering the sucrose metabolism at guard cell and leaf apoplast level is a promising strategy to control the stomatal movement behavior.

REFERENCES

ALMEIDA, D.; HUBER, D. Chilling-induced changes in the apoplastic solution of tomato pericarp. **The Journal of Horticultural Science and Biotechnology**, [*s. l.*], v. 85, n. 4, p. 312–316, 2010. Disponível em: http://www.tandfonline.com/doi/full/10.1080/14620316.2010.11512673.

AMODEO, G.; TALBOTT, L. D.; ZEIGER, E. Use of potassium and sucrose by onion guard cells during a daily cycle of osmoregulation. **Plant and Cell Physiology**, [*s. l.*], v. 37, n. 5, p. 575–579, 1996.

ANTUNES, W. C. *et al.* Changes in stomatal function and water use efficiency in potato plants with altered sucrolytic activity. **Plant, Cell and Environment**, [*s. l.*], v. 35, n. 4, p. 747–759, 2012.

ANTUNES, W. C. *et al.* Guard cell-specific down-regulation of the sucrose transporter SUT1 leads to improved water use efficiency and reveals the interplay between carbohydrate metabolism and K+ accumulation in the regulation of stomatal opening. **Environmental and Experimental Botany**, [*s. l.*], v. 135, p. 73–85, 2017. Disponível em: http://dx.doi.org/10.1016/j.envexpbot.2016.12.004.

ARAÚJO, W. L. *et al.* Antisense Inhibition of the Iron-Sulphur Subunit of Succinate Dehydrogenase Enhances Photosynthesis and Growth in Tomato via an Organic Acid–Mediated Effect on Stomatal Aperture. **The Plant Cell**, [*s. l.*], v. 23, n. 2, p. 600–627, 2011. Disponível em: http://www.plantcell.org/lookup/doi/10.1105/tpc.110.081224.

AZEVEDO, I. G. *et al.* P-type H+-ATPases activity, membrane integrity, and apoplastic pH during papaya fruit ripening. **Postharvest Biology and Technology**, [*s. l.*], v. 48, n. 2, p. 242–247, 2008. Disponível em: https://linkinghub.elsevier.com/retrieve/pii/S0925521407003730.

AZOULAY-SHEMER, T. *et al.* Starch Biosynthesis in Guard Cells But Not in Mesophyll Cells Is Involved in CO2-Induced Stomatal Closing. **Plant physiology**, [*s. l.*], v. 171, n. 2, p. 788–798, 2016.

BATES, G. W. *et al.* A Comparative Study of the Arabidopsis thaliana Guard-Cell Transcriptome and Its Modulation by Sucrose. **PLoS ONE**, [*s. l.*], v. 7, n. 11, p. e49641, 2012. Disponível em: https://dx.plos.org/10.1371/journal.pone.0049641.

BAUER, H. *et al.* The stomatal response to reduced relative humidity requires guard cell-autonomous ABA synthesis. **Current Biology**, [*s. l.*], v. 23, n. 1, p. 53–57, 2013.

BERNSTEIN, L. Method for Determining Solutes in the Cell Walls of Leaves. **Plant Physiology**, [*s. l.*], v. 47, n. 3, p. 361–365, 1971.

BRODRIBB, T. J.; SUSSMILCH, F.; MCADAM, S. A. M. From Reproduction to Production, Stomata are the Master Regulators. **The Plant Journal**, [*s. l.*], p. tpj.14561, 2019.

CÂNDIDO-SOBRINHO, S. A. *et al.* Metabolism-mediated mechanisms underpin the differential stomatal speediness regulation among ferns and angiosperms. **Plant, Cell & Environment**, [*s. l.*], v. 45, n. 2, p. 296–311, 2022. Disponível em:

https://onlinelibrary.wiley.com/doi/10.1111/pce.14232.

CARRIQUÍ, M. *et al.* Diffusional limitations explain the lower photosynthetic capacity of ferns as compared with angiosperms in a common garden study. **Plant, Cell and Environment**, [*s. l.*], v. 38, n. 3, p. 448–460, 2015.

CECILIATO, P. H. O. O. *et al.* Intact leaf gas exchange provides a robust method for measuring the kinetics of stomatal conductance responses to abscisic acid and other small molecules in Arabidopsis and grasses. **Plant Methods**, [*s. l.*], v. 15, n. 1, p. 1–11, 2019. Disponível em: https://doi.org/10.1186/s13007-019-0423-y.

CHATER, C. C. C. *et al.* Origins and Evolution of Stomatal Development. **Plant Physiology**, [*s. l.*], v. 174, n. 2, p. 624–638, 2017. Disponível em: http://www.plantphysiol.org/lookup/doi/10.1104/pp.17.00183.

CHEN, Q. X. *et al.* Effect of methanol on the activity and conformation of acid phosphatase from the prawn Penaeus penicillatus. **Biochemistry. Biokhimiia**, [*s. l.*], v. 65, n. 4, p. 452–456, 2000. Disponível em: http://www.ncbi.nlm.nih.gov/pubmed/10810183.

CHEN, L. Q. *et al.* Sucrose efflux mediated by SWEET proteins as a key step for phloem transport. **Science**, [*s. l.*], v. 335, n. 6065, p. 207–211, 2012.

CHIKOV, V. I.; BAKIROVA, G. G. Role of the Apoplast in the Control of Assimilate Transport, Photosynthesis, and Plant Productivity. **Russian Journal of Plant Physiology**, [*s. l.*], v. 51, n. 3, p. 420–431, 2004. Disponível em: http://link.springer.com/10.1023/B:RUPP.0000028691.49600.c2.

CHINCINSKA, I. A. Leaf infiltration in plant science: old method, new possibilities. **Plant Methods**, [*s. l.*], v. 17, n. 1, p. 1–21, 2021. Disponível em: https://doi.org/10.1186/s13007-021-00782-x.

CHONG, J. *et al.* MetaboAnalyst 4.0: towards more transparent and integrative metabolomics analysis. **Nucleic Acids Research**, [*s. l.*], v. 46, n. W1, p. W486–W494, 2018. Disponível em: https://academic.oup.com/nar/article/46/W1/W486/4995686.

COCKBURN, W. Stomatal mechanism as the basis of the evolution of CAM and C4 photosynthesis. **Plant, Cell & Environment**, [*s. l.*], v. 6, n. 4, p. 275–279, 1983.

CRAMER, G. R. *et al.* Effects of abiotic stress on plants: a systems biology perspective. **BMC Plant Biology**, [*s. l.*], v. 11, n. 1, p. 163, 2011. Disponível em: http://www.biomedcentral.com/content/pdf/1471-2229-11-163.pdf.

DALOSO, D. M. *et al.* Guard cell-specific upregulation of sucrose synthase 3 reveals that the role of sucrose in stomatal function is primarily energetic. **New Phytologist**, [*s. l.*], v. 209, n. 4, p. 1470–1483, 2016.

DALOSO, D. M. *et al.* Metabolism within the specialized guard cells of plants. **New Phytologist**, [*s. l.*], v. 216, n. 4, p. 1018–1033, 2017.

DALOSO, D. M. *et al.* Tobacco guard cells fix CO2 by both Rubisco and PEPcase while sucrose acts as a substrate during light-induced stomatal opening. **Plant Cell and**

Environment, [*s. l.*], v. 38, n. 11, p. 2353–2371, 2015.

DALOSO, D. M.; DOS ANJOS, L.; FERNIE, A. R. Roles of sucrose in guard cell regulation. **New Phytologist**, [*s. l.*], v. 211, n. 3, p. 809–818, 2016.

DAUBERMANN, A. G. *et al.* Novel guard cell sink characteristics revealed by a multi-species/cell-types meta-analysis of 13C-labelling experiments. **Theoretical and Experimental Plant Physiology**, [*s. l.*], n. 0123456789, 2024. Disponível em: https://doi.org/10.1007/s40626-023-00299-9.

DRAGIŠIC MAKSIMOVIC, J. J. *et al.* Filter strip as a method of choice for apoplastic fluid extraction from maize roots. **Plant Science**, [*s. l.*], v. 223, p. 49–58, 2014.

DURAN-CARRIL, M. V; BUJAN, C. R. Antioxidant systems in the leaf apoplast compartment of Pinus pinaster Ait. and Pinus radiata D. Don. Plants exposed to SO 2. **Annals of Applied Biology**, [*s. l.*], v. 133, n. 3, p. 455–466, 1998. Disponível em: https://onlinelibrary.wiley.com/doi/10.1111/j.1744-7348.1998.tb05843.x.

DYRDA, G. *et al.* The effect of organic solvents on selected microorganisms and model liposome membrane. **Molecular Biology Reports**, [*s. l.*], v. 46, n. 3, p. 3225–3232, 2019. Disponível em: http://link.springer.com/10.1007/s11033-019-04782-y.

EISENACH, C.; DE ANGELI, A. Ion Transport at the Vacuole during Stomatal Movements. **Plant Physiology**, [*s. l.*], v. 174, n. 2, p. 520–530, 2017. Disponível em: http://www.plantphysiol.org/lookup/doi/10.1104/pp.17.00130.

EKANAYAKE, G.; GOHMANN, R.; MACKEY, D. A method for quantitation of apoplast hydration in Arabidopsis leaves reveals water-soaking activity of effectors of Pseudomonas syringae during biotrophy. **Scientific Reports**, [*s. l.*], v. 12, n. 1, p. 1–11, 2022. Disponível em: https://doi.org/10.1038/s41598-022-22472-x.

ERNST, O.; ZOR, T. Linearization of the Bradford Protein Assay. **Journal of Visualized Experiments**, [*s. l.*], v. 38, n. e1918, 2010. Disponível em: http://www.jove.com/index/Details.stp?ID=1918.

FARVARDIN, A. *et al.* The apoplast: A key player in plant survival. **Antioxidants**, [*s. l.*], v. 9, n. 7, p. 1–26, 2020.

FETTKE, J.; FERNIE, A. R. Intracellular and cell-to-apoplast compartmentation of carbohydrate metabolism. **Trends in Plant Science**, [*s. l.*], v. 20, n. 8, p. 490–497, 2015.

FIGUEIREDO, J. *et al.* An apoplastic fluid extraction method for the characterization of grapevine leaves proteome and metabolome from a single sample. **Physiologia Plantarum**, [*s. l.*], v. 171, n. 3, p. 343–357, 2021.

FLOERL, S. *et al.* Verticillium longisporum Infection Affects the Leaf Apoplastic Proteome, Metabolome, and Cell Wall Properties in Arabidopsis thaliana. **PLoS ONE**, [*s. l.*], v. 7, n. 2, p. e31435, 2012. Disponível em: https://dx.plos.org/10.1371/journal.pone.0031435.

FLÜTSCH, S. *et al.* Glucose uptake to guard cells via STP transporters provides carbon sources for stomatal opening and plant growth. **EMBO reports**, [*s. l.*], v. 21, n. 8, 2020.

Disponível em: https://onlinelibrary.wiley.com/doi/abs/10.15252/embr.201949719.

FLÜTSCH, S. *et al.* Guard cell starch degradation yields glucose for rapid stomatal opening in Arabidopsis. **Pant Cell, in press**, [*s. l.*], 2020.

FLÜTSCH, S.; HORRER, D.; SANTELIA, D. Starch biosynthesis in guard cells has features of both autotrophic and heterotrophic tissues. **Plant Physiology**, [*s. l.*], p. 541–556, 2022.

FLÜTSCH, S.; SANTELIA, D. Mesophyll-derived sugars are positive regulators of light-driven stomatal opening. **New Phytologist**, [*s. l.*], v. 230, n. 5, p. 1754–1760, 2021.

FLÜTSCH, S.; SANTELIA, D. Mesophyll-derived sugars are positive regulators of light-driven stomatal opening. **New Phytologist**, [*s. l.*], v. 230, n. 5, p. 1754–1760, 2021. Disponível em: https://onlinelibrary.wiley.com/doi/10.1111/nph.17322.

FREIRE, F. B. S. *et al.* Mild reductions in guard cell sucrose synthase 2 expression leads to slower stomatal opening and decreased whole plant transpiration in Nicotiana tabacum L. **Environmental and Experimental Botany**, [*s. l.*], v. 184, n. October 2020, 2021.

GAGO, J. *et al.* Photosynthesis Optimized across Land Plant Phylogeny. **Trends in Plant Science**, [*s. l.*], v. 73, p. 1–12, 2019.

GAGO, J. *et al.* Relationships of Leaf Net Photosynthesis, Stomatal Conductance, and Mesophyll Conductance to Primary Metabolism: A Multispecies Meta-Analysis Approach. **Plant Physiology**, [*s. l.*], v. 171, n. 1, p. 265–279, 2016.

GARCHERY, C. *et al.* A diminution in ascorbate oxidase activity affects carbon allocation and improves yield in tomato under water deficit. **Plant, Cell & Environment**, [*s. l.*], v. 36, n. 1, p. 159–175, 2013. Disponível em: https://onlinelibrary.wiley.com/doi/10.1111/j.1365-3040.2012.02564.x.

GENTZEL, I. *et al.* A simple method for measuring apoplast hydration and collecting apoplast contents. **Plant Physiology**, [*s. l.*], v. 179, n. 4, p. 1265–1272, 2019.

GRANOT, D.; KELLY, G. Evolution of Guard-Cell Theories: The Story of Sugars. **Trends in Plant Science**, [*s. l.*], v. 24, n. 6, p. 507–518, 2019. Disponível em: https://doi.org/10.1016/j.tplants.2019.02.009.

GREGORY, A. L. *et al.* In vivo regulatory phosphorylation of the phosphoenolpyruvate carboxylase AtPPC1 in phosphate-starved Arabidopsis thaliana. **Biochemical Journal**, [*s. l.*], v. 420, n. 1, p. 57–65, 2009. Disponível em: https://portlandpress.com/biochemj/article/420/1/57/44523/In-vivo-regulatory-phosphorylation-of-the.

GUPTA, S. K. *et al.* Effects of ethylenediurea (EDU) on apoplast and chloroplast proteome in two wheat varieties under high ambient ozone: an approach to investigate EDU's mode of action. **Protoplasma**, [*s. l.*], v. 258, n. 5, p. 1009–1028, 2021. Disponível em: https://link.springer.com/10.1007/s00709-021-01617-1.

GUPTA, M. N. Enzyme function in organic solvents. **European Journal of Biochemistry**, [*s. l.*], v. 203, n. 1–2, p. 25–32, 1992. Disponível em:

https://onlinelibrary.wiley.com/doi/10.1111/j.1432-1033.1992.tb19823.x.

HARTUNG, W.; RADIN, J. W.; HENDRIX, D. L. Abscisic Acid Movement into the Apoplastic solution of Water-Stressed Cotton Leaves. **Plant Physiology**, [*s. l.*], v. 86, n. 3, p. 908–913, 1988.

HEDRICH, R.; MARTEN, I. Malate-induced feedback regulation of plasma membrane anion channels could provide a CO2 sensor to guard cells. **The EMBO journal**, [*s. l.*], v. 12, n. 3, p. 897–901, 1993.

HETHERINGTON, A. M.; WOODWARD, F. I. The role of stomata in sensing and driving environmental change. **Nature**, [*s. l.*], v. 424, n. 6951, p. 901–908, 2003. Disponível em: http://www.nature.com/articles/nature01843.

HITE, D. R. C.; OUTLAW, W. H.; TARCZYNSKI, M. C. Elevated levels of both sucrose-phosphate synthase and sucrose synthase in Vicia guard cells indicate cell-specific carbohydrate interconversions. **Plant physiology**, [*s. l.*], v. 101, n. 4, p. 1217–1221, 1993.

HOAGLAND, D. R.; ARNON, D. I. The water-culture method for growing plants without soil. **California Agricultural Experiment Station Circular**, [*s. l.*], v. 347, p. 1–32, 1950.

HÕRAK, H.; KOLLIST, H.; MERILO, E. Fern Stomatal Responses to ABA and CO 2 Depend on Species and Growth Conditions. **Plant Physiology**, [*s. l.*], v. 174, n. 2, p. 672–679, 2017. Disponível em: https://academic.oup.com/plphys/article/174/2/672-679/6117579.

HORRER, D. *et al.* Blue light induces a distinct starch degradation pathway in guard cells for stomatal opening. **Current Biology**, [*s. l.*], v. 26, n. 3, p. 362–370, 2016.

HUBBARD, K. E.; WEBB, A. A. R. Circadian Rhythms in Stomata: Physiological and Molecular Aspects. *In*: RHYTHMS IN PLANTS. Cham: Springer International Publishing, 2015. p. 231–255. Disponível em: http://link.springer.com/10.1007/978-3-319-20517-5_9.

INOUE, S. I.; KINOSHITA, T. Blue light regulation of stomatal opening and the plasma membrane H+-ATPase. **Plant Physiology**, [*s. l.*], v. 174, n. 2, p. 531–538, 2017.

JASWANTHI, N. *et al.* Apoplast proteomic analysis reveals drought stress-responsive protein datasets in chilli (Capsicum annuum L.). **Data in Brief**, [*s. l.*], v. 25, p. 104041, 2019. Disponível em: https://linkinghub.elsevier.com/retrieve/pii/S2352340919303944.

JAYASINGHE, N. S. *et al.* Chapter 15 - Quantification of sugars and organic acids in biological matrices using GC-QqQ-MS. *In*: METHODS IN MOLECULAR BIOLOGY. [*S. l.: s. n.*], 2018. v. 1778, p. 207–223. Disponível em: http://link.springer.com/10.1007/978-1-4939-7819-9_15.

JOO, H.-J. *et al.* The Effect of Methanol on the Structural Parameters of Neuronal Membrane Lipid Bilayers. **The Korean Journal of Physiology & Pharmacology**, [*s. l.*], v. 16, n. 4, p. 255, 2012. Disponível em: https://synapse.koreamed.org/DOIx.php?id=10.4196/kjpp.2012.16.4.255.

JOOSTEN, M. H. A. J. A. J. Isolation of Apoplastic Fluid from Leaf Tissue by the Vacuum Infiltration-Centrifugation Technique. *In*: METHODS IN MOLECULAR BIOLOGY. [*S. l.: s.*

n.], 2012. v. 835, p. 603–610. Disponível em: https://link.springer.com/10.1007/978-1-61779-501-5_38.

JORGE, T. F.; ANTÓNIO, C. Quantification of Low-Abundant Phosphorylated Carbohydrates Using HILIC-QqQ-MS/MS. *In*: PLANT METABOLOMICS: METHODS AND PROTOCOLS. [*S. l.: s. n.*], 2018. p. 71–86. Disponível em: http://link.springer.com/10.1007/978-1-4939-7819-9_6.

KANG, YUN *et al.* Guard-cell apoplastic sucrose concentration – a link between leaf photosynthesis and stomatal aperture size in the apoplastic phloem loader Vicia faba L. **Plant, Cell & Environment**, [*s. l.*], v. 30, n. 5, p. 551–558, 2007. Disponível em: http://doi.wiley.com/10.1111/j.1365-3040.2007.01635.x.

KANG, Yun *et al.* Guard cell apoplastic photosynthate accumulation corresponds to a phloem-loading mechanism. **Journal of Experimental Botany**, [*s. l.*], v. 58, n. 15–16, p. 4061–4070, 2007.

KEHR, J.; MORRIS, R. J.; KRAGLER, F. Long-Distance Transported RNAs: From Identity to Function. **Annual Review of Plant Biology**, [*s. l.*], v. 73, p. 457–474, 2022.

KELLY, G. *et al.* Guard-Cell Hexokinase Increases Water-Use Efficiency Under Normal and Drought Conditions. **Frontiers in plant science**, [*s. l.*], v. 10, p. 1499, 2019. Disponível em: https://www.frontiersin.org/article/10.3389/fpls.2019.01499/full.

KELLY, G. *et al.* Hexokinase mediates stomatal closure. **Plant Journal**, [*s. l.*], v. 75, n. 6, p. 977–988, 2013.

KELLY, G. *et al.* The Solanum tuberosum KST1 partial promoter as a tool for guard cell expression in multiple plant species. **Journal of Experimental Botany**, [*s. l.*], v. 68, n. 11, p. 2885–2897, 2017.

KINGSBURY, N. J.; MCDONALD, K. A. Quantitative Evaluation of E1 Endoglucanase Recovery from Tobacco Leaves Using the Vacuum Infiltration-Centrifugation Method. **BioMed Research International**, [*s. l.*], v. 2014, p. 1–10, 2014. Disponível em: http://www.hindawi.com/journals/bmri/2014/483596/.

KOLEY, S. *et al.* An efficient LC-MS method for isomer separation and detection of sugars, phosphorylated sugars, and organic acids. **Journal of Experimental Botany**, [*s. l.*], v. 73, n. 9, p. 2938–2952, 2022.

KOPKA, J. *et al.* GMD@CSB.DB: the Golm Metabolome Database. **Bioinformatics**, [*s. l.*], v. 21, n. 8, p. 1635–1638, 2005. Disponível em: https://academic.oup.com/bioinformatics/article-lookup/doi/10.1093/bioinformatics/bti236.

KOPKA, J.; PROVART, N. J.; MULLER-ROBER, B. Potato guard cells respond to drying soil by a complex change in the expression of genes related to carbon metabolism and turgor regulation. **The Plant Journal**, [*s. l.*], v. 11, n. 4, p. 871–882, 1997. Disponível em: http://doi.wiley.com/10.1046/j.1365-313X.1997.11040871.x.

KOTTAPALLI, J. *et al.* Sucrose-induced stomatal closure is conserved across evolution. **PLoS ONE**, [*s. l.*], v. 13, n. 10, p. 1–17, 2018.

LAWSON, T. Guard cell photosynthesis and stomatal function. **New Phytologist**, [*s. l.*], v. 181, n. 1, p. 13–34, 2009. Disponível em: http://doi.wiley.com/10.1111/j.1469-8137.2008.02685.x.

LAWSON, T. *et al.* Mesophyll photosynthesis and guard cell metabolism impacts on stomatal behaviour. **New Phytologist**, [*s. l.*], v. 203, n. 4, p. 1064–1081, 2014.

LAWSON, T.; MATTHEWS, J. Guard Cell Metabolism and Stomatal Function. **Annual Review ofPlant Biology**, [*s. l.*], v. 71, p. 273–302, 2020.

LEAKEY, A. D. B. *et al.* Water Use Efficiency as a Constraint and Target for Improving the Resilience and Productivity of C 3 and C 4 Crops. **Annual Review of Plant Biology**, [*s. l.*], v. 70, n. 1, p. 781–808, 2019. Disponível em: https://www.annualreviews.org/doi/10.1146/annurev-arplant-042817-040305.

LEONHARDT, N. *et al.* Microarray Expression Analyses of Arabidopsis Guard Cells and Isolation of a Recessive Abscisic Acid Hypersensitive Protein Phosphatase 2C Mutant. **The Plant Cell**, [*s. l.*], v. 16, n. 3, p. 596–615, 2004. Disponível em: http://www.plantcell.org/lookup/doi/10.1105/tpc.019000.

LI, Y. *et al.* Glucose triggers stomatal closure mediated by basal signaling through HXK1 and PYR/RCAR receptors in Arabidopsis. **Journal of Experimental Botany**, [*s. l.*], v. 69, n. 7, p. 1471–1484, 2018. Disponível em: https://academic.oup.com/jxb/article/69/7/1471/4850518.

LIM, S.-L. *et al.* Arabidopsis guard cell chloroplasts import cytosolic ATP for starch turnover and stomatal opening. **Nature Communications**, [*s. l.*], v. 13, n. 1, p. 652, 2022. Disponível em: https://www.nature.com/articles/s41467-022-28263-2.

LIMA, V. F. *et al.* Establishment of a GC-MS-based 13 C-positional isotopomer approach suitable for investigating metabolic fluxes in plant primary metabolism. **The Plant Journal**, [*s. l.*], p. 1–21, 2021. Disponível em: https://onlinelibrary.wiley.com/doi/10.1111/tpj.15484.

LIMA, V. F. *et al.* The sucrose-to-malate ratio correlates with the faster CO2 and light stomatal responses of angiosperms compared to ferns. **New Phytologist**, [*s. l.*], v. 223, n. 4, p. 1873–1887, 2019. Disponível em: https://onlinelibrary.wiley.com/doi/abs/10.1111/nph.15927.

LIMA, V. F. *et al.* Toward multifaceted roles of sucrose in the regulation of stomatal movement. **Plant Signaling and Behavior**, [*s. l.*], v. 13, n. 8, p. 1–8, 2018. Disponível em: https://doi.org/10.1080/15592324.2018.1494468.

LIMA, V. F. *et al.* Unveiling the dark side of guard cell metabolism. **Plant Physiology and Biochemistry**, [*s. l.*], p. 107862, 2023. Disponível em: https://doi.org/10.1016/j.plaphy.2023.107862.

LISEC, J. *et al.* Gas chromatography mass spectrometry–based metabolite profiling in plants. **Nature Protocols**, [*s. l.*], v. 1, n. 1, p. 387–396, 2006. Disponível em: https://www.nature.com/articles/nprot.2006.59.

LIU, F. L. *et al.* Chemical Tagging Assisted Mass Spectrometry Analysis Enables Sensitive Determination of Phosphorylated Compounds in a Single Cell. **Analytical Chemistry**, [*s. l.*], v. 93, n. 17, p. 6848–6856, 2021.

LLOYD, F. . E. The physiology of stomata. **Publications of the Carnegie Institution of Washington**, [*s. l.*], v. 82, p. 1–42, 1908.

LOHAUS, G. *et al.* Is the infiltration-centrifugation technique appropriate for the isolation of apoplastic fluid? A critical evaluation with different plant species. **Physiologia Plantarum**, [*s. l.*], v. 111, n. 4, p. 457–465, 2001.

LONG, J. M.; WIDDERS, I. E. Quantification of apoplastic potassium content by elution analysis of leaf lamina tissue from pea (Pisum sativum L. cv Argenteum). **Plant Physiology**, [*s. l.*], v. 94, n. 3, p. 1040–1047, 1990.

LU, P. *et al.* A New Mechanism for the Regulation of Stomatal Aperture Size in Intact Leaves (Accumulation of Mesophyll-Derived Sucrose in the Guard-Cell Wall of Vicia faba). **Plant Physiology**, [*s. l.*], v. 114, n. 1, p. 109–118, 1997. Disponível em: https://academic.oup.com/plphys/article/114/1/109/6071024.

LU, P. *et al.* Sucrose: a solute that accumulates in the guard-cell apoplast and guard-cell symplast of open stomata. **FEBS Letters**, [*s. l.*], v. 362, n. 2, p. 180–184, 1995. Disponível em: http://doi.wiley.com/10.1016/0014-5793%2895%2900239-6.

LUGASSI, N. *et al.* Expression of Arabidopsis Hexokinase in Citrus Guard Cells Controls Stomatal Aperture and Reduces Transpiration. **Frontiers in Plant Science**, [*s. l.*], v. 6, n. December, p. 1–11, 2015. Disponível em: http://journal.frontiersin.org/Article/10.3389/fpls.2015.01114/abstract.

LUGASSI, N. *et al.* Expression of Arabidopsis Hexokinase in Tobacco Guard Cells Increases Water-Use Efficiency and Confers Tolerance to Drought and Salt Stress. **Plants**, [*s. l.*], v. 8, n. 12, p. 613, 2019. Disponível em: https://www.mdpi.com/2223-7747/8/12/613.

LUGASSI, N. *et al.* Expression of Hexokinase in Stomata of Citrus Fruit Reduces Fruit Transpiration and Affects Seed Development. **Frontiers in Plant Science**, [*s. l.*], v. 11, n. March, p. 1–10, 2020.

MADSEN, S. R.; NOUR-ELDIN, H. H.; HALKIER, B. A. Collection of Apoplastic Fluids from Arabidopsis thaliana Leaves. *In*: FETT-NETO, A. G.; WALKER, J. M. (org.). **Biotechnology of Plant Secondary Metabolism: Methods and Protocols**. New York, NY: Springer New York, 2016. (Methods in Molecular Biology). v. 1405, p. 35–42. Disponível em: http://link.springer.com/10.1007/978-1-4939-3393-8.

MALINOVA, I. *et al.* Identification of Two Arabidopsis thaliana Plasma Membrane Transporters Able to Transport Glucose 1-Phosphate. **Plant and Cell Physiology**, [*s. l.*], v. 61, n. 2, p. 381–392, 2020. Disponível em: https://academic.oup.com/pcp/article/61/2/381/5625160.

MARENTES, E. *et al.* Proteins accumulate in the apoplast of winter rye leaves during cold acclimation. [*s. l.*], p. 499–508, 1993.

MARTÍNEZ-GONZÁLEZ, A. P. *et al.* What proteomic analysis of the apoplast tells us about plant–pathogen interactions. **Plant Pathology**, [*s. l.*], v. 67, n. 8, p. 1647–1668, 2018. Disponível em: https://bsppjournals.onlinelibrary.wiley.com/doi/10.1111/ppa.12893.

MATSUO, K.; FUKUZAWA, N.; MATSUMURA, T. A simple agroinfiltration method for transient gene expression in plant leaf discs. **Journal of Bioscience and Bioengineering**, [*s. l.*], v. 122, n. 3, p. 351–356, 2016. Disponível em: https://linkinghub.elsevier.com/retrieve/pii/S1389172316000347.

MATTHEWS, J. S. A.; VIALET-CHABRAND, S. R. M.; LAWSON, T. Diurnal variation in gas exchange: The balance between carbon fixation and water loss. **Plant Physiology**, [*s. l.*], v. 174, n. 2, p. 614–623, 2017.

MCAUSLAND, L. *et al.* Effects of kinetics of light-induced stomatal responses on photosynthesis and water-use efficiency. **The New phytologist**, [*s. l.*], v. 211, n. 4, p. 1209–1220, 2016.

MCCORMICK, S. A 3-dimensional biomechanical model of guard cell mechanics. **The Plant Journal**, [*s. l.*], v. 92, n. 1, p. 3–4, 2017. Disponível em: https://onlinelibrary.wiley.com/doi/abs/10.1111/tpj.13665.

MEDEIROS, D. B. *et al.* Metabolomics for understanding stomatal movements. **Theoretical and Experimental Plant Physiology**, [*s. l.*], v. 31, n. 1, p. 91–102, 2019.

MEDEIROS, D. B. *et al.* Sucrose breakdown within guard cells provides substrates for glycolysis and glutamine biosynthesis during light-induced stomatal opening. **Plant Journal**, [*s. l.*], v. 94, n. 4, p. 583–594, 2018.

MEDEIROS, D. B. *et al.* Utilizing systems biology to unravel stomatal function and the hierarchies underpinning its control. **Plant, Cell & Environment**, [*s. l.*], v. 38, n. 8, p. 1457–1470, 2015. Disponível em: http://doi.wiley.com/10.1111/pce.12517.

MONTANO, J. *et al.* Salmonella enterica Serovar Typhimurium 14028s Genomic Regions Required for Colonization of Lettuce Leaves. **Frontiers in Microbiology**, [*s. l.*], v. 11, 2020. Disponível em: https://www.frontiersin.org/article/10.3389/fmicb.2020.00006/full.

NEILL, S. J. *et al.* Nitric Oxide Is a Novel Component of Abscisic Acid Signaling in Stomatal Guard Cells. **Plant Physiology**, [*s. l.*], v. 128, n. 1, p. 13–16, 2002. Disponível em: https://academic.oup.com/plphys/article/128/1/13-16/6110055.

NI, D. A. Role of vacuolar invertase in regulating Arabidopsis stomatal opening. **Acta Physiologiae Plantarum**, [*s. l.*], v. 34, n. 6, p. 2449–2452, 2012. Disponível em: http://link.springer.com/10.1007/s11738-012-1036-5.

NUNES-NESI, A. *et al.* Deficiency of mitochondrial fumarase activity in tomato plants impairs photosynthesis via an effect on stomatal function. **The Plant Journal**, [*s. l.*], v. 50, n. 6, p. 1093–1106, 2007. Disponível em: http://doi.wiley.com/10.1111/j.1365-313X.2007.03115.x.

O'LEARY, B. M. *et al.* Early changes in apoplast composition associated with defence and disease in interactions between Phaseolus vulgaris and the halo blight pathogen Pseudomonas syringae Pv. phaseolicola. **Plant Cell and Environment**, [*s. l.*], v. 39, n. 10, p. 2172–2184, 2016.

O'LEARY, B. M. *et al.* The infiltration-centrifugation technique for extraction of apoplastic

fluid from plant leaves using Phaseolus vulgaris as an example. **Journal of Visualized Experiments**, [*s. l.*], n. 94, p. 1–8, 2014.

OUTLAW, W. H. J. Integration of Cellular and Physiological Functions of Guard Cells. **Critical Reviews in Plant Sciences**, [*s. l.*], v. 22, n. 6, p. 503–5229, 2003.

OUTLAW, W. H. J. Sucrose and stomata: a full circle. *In*: MADORE, M. A.; LUCUS, W. J. (org.). **Carbon Partitioning and Source–Sink Interactions in Plants**. Rockville, MD, USA: American Society of Plant Physiologists, 1995. p. 56–67.

OUTLAW, W. H.; DE VLIEGHERE-HE, X. Transpiration Rate. An Important Factor Controlling the Sucrose Content of the Guard Cell Apoplast of Broad Bean. **Plant Physiology**, [*s. l.*], v. 126, n. 4, p. 1716–1724, 2001. Disponível em: http://www.plantphysiol.org/lookup/doi/10.1104/pp.126.4.1716.

OUTLAW, W. H.; MANCHESTER, J. Guard cell starch concentration quantitatively related to stomatal aperture. **Plant physiology**, [*s. l.*], v. 64, p. 79–82, 1979.

PARKHURST, D. F. Stereological methods for measuring internal leaf structure variables. **American Journal of Botany**, [*s. l.*], v. 69, n. 1, p. 31–39, 1982.

PEI, Z.-M. *et al.* Calcium channels activated by hydrogen peroxide mediate abscisic acidsignalling in guard cells. **Nature**, [*s. l.*], v. 406, n. 6797, p. 731–734, 2000. Disponível em: http://www.nature.com/articles/35021067.

PEREZ DE SOUZA, L. *et al.* Ultra-high-performance liquid chromatography high-resolution mass spectrometry variants for metabolomics research. **Nature Methods**, [*s. l.*], 2021.

PIRO, L.; FLÜTSCH, S.; SANTELIA, D. Arabidopsis Sucrose Synthase 3 (SUS3) regulates starch accumulation in guard cells at the end of day. **Plant Signaling and Behavior**, [*s. l.*], v. 18, n. 1, p. 4–8, 2023.

ROBAINA-ESTÉVEZ, S. *et al.* Resolving the central metabolism of Arabidopsis guard cells. **Scientific Reports**, [*s. l.*], v. 7, n. 1, p. 1–13, 2017.

RODRÍGUEZ-CELMA, J. *et al.* Plant fluid proteomics: Delving into the xylem sap, phloem sap and apoplastic fluid proteomes. **Biochimica et Biophysica Acta (BBA) - Proteins and Proteomics**, [*s. l.*], v. 1864, n. 8, p. 991–1002, 2016. Disponível em: https://linkinghub.elsevier.com/retrieve/pii/S1570963916300565.

ROELFSEMA, M. R. G.; HEDRICH, R. In the light of stomatal opening: new insights into ‘the Watergate’. **New Phytologist**, [*s. l.*], v. 167, n. 3, p. 665–691, 2005. Disponível em: http://doi.wiley.com/10.1111/j.1469-8137.2005.01460.x.

ROESSNER-TUNALI, U. *et al.* Kinetics of labelling of organic and amino acids in potato tubers by gas chromatography-mass spectrometry following incubation in 13 C labelled isotopes. **The Plant Journal**, [*s. l.*], v. 39, n. 4, p. 668–679, 2004. Disponível em: https://onlinelibrary.wiley.com/doi/10.1111/j.1365-313X.2004.02157.x.

ROHWER, J. M. Kinetic modelling of plant metabolic pathways. **Journal of Experimental Botany**, [*s. l.*], v. 63, n. 6, p. 2275–2292, 2012.

ROSADO-SOUZA, L. *et al.* Cassava Metabolomics and Starch Quality. **Current Protocols in Plant Biology**, [*s. l.*], v. 4, n. 4, 2019. Disponível em: https://onlinelibrary.wiley.com/doi/10.1002/cppb.20102.

SATTELMACHER, B. The apoplast and its significance for plant mineral nutrition. **New Phytologist**, [*s. l.*], v. 149, n. 2, p. 167–192, 2001. Disponível em: https://nph.onlinelibrary.wiley.com/doi/10.1046/j.1469-8137.2001.00034.x.

SCARPECI, T.; ZANOR, M.; VALLE, E. Estimation of Stomatal Aperture in Arabidopsis thaliana Using Silicone Rubber Imprints. **Bio-Protocol**, [*s. l.*], v. 7, n. 12, p. 1–6, 2017.

SCHNEIDER, C. A.; RASBAND, W. S.; ELICEIRI, K. W. NIH Image to ImageJ: 25 years of image analysis. **Nature Methods**, [*s. l.*], v. 9, n. 7, p. 671–675, 2012. Disponível em: https://www.nature.com/articles/nmeth.2089.

SHI, J. *et al.* Phospho enol pyruvate Carboxylase in Arabidopsis Leaves Plays a Crucial Role in Carbon and Nitrogen Metabolism. **Plant Physiology**, [*s. l.*], v. 167, n. 3, p. 671–681, 2015. Disponível em: https://academic.oup.com/plphys/article/167/3/671/6113635.

SMITH, R. R.; CANADY, W. J. Solvation effects upon the thermodynamic substrate activity; correlation with the kinetics of enzyme catalyzed reactions. I. Effects of added reagents such as methanol upon alpha-chymotrypsin. **Biophysical Chemistry**, [*s. l.*], v. 43, n. 2, p. 173–187, 1992. Disponível em: https://linkinghub.elsevier.com/retrieve/pii/030146229280032Z.

STEUDLE, E.; FRENSCH, J. Water transport in plants: Role of the apoplast. **Plant and Soil**, [*s. l.*], v. 187, n. 1, p. 67–79, 1996. Disponível em: http://link.springer.com/10.1007/BF00011658.

STURM, A.; TANG, G.-Q. The sucrose-cleaving enzymes of plants are crucial for development, growth and carbon partitioning. **Trends in Plant Science**, [*s. l.*], v. 4, n. 10, p. 401–407, 1999. Disponível em: https://linkinghub.elsevier.com/retrieve/pii/S1360138599014703.

TALBOTT, L. D.; ZEIGER, E. Central roles for potassium and sucrose in guard-cell osmoregulation. **Plant Physiology**, [*s. l.*], v. 111, n. 4, p. 1051–1057, 1996.

TALBOTT, L. D.; ZEIGER, E. The role of sucrose in guard cell osmoregulation. **Journal of Experimental Botany**, [*s. l.*], v. 49, n. Special, p. 329–337, 1998. Disponível em: https://academic.oup.com/jxb/article-lookup/doi/10.1093/jxb/49.Special_Issue.329.

TOSENS, T. *et al.* The photosynthetic capacity in 35 ferns and fern allies: Mesophyll CO2diffusion as a key trait. **New Phytologist**, [*s. l.*], v. 209, n. 4, p. 1576–1590, 2016.

VAVASSEUR, A.; RAGHAVENDRA, A. S. Guard cell metabolism and CO 2 sensing. **New Phytologist**, [*s. l.*], v. 165, n. 3, p. 665–682, 2005. Disponível em: https://onlinelibrary.wiley.com/doi/10.1111/j.1469-8137.2004.01276.x.

VOSS, L. J. *et al.* Guard cells in fern stomata are connected by plasmodesmata, but control cytosolic Ca2+ levels autonomously. **New Phytologist**, [*s. l.*], v. 219, n. 1, p. 206–215, 2018.

WANG, H. *et al.* A Subsidiary Cell-Localized Glucose Transporter Promotes Stomatal

Conductance and Photosynthesis. **The Plant cell**, [*s. l.*], v. 31, n. 6, p. 1328–1343, 2019.

WANG, R.-S. *et al.* Common and unique elements of the ABA-regulated transcriptome of Arabidopsis guard cells. **BMC Genomics**, [*s. l.*], v. 12, n. 1, p. 216, 2011. Disponível em: http://bmcgenomics.biomedcentral.com/articles/10.1186/1471-2164-12-216.

WILLE, A. C.; LUCAS, W. J.; ZEA, L. Ultrastructural and histochemical studies on guard cells. **Planta**, [*s. l.*], v. 160, n. 2, p. 129–142, 1984. Disponível em: http://link.springer.com/10.1007/BF00392861.

WILLMER, C.; FRICKER, M. **Stomata**. 2. ed. Dordrecht: Springer Netherlands, 1996. Disponível em: http://link.springer.com/10.1007/978-94-011-0579-8.

WOOLFENDEN, H. C. *et al.* A computational approach for inferring the cell wall properties that govern guard cell dynamics. **The Plant Journal**, [*s. l.*], v. 92, n. 1, p. 5–18, 2017. Disponível em: https://onlinelibrary.wiley.com/doi/abs/10.1111/tpj.13640.

YAHIA, E. M.; CARRILLO-LÓPEZ, A.; BELLO-PEREZ, L. A. Carbohydrates. *In*: POSTHARVEST PHYSIOLOGY AND BIOCHEMISTRY OF FRUITS AND VEGETABLES. [*S. l.*]: Elsevier, 2019. p. 175–205. Disponível em: https://linkinghub.elsevier.com/retrieve/pii/B9780128132784000099.

YU, Y. *et al.* The effects of organic solvents on the folding pathway and associated thermodynamics of proteins: a microscopic view. **Scientific Reports**, [*s. l.*], v. 6, n. 1, p. 19500, 2016. Disponível em: https://www.nature.com/articles/srep19500.

ZAKHARTSEV, M. *et al.* Metabolic model of central carbon and energy metabolisms of growing Arabidopsis thaliana in relation to sucrose translocation. **BMC Plant Biology**, [*s. l.*], v. 16, n. 1, 2016. Disponível em: http://dx.doi.org/10.1186/s12870-016-0868-3.

ZEIGER, E. *et al.* The guard cell chloroplast: a perspective for the twenty-first century. **New Phytologist**, [*s. l.*], v. 153, n. 3, p. 415–424, 2002. Disponível em: http://doi.wiley.com/10.1046/j.0028-646X.2001.NPH328.doc.x.

ZEIGER1, E.; ZHU, J. Role of zeaxanthin in blue light photoreception and the modulation of light–CO 2 interactions in guard cells. **Journal of Experimental Botany**, [*s. l.*], v. 49, n. March, p. 433–442, 1998.